MICROCOPY RESOLUTION TEST CHART

NATIONAL BUREAU OF STANDARDS-1963-A

AFWAL-TR-83-3087

THRUST AUGMENTATION STUDY OF
HIGH PERFORMANCE EJECTORS

J. E. MINARDI
H. P. VON OHAIN

UNIVERSITY OF DAYTON RESEARCH INSTITUTE
300 COLLEGE PARK AVENUE
DAYTON, OHIO 45469

NOVEMBER 1983

FINAL REPORT FOR PERIOD 15 MARCH 1982 - 15 MARCH 1983

APPROVED FOR PUBLIC RELEASE; DISTRIBUTION UNLIMITED.

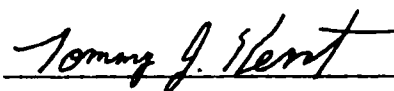AD-A142 650

DTIC FILE COPY

84 07 02 074

NOTICE

When Government drawings, specifications, or other data are used for any
purpose other than in connection with a definately related Government procure-
ment operation, the United States Government thereby incurs no responsibility
nor any obligation whatsoever; and the fact that the Government may have
formulated, furnished, or in any way supplied the said drawings, specifications,
or other data, is not to be regarded by implication or otherwise as in any
manner licensing the holder or any other person or corporation, or conveying
any rights or permission to manufacture use, or sell any patented invention
that may in any way be related thereto.

This report has been reviewed by the Office of Public Affairs (ASD/PA) and is
releasable to the National Technical Information Service (NTIS). At NTIS, it
will be available to the general public, including foreign nations.

This technical report has been reviewed and is approved for publication.

K. S. NAGARAJA   Tommy J. Kent, Maj., USAF
Project Engineer   Chief, Aerodynamics and Airframe Branch

FOR THE COMMANDER

Ralph W. Holm
Colonel, USAF
Chief, Aeromechanics Division

REPORT DOCUMENTATION PAGE	READ INSTRUCTIONS BEFORE COMPLETING FORM

1. REPORT NUMBER	2. GOVT ACCESSION NO.	3. RECIPIENT'S CATALOG NUMBER
AFWAL-TR-83-3087	A142650	

4. TITLE (and Subtitle)	5. TYPE OF REPORT & PERIOD COVERED
THRUST AUGMENTATION STUDY OF HIGH PERFORMANCE EJECTORS	Final 3/15/82 to 3/15/83
	6. PERFORMING ORG. REPORT NUMBER UDR-TR-83-37

7. AUTHOR(s)	8. CONTRACT OR GRANT NUMBER(s)
J. E. Minardi H. P. von Ohain	F33615-82-K-3016

9. PERFORMING ORGANIZATION NAME AND ADDRESS	10. PROGRAM ELEMENT, PROJECT, TASK AREA & WORK UNIT NUMBERS
University of Dayton Research Institute 300 College Park Avenue Dayton, Ohio 45469	P.E. 62201F JON: 24041067

11. CONTROLLING OFFICE NAME AND ADDRESS	12. REPORT DATE
AFWAL/FIMM Wright-Patterson AFB, Ohio 45433	November 1983
	13. NUMBER OF PAGES 86

14. MONITORING AGENCY NAME & ADDRESS(If different from Controlling Office)	15. SECURITY CLASS. (of this report)
	Unclassified
	15a. DECLASSIFICATION DOWNGRADING SCHEDULE

16. DISTRIBUTION STATEMENT (of this Report)

Approved for public release; distribution unlimited.

17. DISTRIBUTION STATEMENT (of the abstract entered in Block 20, If different from Report)

18. SUPPLEMENTARY NOTES

19. KEY WORDS (Continue on reverse side if necessary and identify by block number)

Ejectors
Thrust Augmentation
High Pressure Ratio Ejectors
Supersonic Ejectors
Propulsive Ejectors

Mixing Devices for Thrust
Augmentation

20. ABSTRACT (Continue on reverse side If necessary and identify by block number)

The use of ejectors in energy conversion processes and thrust augmentation requires that the mixed flow be produced at a high efficiency. Although many definitions of efficiency have been used to describe the efficiency of an ejector, we have used an efficiency based on thermodynamic availability which is referenced to the stagnation properties of the secondary flow (the flow being "pumped"). As is well known, a compressible-flow,

DD FORM 1473 EDITION OF 1 NOV 65 IS OBSOLETE
1 JAN 73

20.   control-volume approach to analyzing a constant area ejector yields two solutions: one with a subsonic mixed flow and one with a supersonic mixed flow. The supersonic mixed flow produces the best efficiencies and highest total pressures. The properties of the supersonic mixed flow are of necessity related to the properties of the subsonic mixed flow by the normal shock relations. Nonetheless, in practice, the subsonic mixed flow is, in general, not achieved through a normal shock (or pseudo-normal shock) from the supersonic mixed flow solution.

A technique is developed for determining a representative value of the maximum efficiency that can be achieved with high performance ejectors when operating on the supersonic solution branch of an ejector. These efficiencies are used to calculate thrust augmentation for an ejector over a wide range of parameters including operation with a hypothetical engine.

Reasonable values of thrust augmentation can be achieved at low subsonic flight Mach numbers. However, at flight Mach numbers near one, little or no thrust augmentation was found. At supersonic flight Mach numbers, thrust augmentation was achieved.

Basic studies indicated that the effects of temperature was opposite at subsonic and supersonic flight Mach numbers. Thrust augmentation decreased with increasing temperature at subsonic Mach numbers and increased with increasing temperature at supersonic Mach numbers.

Basic concepts are presented for cross flow and counter flow momentum exchangers which may afford more efficient transfer of kinetic energy between fluid streams.

FOREWORD

iii

TABLE OF CONTENTS

LIST OF ILLUSTRATIONS

LIST OF TABLES

LIST OF SYMBOLS

β	bypass ratio
γ	ratio of specific heats
η	efficiency
η_c	compressor polytropic component efficiency
η_t	turbine polytropic component efficiency
τ	thrust
τ_m	mixed flow thrust
τ_p	thrust of the primary flow
ϕ	thrust augmentation ratio
A_p	primary flow area at the inlet
A_s	secondary flow area at the inlet
A_{ep}	primary flow area at the station e
A_{es}	secondary flow area at the station e
C_p	specific heat at constant pressure
M_∞	flight Mach number
M_p	primary inlet Mach number
M_s	secondary inlet Mach number
M^*	ratio of velocity to the speed of sound at Mach one
M_p^*	primary M^*
M_s^*	secondary M^*
M_{ep}	primary Mach number at the station e
M_{es}	secondary Mach number at the station e
$\dot{m}$	mass flow rate
P	pressure
P_{amb}	ambient pressure
P_{comp}	compressor pressure
P_e	compressor pressure ratio
P_{1p}	primary inlet static pressure
P_{1s}	secondary inlet static pressure
P_{op}	primary total pressure
P_{os}	secondary total pressure
P_R	P_{op}/P_{os}

R	gas constant
T	temperature
T_{op}	primary total temperature
T_{os}	secondary total temperature
T_R	T_{op}/T_{os}
U	transport velocity
V	velocity
W	molecular weight
—	bar over a symbol is a ratio of primary to secondary

LIST OF SYMBOLS
FOR TABLES 1 THROUGH 5

A/AP*	value of A/A_p^* mixing tube area to primary nozzle throat area
AP/AS	area ratio A_p/A_s required to match the inlet pressure
EFAVL	efficiency based on availability
EFPOS	efficiency based on expansion to P_{os}
GM	gamma value of the mixture
GP	primary gamma value
GS	secondary gamma value
MM	mixed flow Mach number
MP	primary Mach number
MS	secondary Mach number
PR	pressure ratio
P1P/POS	primary nozzle pressure ratio: P_{1p}/P_{op}
P1S/	secondary nozzle pressure ratio: P_{1s}/P_{os}
PM/	pressure ratio P_m/P_{os}
POM/	total pressure ratio P_{om}/P_{os}
SR	entropy increase
TR	temperature ratio
T1P/TOS	primary nozzle temperature ratio: T_{1p}/T_{op}
T1S/	secondary nozzel temperature ratio: T_{1s}/T_{os}
TM/	temperature ratio T_m/T_{os}
VP/VS	ratio of primary velocity to the secondary velocity
VM/VS	ratio of the mixed velocity to the secondary velocity
WP	primary molecular weight
WS	secondary molecular weight
WR	ratio of molecular weights

SECTION 1
INTRODUCTION

Ejectors have been used in man, useful applications in
industry. Ejectors have also been investigated for flight appli-
cations and their potential usefulness has been demonstrated in
experimental aircraft.

It has been known for some time (see, for example, references
1 through 4) that a control volume analysis of a constant area
ejector leads to a double-valued solution: one where the mixed
flow is subsonic, and the other where the mixed flow is supersonic.
Further, it is well known that these two solutions are related
by the normal shock relations.

Recently, Alperin and Wu[5] have pointed out the potential
advantages of the supersonic branch for applications to thrust
augmentation. Minardi et al.[6], who were studying two fluid
ejectors for applications in turbines, also found better results
for their applications when the supersonic branch was utilized.

Extremely high efficiencies (based on thermodynamic avail-
ability) are indicated on the supersonic solution branch. In fact,
following Hoge[3], it can be shown[7,8] that extremely high efficiencies
can also occur on the subsonic solution branch. However, as dis-
cussed in reference 7, these extremely high efficiencies cannot
be achieved in an ejector. Rather, they would require rotating
machinery within the control volume to produce the extremely high
efficiencies. It was shown in reference 7 that an ejector with
a subsonic inlet for the secondary flow (the primary is supersonic
at the inlet) operates at a single operating point when the exit
flow is supersonic. This operating point can be determined by
the methods described by Fabri and Siestrunck[2]. Thus, a procedure
is available to evaluate the performance of an ejector operating
on the supersonic solution branch.

It was the purpose of the study reported herein to determine
reasonable estimates of thrust augmentation that could be achieved
with an ejector over a range of Mach numbers from zero to supersonic.

1

SECTION 2

DISCUSSION OF THE SUPERSONIC SOLUTION BRANCH

In reference 7 an analysis for a constant area ejector, such as shown in Figure 1, is presented. The equations resulting from the solution are presented in Appendix A. Figure 2 presents supersonic branch solutions to the equations for air driving air for a pressure ratio of six and a temperature ratio of 3.7 and for a series of bypass ratios, β, from 0.5 to 10. The curves show efficiency, based on thermodynamic availability, versus the secondary, inlet Mach number, M_s. As stated earlier there is also a subsonic solution branch (not shown on Figure 2) which is related to the supersonic solution branch by the normal shock relations: if the supersonic mixed flow experiences a normal shock, the conditions would be the same as the conditions on the subsonic solution branch at the same value of M_s.

At the higher values of β the mixed flow becomes choked, i.e., the mixed flow Mach number is one. This choking eliminates a section of the curve as indicated on the bypass ratios of five and ten. The region over which the solutions do not exist are referred to by Hoge[3] as the forbidden region. We have indicated the boundaries of the forbidden region on Figure 2.

Hoge[3] also showed that the control volume equations developed for an ejector could be solved over the entire region of the $M_p^* - M_s^*$ plane. The parameter M^* (the ratio of velocity to the speed of sound at Mach one) was chosen in place of the Mach number since a finite range of the parameter M^* covers all Mach numbers from zero to infinity. An efficiency map for a pressure ratio of six, temperature ratio of 3.7, and a bypass ratio of 10 is shown on Figure 3. On Figure 3 the forbidden region becomes egg-shaped, as shown cross-hatched. In calculating the data for Figure 2, it was assumed that the inlet static pressures of the primary, P_{1p}, and secondary, P_{1s}, were equal. In Figure 3 we show the curve in the $M_p^* - M_s^*$ plane for which $P_{1p} = P_{1s}$. After

2
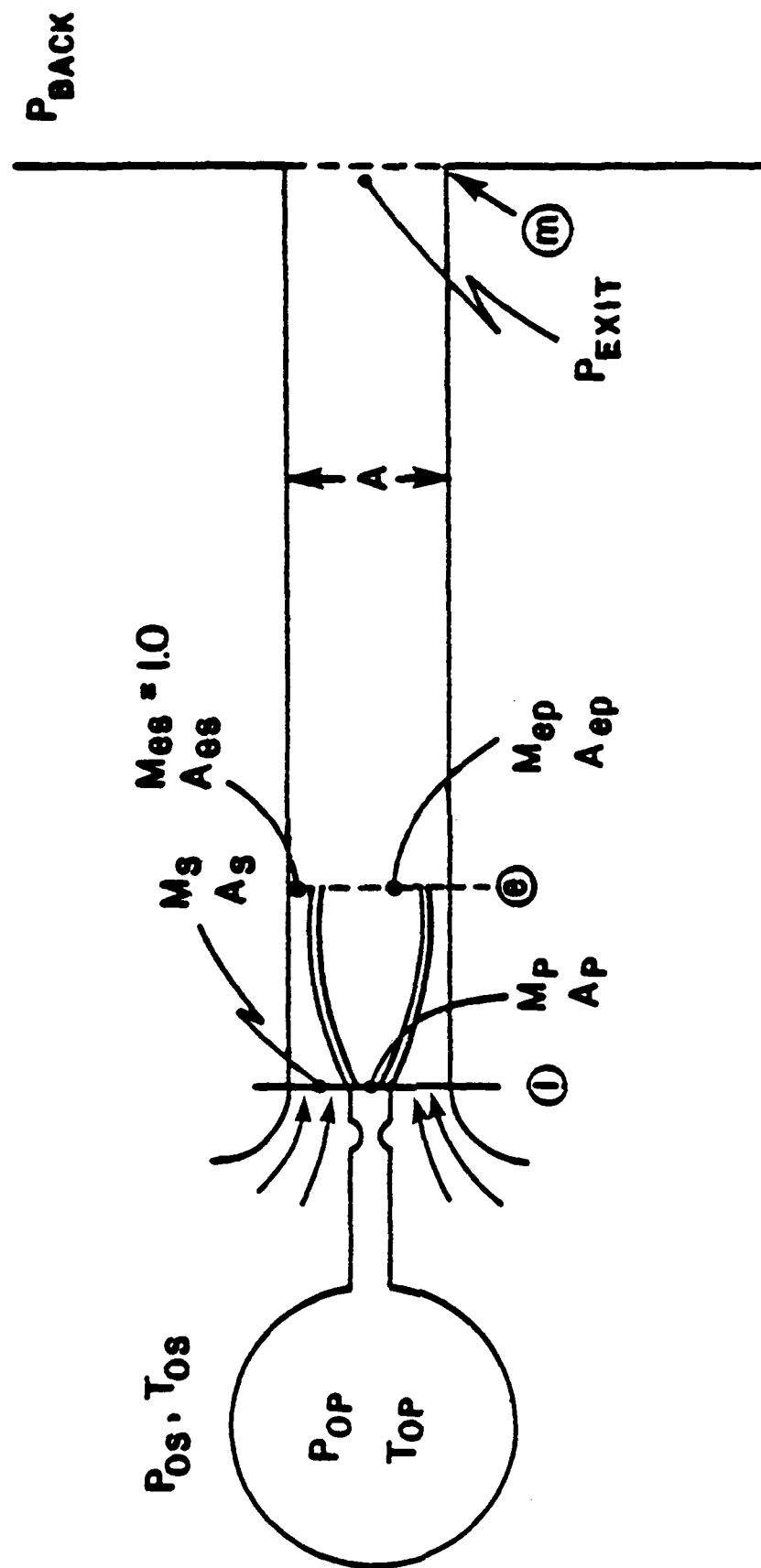
Figure 1. Inlet Flow Pattern for an Ejector Operating with a Supersonic Mixed Flow and Having a Supersonic Primary Flow and a Subsonic Secondary Flow.
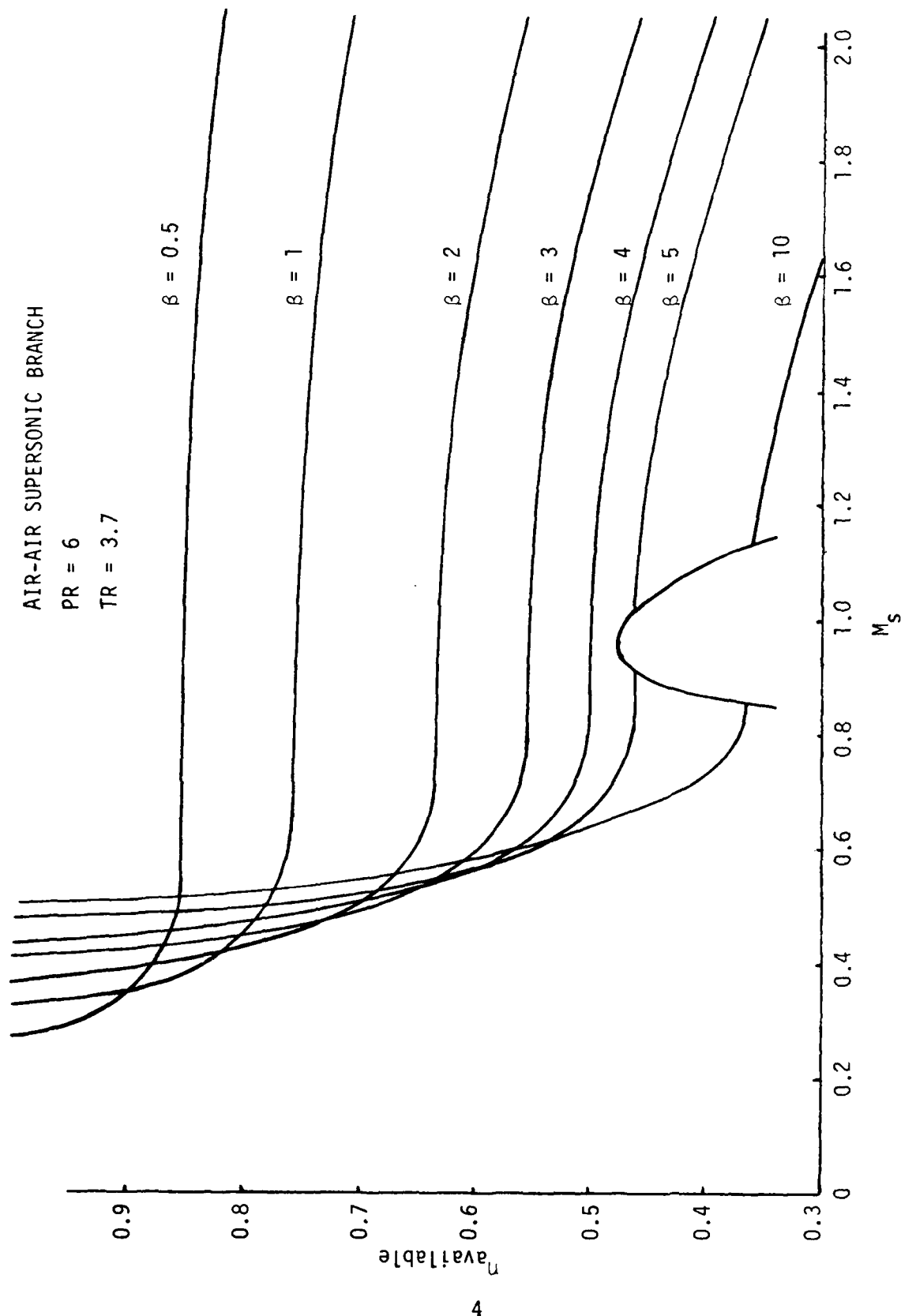
Figure 2. Supersonic Branch Solutions Showing Efficiency Versus Secondary Inlet Mach Number, M_s, for Various Bypass Ratios, β, at the Indicated Conditions. This is a Design Curve Because the Physical Size of the Ejector Changes as One Moves Along the Curves.

4

SUPERSONIC BRANCH EFFICIENCY
$\beta = 10$ PR = 6.0   TR = 3.7
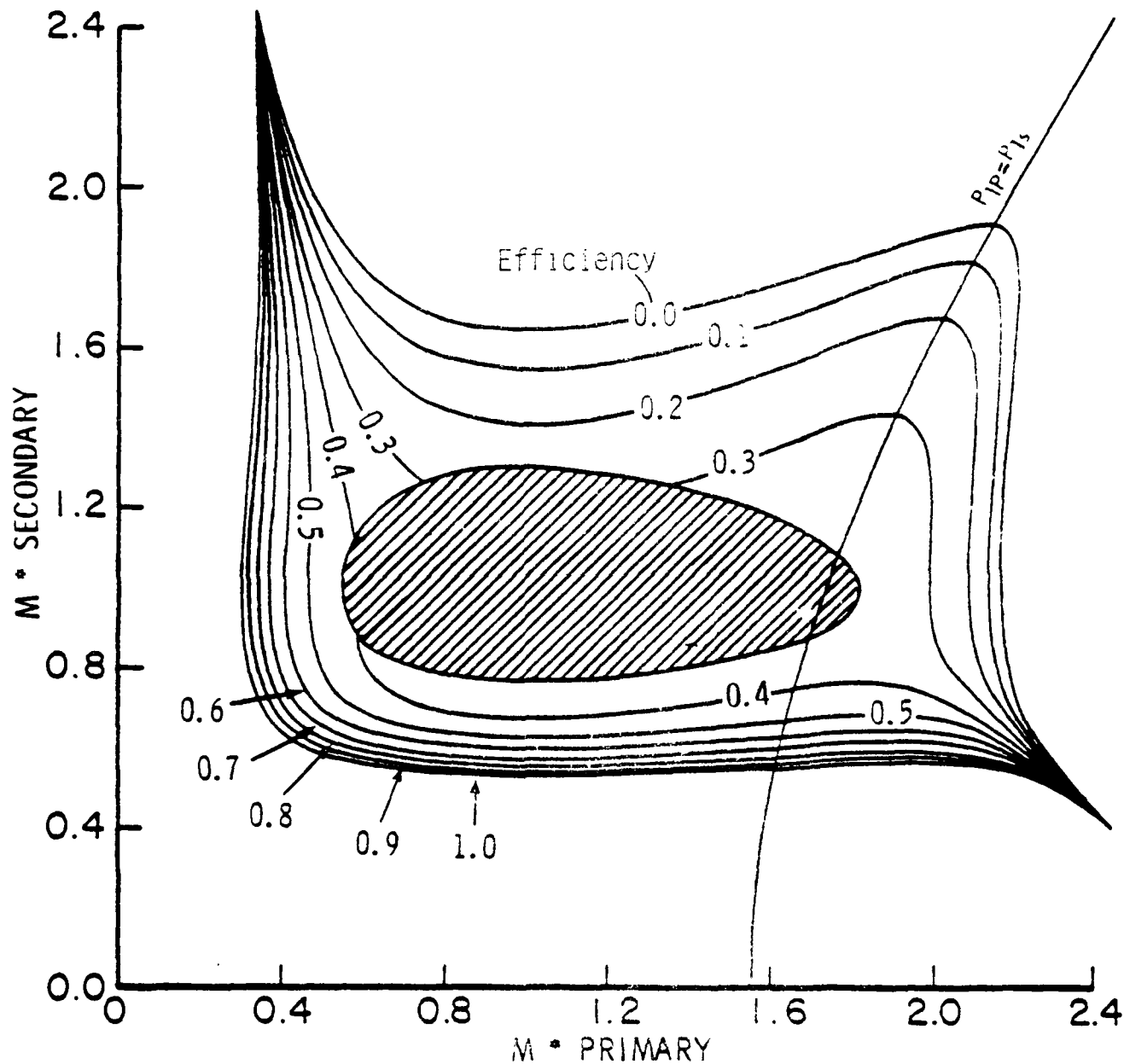
Figure 3. Supersonic Branch Efficiency Map. Also Shown
is the Curve for which $P_{1p}=P_{1s}$. The Curve is
a Design Curve Because the Physical Size of the
Ejector Has to Change as One Moves Along the
Curve.

proper adjustments for changing M_s^* to M_s we could take data from
Figure 3 along the curve $P_{1p} = P_{1s}$ and plot the corresponding
curve for $\beta = 10$ on Figure 2.

The shape of the forbidden region is independent of the
pressure ratio and depends only on the value of the bypass ratio
and the temperature ratio. Hoge[3] gives the equation for the
boundaries of the forbidden region as

$$(M_p^*+1/M_p^*) + \beta(M_s^*+1/M_s^*)/\sqrt{TR} = 2\sqrt{(1+\beta)(1+\beta/TR)}. \tag{1}$$

It is interesting to note that for either the primary or the
secondary flow that if M^* satisfies Equation (1), then so does
the value of M^* equal to the reciprocal of the first value. Also,
the curve for which $P_{1p} = P_{1s}$ can be obtained from the isentropic
relations which yield

$$M_p^* = \sqrt{\frac{\gamma+1}{\gamma-1} - PR^{-\left(\frac{\gamma-1}{\gamma}\right)}\left(\frac{\gamma+1}{\gamma-1} - M_s^{*2}\right)}. \tag{2}$$

The simulataneous solution of Equations (1) and (2) yields the
pair of points where the curve $P_{1p} = P_{1s}$ intersects the boundaries
of the forbidden region. These results will be used in Section 5.

At this time, however, we wish to consider Figure 2 and 3
further. The very high values of efficiency located at the low
subsonic values of M_s for all of the bypass ratios would provide
excellent values of thrust augmentation if they could be achieved
in an ejector. However, Figure 2 raises serious doubts that this
could happen in an ejector. For example, the data of Figure 2
indicate that at a Mach number of $M_s = 0.51$ the efficiency at
a bypass ratio of 10 is about 0.9 which is higher than the effi-
ciency (at the same M_s) associated with any other value of β
indicated on Figure 2. Even though the value of efficiency of 0.9
does not violate the second law (since it is less than one) it is
highly unlikely that such a result could be achieved in an ejector.

It was considerations such as these that led us to consider
the control volume solution in more detail in reference 7. It

was concluded that although the constant area geometry shown in Figure 1 was a sufficient condition to derive the set of equations used in the analysis, it was not a necessary condition. Thus, some of the solutions generated from the equations might not be valid solutions for an ejector. On the other hand, all of the solutions valid for an ejector would be obtained from the solutions to the equations.

Thus, some other criteria would be required to sort out those solutions that are valid in an ejector. Such criteria are discussed further in the next section.

SECTION 3

INLET CONDITIONS

The curves of Figures 2 and 3 should be considered design
curves since the physical size of the various ejector areas (and
area ratios) would have to change to obtain the performance indi-
cated at various points on the curves. However, once an ejector
design is selected its operation will be determined by the boundary
conditions imposed on the ejector.

In addition to the primary and secondary total pressures
and total temperatures, the back pressure (see Figure 1) must also
be known to determine the ejector operation. At any value of M_s
the design is the same for a point on the supersonic or subsonic
branch. Thus, if the back pressure is set at a value equal to
the mixed-flow, static pressure on the subsonic branch, then the
ejector would operate at that design point and P_{1p} would be equal
to P_{1s}. This follows since the exit flow is subsonic.

A whole series of values of M_s could be achieved in the
ejector on the subsonic branch by adjusting the back pressure.

On the supersonic branch this is not the case. If the back
pressure is reduced sufficiently, the ejector will make a trans-
ition to the supersonic solution branch and the operation becomes
independent of further reductions in pressure. Thus, there is
only one operating point that the ejector will achieve on the
supersonic branch. This operating point can be determined by the
methods described by Fabri and Siestrunck[2]. We have developed
equations based on their approach in reference 7 and these equations
are also presented in Appendix A.

In reference 7, using the Fabri and Siestrunck approach, we
calculated the data presented in Figure 4 for a temperature ratio
of 3.7 and the other conditions shown on the figure. We chose
various area ratios and plotted the efficiency versus the mass
flow ratio achieved at various pressure ratios. Each curve

8
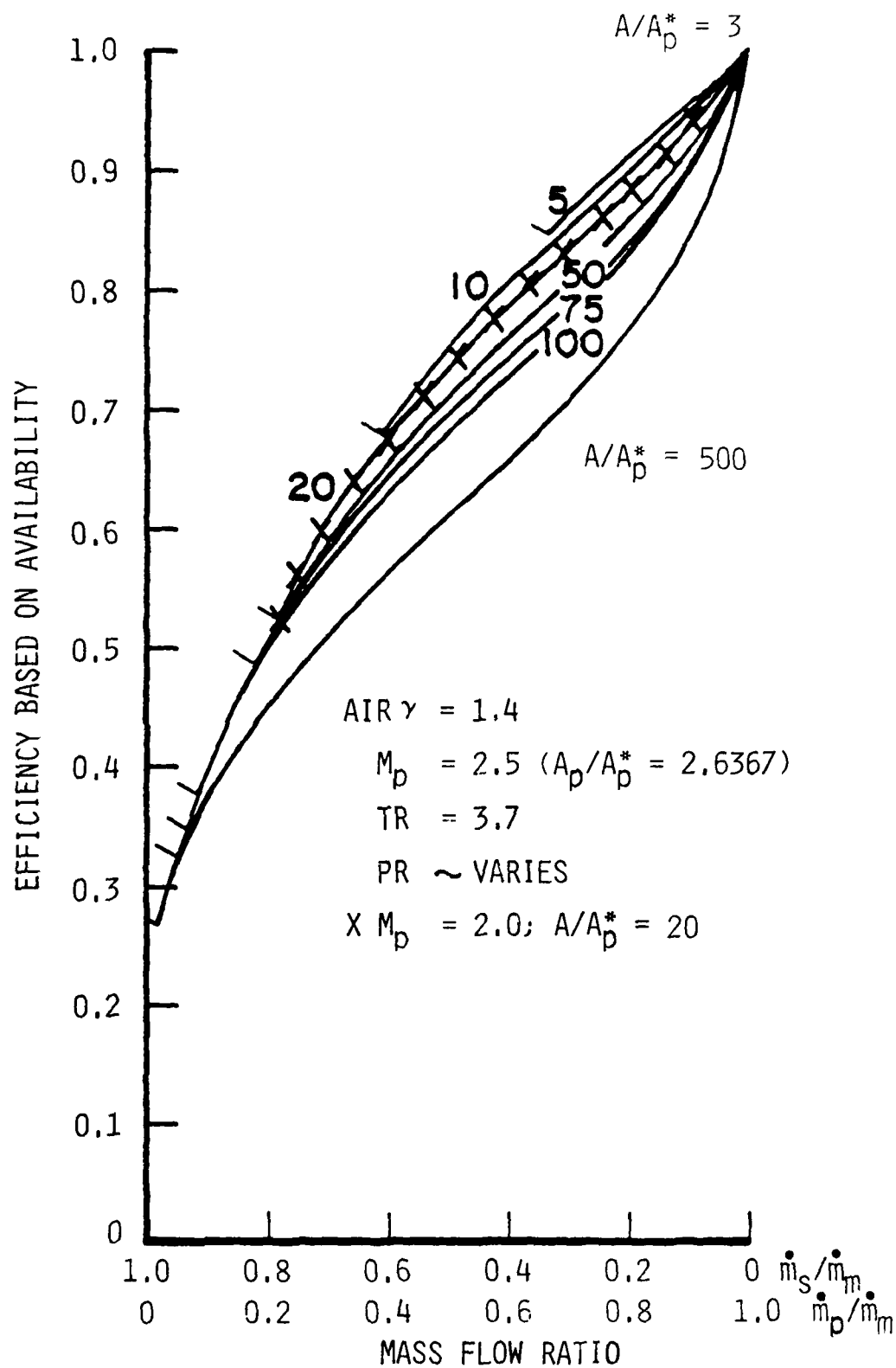
Figure 4. Efficiency Versus Mass-Flow Ratio for Different Geometry Mixing Tubes.

9

terminates at the point where the value of M_s^* first reaches Mach
one. The points are indicated by the hack marks on Figure 4
along each area ratio curve. It is clear from Figure 4 that the
maximum efficiency is achieved for a given mass flow ratio with
the smallest diameter tube operating at a value of M_s^* nearly
equal to one.

These results were achieved for an ejector that operates
at a value of $M_s \leq 1$. However, from Figure 2 we see that for all
of the data shown that the efficiency at $M_s = 1$, on a curve for
a given bypass ratio, is higher than at any supersonic values of
M_s. However, as shown on Figure 5, this result does not hold
for all temperature ratios. At the low temperature ratios (e.g.,
1.0 and 1.5) there is an increase in efficiency at higher values
of M_s. Since most of our applications are concerned with tem-
perature ratios higher than two, we will not consider the in-
creased efficiencies resulting from operation at values of
$M_s \geq 1$ at the lower temperature ratios.

In Table 1 we present a computer printout of the supersonic
branch solution for a pressure ratio of six, temperature ratio
of 3.7, and a bypass ratio of four. The first column contains
the secondary Mach number M_s which is taken as the independent
variable. The second column is P_{1s}/P_{os} (because of lack of space,
it is labeled (Pls) and the third column is the temperature ratio
T_{1s}/T_{os}. Each of these values is obtained from M_s using isen-
tropic relations. The exit area of the primary nozzle is chosen
to match the pressure of the primary to the secondary. This
sets the value of the primary Mach number, M_p (located in column
10), and enables one to find T_{1p}/T_{op} and P_{1p}/P_{op} (located in
columns 11 and 12).

Column four gives the ratio of the primary velocity to the
secondary velocity V_p/V_s and column five gives the ratio of the
mixed velocity to the secondary velocity.

Column six gives the mixed flow Mach number. Column seven
is the pressure ratio P_m/P_{os} and column eight is the temperature

10

AIR-AIR SUPERSONIC BRANCH

$\beta = 1$

$PR = 6$

$\eta_{available}$

M_s

Figure 5. Efficiency Versus M_s for Various Temperature Ratios at Indicated Conditions.

11

TABLE 1

SUPERSONIC BRANCH SOLUTION

CONSTANT MASS FLOW
CONSTANT AREA SUPERSONIC
PRIMARY VAPOR AIR   SECONDARY GAS AIR
PR= 6.000 TR= 3.700 GP=1.400 GS=1.400 WR= 1.00 WP= 29.00 WE= 29.00
BY-PASS RATIO= 4.000

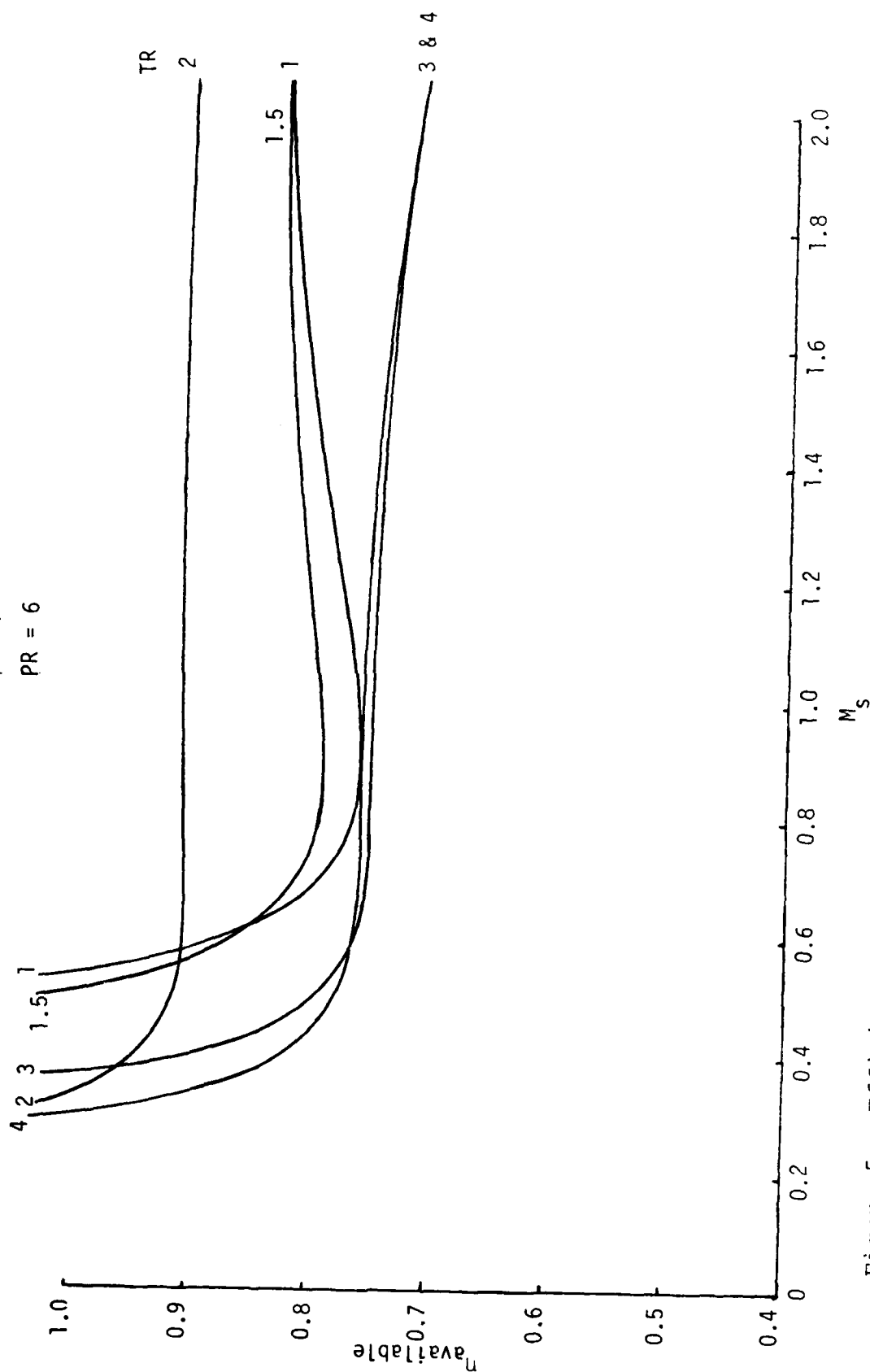| MS	PIS/	TIS/	VP/VS	VM/VS	MM	PM/	TM/	GM	MP	TIP/TOS	PIP/PCP	AP/AS	A/AP*	EFPOS	POM/	EFAVI	SE
0.0500	VIOLATION OF 2ND LAW REQUIRES NEGATIVE TEMPERATURES																
0.1000	VIOLATION OF 2ND LAW REQUIRES NEGATIVE TEMPERATURES																
0.1500	VIOLATION OF 2ND LAW REQUIRES NEGATIVE TEMPERATURES																
0.2000	VIOLATION OF 2ND LAW REQUIRES NEGATIVE TEMPERATURES																
0.2500	VIOLATION OF 2ND LAW REQUIRES NEGATIVE TEMPERATURES																
0.3000	VIOLATION OF 2ND LAW REQUIRES NEGATIVE TEMPERATURES																
0.3500	VIOLATION OF 2ND LAW FOR ADIABATIC SYSTEMS REQUIRES WORK INPUT AND COOLING																
0.4000	VIOLATION OF 2ND LAW FOR ADIABATIC SYSTEMS REQUIRES WORK INPUT AND COOLING																
0.4500	0.870	0.961	6.349	4.543	2.335	0.169	0.737	1.400	1.92	0.576	0.145	0.087	19.653	1.06	2.23	0.986	0.152
0.5000	0.843	0.952	5.775	3.776	1.986	0.230	0.861	1.400	1.94	0.571	0.141	0.096	18.322	0.78	1.76	0.709	0.388
0.5500	0.814	0.943	5.311	3.201	1.749	0.292	0.956	1.400	1.96	0.565	0.136	0.104	17.293	0.61	1.55	0.613	0.515
0.6000	0.784	0.933	4.928	2.759	1.575	0.352	1.029	1.400	1.99	0.559	0.131	0.112	16.493	0.52	1.44	0.560	0.586
0.6500	0.753	0.922	4.609	2.409	1.442	0.411	1.088	1.400	2.01	0.553	0.125	0.120	15.873	0.47	1.39	0.531	0.625
0.7000	0.721	0.911	4.339	2.130	1.336	0.467	1.135	1.400	2.04	0.546	0.120	0.128	15.399	0.44	1.36	0.515	0.646
0.7500	0.689	0.899	4.108	1.904	1.250	0.520	1.173	1.400	2.07	0.539	0.115	0.135	15.045	0.42	1.35	0.508	0.656
0.8000	0.656	0.887	3.909	1.719	1.180	0.568	1.205	1.400	2.10	0.531	0.109	0.142	14.791	0.42	1.34	0.504	0.660
0.8500	0.624	0.874	3.736	1.569	1.125	0.608	1.229	1.400	2.13	0.524	0.104	0.148	14.625	0.42	1.34	0.504	0.661
0.9000	0.591	0.861	3.585	1.454	1.087	0.637	1.245	1.400	2.17	0.516	0.099	0.155	14.534	0.42	1.34	0.504	0.661
0.9500	0.559	0.847	3.452	1.377	1.077	0.646	1.250	1.400	2.20	0.508	0.093	0.161	14.512	0.42	1.34	0.504	0.661
1.0000	0.528	0.833	3.334	1.336	1.094	0.632	1.243	1.400	2.24	0.499	0.088	0.166	14.552	0.42	1.34	0.504	0.662
1.0500	0.498	0.819	3.228	1.314	1.127	0.606	1.228	1.400	2.28	0.491	0.083	0.172	14.649	0.41	1.34	0.503	0.663
1.1000	0.468	0.805	3.135	1.299	1.165	0.576	1.211	1.400	2.32	0.483	0.078	0.177	14.800	0.41	1.34	0.501	0.665
1.1500	0.440	0.791	3.050	1.283	1.207	0.545	1.193	1.400	2.36	0.474	0.073	0.182	15.002	0.41	1.33	0.499	0.667
1.2000	0.412	0.776	2.974	1.280	1.249	0.513	1.174	1.400	2.40	0.465	0.069	0.186	15.253	0.40	1.33	0.497	0.670
1.2500	0.386	0.762	2.906	1.272	1.291	0.483	1.155	1.400	2.44	0.457	0.064	0.191	15.552	0.40	1.32	0.494	0.674
1.3000	0.361	0.747	2.844	1.265	1.334	0.453	1.136	1.400	2.48	0.448	0.060	0.195	15.898	0.39	1.32	0.491	0.679
1.3500	0.337	0.733	2.787	1.257	1.377	0.425	1.117	1.400	2.53	0.439	0.056	0.199	16.291	0.39	1.31	0.487	0.684
1.4000	0.314	0.718	2.735	1.254	1.420	0.398	1.097	1.400	2.57	0.431	0.052	0.203	16.730	0.38	1.30	0.483	0.689
1.4500	0.293	0.704	2.688	1.249	1.463	0.372	1.079	1.400	2.62	0.422	0.049	0.206	17.217	0.37	1.29	0.478	0.695
1.5000	0.272	0.690	2.645	1.244	1.505	0.348	1.060	1.400	2.66	0.413	0.045	0.210	17.751	0.36	1.29	0.473	0.702
1.5500	0.253	0.675	2.605	1.240	1.548	0.325	1.041	1.400	2.71	0.405	0.042	0.213	18.334	0.35	1.28	0.468	0.709
1.6000	0.235	0.661	2.568	1.236	1.590	0.303	1.023	1.400	2.76	0.396	0.039	0.216	18.967	0.34	1.27	0.462	0.716
1.6500	0.218	0.647	2.534	1.232	1.632	0.282	1.005	1.400	2.81	0.388	0.036	0.219	19.650	0.33	1.26	0.456	0.724
1.7000	0.203	0.634	2.503	1.229	1.674	0.263	0.987	1.400	2.86	0.380	0.034	0.221	20.386	0.32	1.25	0.450	0.733
1.7500	0.188	0.620	2.474	1.226	1.716	0.245	0.969	1.400	2.91	0.372	0.031	0.224	21.176	0.31	1.24	0.444	0.742
1.8000	0.174	0.607	2.447	1.223	1.757	0.228	0.952	1.400	2.96	0.364	0.029	0.227	22.022	0.29	1.23	0.437	0.751
1.8500	0.161	0.594	2.422	1.220	1.799	0.212	0.935	1.400	3.01	0.356	0.027	0.229	22.926	0.28	1.21	0.430	0.760
1.9000	0.149	0.581	2.399	1.218	1.843	0.197	0.918	1.400	3.06	0.348	0.025	0.231	23.890	0.27	1.20	0.423	0.770
1.9500	0.138	0.568	2.377	1.215	1.883	0.183	0.902	1.400	3.11	0.340	0.023	0.233	24.917	0.25	1.19	0.414	0.783
2.0000	0.128	0.556	2.356	1.213	1.921	0.170	0.886	1.400	3.16	0.333	0.021	0.235	26.008	0.24	1.18	0.406	0.791
2.0500	0.118	0.543	2.337	1.211	1.961	0.158	0.870	1.400	3.22	0.326	0.020	0.237	27.169	0.22	1.16	0.398	0.802

ratio T_m/T_{os}. The gamma value of the mixture is given in column nine which would vary if two different species were being used.

Column thirteen gives the area ratio A_p/A_s required to match the inlet pressures and column fourteen gives the value of A/A_p^*. The last four columns give the two efficiencies, total pressure, and the entropy increase. The efficiency based on availability, labeled ERAVL, is plotted on Figure 2.

The Fabri conditions cannot be directly applied to the solution given in Table 1 since the geometry changes at each point. However, if we select designs (i.e., fix the geometry) from those presented in Table 1 we can then apply the inlet criteria to determine the ejector operating point for each of the selected designs. We have marked four such selections in Table 1 at values of $M_s \le 1$.

Each of these four selections was used to generate an operating characteristic. These solutions, for the supersonic branch, are presented in Tables 2, 3, 4, and 5. The occurrence of the design points is indicated in each of the tables. These tables are basically different from Table 1 since they are for an ejector of given geometry which is presented at the top of each table. The columns referring to the primary conditions and to area ratios have been removed and replaced by the mass flow ratio of primary to secondary flow which is labeled M.P/M.S (the reciprocal of the bypass ratio).

Following the procedures that we developed in reference 7 for applying the Fabri and Siestrunck inlet conditions (the equations are given in Appendix A) we constructed the graphs presented in Figure 6 for each of the four designs. Figure 6 presents the total pressure ratio required to operate at the indicated value of M_s. Thus, the intersection of each of the curves with the pressure ratio of six gives the value of M_s at which the particular ejector would operate. Only the design labeled "4" operates at the chosen design value of M_s which was $M_s = 1$. One can prove (see Appendix B) that the inlet conditions always allow for operation at $M_s = 1$ and $P_{1p} = P_{1s}$.

13

TABLE 2

CASE 1

CONSTANT GEOMETRY
CONSTANT AREA SUPERSONIC
PRIMARY VAPOR AIR SECONDARY GAS AIR
PR= 6 000 TR= 3 700 GP=1 400 GS=1 400 WR= 1 00 WP= 29 00 WS= 29 00
A/AP*= 19 653 AP/AP*= 1 580 AP/AS= 0 087
MP= 1 92 TIP/TOP=0 576 PIP/POS=0 145

ME	PIS	TIS	VP/VS	VM/VS	MM	PM/	TM/	GM	MS/MP	EFPOS	POM/	EFAVL	ER
0 0500	VIOLATION OF 2ND LAW REQUIRES NEGATIVE TEMPERATURES												
0 1000	VIOLATION OF 2ND LAW REQUIRES NEGATIVE TEMPERATURES												
0 1500	VIOLATION OF 2ND LAW REQUIRES NEGATIVE TEMPERATURES												
0 2000	VIOLATION OF 2ND LAW REQUIRES NEGATIVE TEMPERATURES												
0 2500	VIOLATION OF 2ND LAW REQUIRES NEGATIVE TEMPERATURES												
0 3000	VIOLATION OF 2ND LAW FOR ADIABATIC SYSTEMS REQUIRES WORK INPUT AND COOLING												
0 3500	VIOLATION OF 2ND LAW FOR ADIABATIC SYSTEMS REQUIRES WORK INPUT AND COOLING												
0 4000	VIOLATION OF 2ND LAW FOR ADIABATIC SYSTEMS REQUIRES WORK INPUT AND COOLING												
0 4500	0 870	0 962	6 351	4 543	2 335	0 169	0 737	1 400	3 999	1 06	2 230	0 986	0 152
0 5000	0 843	0 952	5 792	3 750	2 000	0 224	0 832	1 400	4 324	0 80	1 751	0 719	0 352
0 5500	0 814	0 943	5 244	3 152	1 761	0 280	0 914	1 400	4 617	0 63	1 516	0 611	0 442
0 6000	0 784	0 933	4 835	2 687	1 578	0 338	0 974	1 400	4 876	0 52	1 389	0 541	0 521
0 6500	0 753	0 922	4 489	2 318	1 430	0 397	1 024	1 400	5 102	0 45	1 317	0 496	0 550
0 7000	0 721	0 911	4 194	2 017	1 305	0 457	1 066	1 400	5 294	0 41	1 276	0 468	0 563
0 7500	0 689	0 899	3 941	1 760	1 190	0 523	1 105	1 400	5 454	0 39	1 254	0 452	0 565
0 8000	0 656	0 887	3 720	1 500	1 051	0 618	1 155	1 400	5 581	0 38	1 243	0 445	0 562
0 8500	IMAGINARY SOLUTION												
0 9000	IMAGINARY SOLUTION												
0 9500	IMAGINARY SOLUTION												
1 0000	IMAGINARY SOLUTION												
1 0500	IMAGINARY SOLUTION												
1 1000	IMAGINARY SOLUTION												
1 1500	IMAGINARY SOLUTION												
1 2000	IMAGINARY SOLUTION												
1 2500	IMAGINARY SOLUTION												
1 3000	0 361	0 747	2 493	1 046	1 100	0 574	1 143	1 400	5 434	0 35	1 226	0 431	0 589
1 3500	0 337	0 733	2 424	1 066	1 162	0 530	1 124	1 400	5 320	0 34	1 223	0 428	0 603
1 4000	0 314	0 718	2 361	1 076	1 212	0 495	1 110	1 400	5 197	0 33	1 219	0 425	0 618
1 4500	0 293	0 704	2 303	1 083	1 257	0 464	1 098	1 400	5 065	0 32	1 214	0 422	0 635
1 5000	0 272	0 690	2 249	1 087	1 298	0 437	1 089	1 400	4 926	0 31	1 209	0 419	0 654
1 5500	0 253	0 675	2 200	1 091	1 337	0 413	1 080	1 400	4 782	0 30	1 204	0 415	0 674
1 6000	0 235	0 661	2 153	1 094	1 374	0 390	1 074	1 400	4 634	0 28	1 198	0 412	0 695
1 6500	0 218	0 647	2 110	1 097	1 409	0 369	1 068	1 400	4 484	0 27	1 191	0 409	0 718
1 7000	0 203	0 634	2 070	1 100	1 443	0 350	1 064	1 400	4 332	0 25	1 184	0 406	0 743
1 7500	0 189	0 620	2 033	1 102	1 475	0 332	1 060	1 400	4 179	0 24	1 176	0 403	0 769
1 8000	0 174	0 607	1 998	1 104	1 506	0 315	1 058	1 400	4 026	0 23	1 167	0 400	0 796
1 8500	0 161	0 594	1 966	1 107	1 535	0 300	1 056	1 400	3 875	0 21	1 158	0 397	0 824
1 9000	0 149	0 581	1 935	1 109	1 562	0 285	1 056	1 400	3 725	0 19	1 148	0 394	0 854
1 9500	0 138	0 568	1 907	1 111	1 589	0 272	1 057	1 400	3 578	0 18	1 137	0 392	0 885
2 0000	0 128	0 556	1 880	1 113	1 614	0 260	1 058	1 400	3 433	0 16	1 126	0 390	0 917
2 0500	0 118	0 543	1 854	1 116	1 637	0 248	1 061	1 400	3 292	0 14	1 114	0 388	0 951

TABLE 3

CASE 2

CONSTANT GEOMETRY
CONSTANT AREA SUPERSONIC
PRIMARY VAPOR AIR   SECONDARY GAS AIR
PR= 6.000 TR= 3.700 GP=1.400 GS=1.400 WR= 1.00 WP=29.00 WS=39.00
A/AP*= 15.399 AP/AP*= 1.745 AP/AS= 0.128
MP= 2.04 TIP/TOP=0.546 PIP/POS=0.120

MS	PIS	TIS	VP/VS	VM/VS	MM	PM/	TM/	GM	MS/MP	EFPOS	POM/	EFAVL	SR
0.0500	VIOLATION OF 2ND LAW REQUIRES NEGATIVE TEMPERATURES												
0.1000	VIOLATION OF 2ND LAW REQUIRES NEGATIVE TEMPERATURES												
0.1500	VIOLATION OF 2ND LAW REQUIRES NEGATIVE TEMPERATURES												
0.2000	VIOLATION OF 2ND LAW REQUIRES NEGATIVE TEMPERATURES												
0.2500	VIOLATION OF 2ND LAW REQUIRES NEGATIVE TEMPERATURES												
0.3000	VIOLATION OF 2ND LAW FOR ADIABATIC SYSTEMS REQUIRES WORK INPUT AND COOLING												
0.3500	VIOLATION OF 2ND LAW FOR ADIABATIC SYSTEMS REQUIRES WORK INPUT AND COOLING												
0.4000	VIOLATION OF 2ND LAW FOR ADIABATIC SYSTEMS REQUIRES WORK INPUT AND COOLING												
0.4500	0.870	0.961	6.571	4.669	2.271	0.188	0.823	1.400	3.022	0.94	2.250	0.823	0.294
0.5000	0.843	0.952	5.941	3.873	1.972	0.243	0.918	1.400	3.267	0.74	1.621	0.703	0.463
0.5500	0.814	0.943	5.428	3.270	1.754	0.299	0.993	1.400	3.488	0.61	1.608	0.629	0.558
0.6000	0.784	0.933	5.002	2.802	1.585	0.355	1.049	1.400	3.684	0.52	1.475	0.572	0.609
0.6500	0.753	0.922	4.644	2.431	1.449	0.411	1.094	1.400	3.855	0.47	1.403	0.537	0.635
0.7000	0.721	0.911	4.339	2.130	1.336	0.467	1.135	1.400	(4.000)	0.44	1.360	0.515	0.646
0.7500	0.689	0.899	4.077	1.881	1.237	0.525	1.169	1.400	4.120	0.42	1.336	0.502	0.648
0.8000	0.656	0.887	3.849	1.666	1.144	0.586	1.203	1.400	4.216	0.41	1.323	0.494	0.646
0.8500	0.624	0.874	3.649	1.429	1.015	0.684	1.253	1.400	4.289	0.41	1.317	0.491	0.641
0.9000	IMAGINARY SOLUTION												
0.9500	IMAGINARY SOLUTION												
1.0000	IMAGINARY SOLUTION												
1.0500	IMAGINARY SOLUTION												
1.1000	IMAGINARY SOLUTION												
1.1500	IMAGINARY SOLUTION												
1.2000	0.412	0.776	2.742	1.109	1.053	0.650	1.249	1.400	4.248	0.40	1.311	0.487	0.651
1.2500	0.386	0.762	2.657	1.133	1.122	0.597	1.215	1.400	4.182	0.39	1.310	0.486	0.660
1.3000	0.361	0.747	2.579	1.142	1.172	0.559	1.199	1.400	4.105	0.39	1.308	0.485	0.672
1.3500	0.337	0.733	2.508	1.147	1.217	0.527	1.187	1.400	4.019	0.38	1.306	0.484	0.684
1.4000	0.314	0.718	2.443	1.150	1.258	0.499	1.176	1.400	3.926	0.37	1.303	0.483	0.699
1.4500	0.293	0.704	2.383	1.152	1.297	0.471	1.167	1.400	3.826	0.37	1.300	0.482	0.715
1.5000	0.272	0.690	2.327	1.153	1.334	0.447	1.159	1.400	3.722	0.36	1.297	0.481	0.733
1.5500	0.253	0.675	2.276	1.155	1.370	0.424	1.153	1.400	3.613	0.35	1.293	0.480	0.751
1.6000	0.235	0.661	2.228	1.156	1.405	0.402	1.147	1.400	3.501	0.34	1.289	0.479	0.772
1.6500	0.218	0.647	2.183	1.158	1.438	0.382	1.143	1.400	3.387	0.33	1.284	0.478	0.793
1.7000	0.203	0.634	2.142	1.159	1.469	0.364	1.140	1.400	3.272	0.32	1.278	0.476	0.815
1.7500	0.188	0.620	2.103	1.161	1.500	0.347	1.138	1.400	3.157	0.31	1.272	0.476	0.841
1.8000	0.174	0.607	2.067	1.163	1.529	0.330	1.136	1.400	3.042	0.30	1.265	0.475	0.866
1.8500	0.161	0.594	2.034	1.165	1.557	0.315	1.135	1.400	2.928	0.28	1.258	0.474	0.892
1.9000	0.149	0.581	2.002	1.167	1.584	0.301	1.137	1.400	2.815	0.27	1.250	0.474	0.920
1.9500	0.138	0.568	1.973	1.169	1.610	0.288	1.139	1.400	2.703	0.26	1.241	0.473	0.948
2.0000	0.128	0.555	1.945	1.171	1.634	0.275	1.141	1.400	2.594	0.25	1.232	0.473	0.977
2.0500	0.118	0.543	1.918	1.173	1.658	0.264	1.145	1.400	2.487	0.23	1.222	0.473	1.007

TABLE 4

CASE 3

CONSTANT GEOMETRY
CONSTANT AREA SUPERSONIC
PRIMARY VAPOR AIR SECONDARY GAS AIR
PR= 6.000 TR= 3.700 CP=1.400 CS=1.400 WR= 1.00 WP= 29.00 WS= 29.00
A/AP*= 14.534 AP/AP*= 1.953 AP/AS= 0.155
MP= 2.17 TIP/TOP=0.515 PIP/POS=0.098

MS	PIS	TIS	VP/VS	VM/VS	MM	PM/	TM/	GM	MS/MP	EFPOS	POM/	EFAVL	GR
0.0500	VIOLATION OF 2ND LAW REQUIRES NEGATIVE TEMPERATURES												
0.1000	VIOLATION OF 2ND LAW REQUIRES NEGATIVE TEMPERATURES												
0.1500	VIOLATION OF 2ND LAW REQUIRES NEGATIVE TEMPERATURES												
0.2000	VIOLATION OF 2ND LAW REQUIRES NEGATIVE TEMPERATURES												
0.2500	VIOLATION OF 2ND LAW REQUIRES NEGATIVE TEMPERATURES												
0.3000	VIOLATION OF 2ND LAW FOR ADIABATIC SYSTEMS REQUIRES WORK INPUT AND COOLING												
0.3500	VIOLATION OF 2ND LAW FOR ADIABATIC SYSTEMS REQUIRES WORK INPUT AND COOLING												
0.4000	VIOLATION OF 2ND LAW FOR ADIABATIC SYSTEMS REQUIRES WORK INPUT AND COOLING												
0.4500	0.870	0.941	6.790	4.754	2.296	0.187	0.634	1.400	2.784	0.94	2.324	0.827	0.305
0.5000	0.843	0.952	6.139	3.953	2.001	0.240	0.929	1.400	3.010	0.75	1.881	0.714	0.475
0.5500	0.814	0.943	5.609	3.347	1.786	0.293	1.002	1.400	3.214	0.62	1.650	0.639	0.571
0.6000	0.784	0.933	5.169	2.877	1.621	0.346	1.058	1.400	3.395	0.54	1.519	0.588	0.624
0.6500	0.753	0.922	4.799	2.506	1.489	0.399	1.104	1.400	3.552	0.49	1.441	0.554	0.652
0.7000	0.721	0.911	4.484	2.208	1.381	0.450	1.141	1.400	3.686	0.45	1.395	0.532	0.665
0.7500	0.689	0.899	4.213	1.966	1.291	0.500	1.172	1.400	3.797	0.43	1.367	0.518	0.669
0.8000	0.656	0.887	3.977	1.765	1.214	0.547	1.199	1.400	3.885	0.42	1.352	0.510	0.668
0.8500	0.624	0.874	3.770	1.598	1.148	0.592	1.223	1.400	3.952	0.42	1.344	0.506	0.665
0.9000	0.591	0.861	3.588	1.457	1.090	0.635	1.244	1.400	(3.998)	0.42	1.340	0.504	0.661
0.9500	0.559	0.847	3.426	1.334	1.037	0.677	1.265	1.400	4.025	0.42	1.339	0.503	0.659
1.0000	IMAGINARY SOLUTION												
1.0500	0.498	0.819	3.152	1.224	1.033	0.680	1.267	1.400	4.025	0.42	1.338	0.503	0.659
1.1000	0.468	0.805	3.035	1.221	1.078	0.644	1.249	1.400	4.002	0.42	1.339	0.503	0.662
1.1500	0.440	0.791	2.929	1.216	1.119	0.612	1.235	1.400	3.964	0.41	1.339	0.503	0.667
1.2000	0.412	0.776	2.833	1.211	1.159	0.582	1.221	1.400	3.914	0.41	1.339	0.503	0.674
1.2500	0.386	0.762	2.745	1.208	1.198	0.553	1.209	1.400	3.853	0.41	1.338	0.503	0.682
1.3000	0.361	0.747	2.665	1.205	1.237	0.526	1.198	1.400	3.783	0.40	1.338	0.503	0.693
1.3500	0.337	0.733	2.592	1.202	1.275	0.500	1.188	1.400	3.704	0.40	1.337	0.503	0.704
1.4000	0.314	0.718	2.524	1.200	1.312	0.475	1.179	1.400	3.618	0.39	1.337	0.503	0.718
1.4500	0.293	0.704	2.462	1.199	1.348	0.451	1.171	1.400	3.526	0.39	1.335	0.502	0.733
1.5000	0.272	0.690	2.405	1.198	1.383	0.429	1.164	1.400	3.429	0.38	1.334	0.502	0.749
1.5500	0.253	0.675	2.351	1.197	1.417	0.408	1.158	1.400	3.329	0.37	1.331	0.502	0.766
1.6000	0.235	0.661	2.302	1.197	1.451	0.389	1.153	1.400	3.226	0.36	1.329	0.502	0.785
1.6500	0.218	0.647	2.256	1.198	1.483	0.370	1.150	1.400	3.121	0.36	1.326	0.502	0.805
1.7000	0.203	0.634	2.213	1.199	1.514	0.353	1.147	1.400	3.015	0.35	1.322	0.502	0.827
1.7500	0.188	0.620	2.174	1.199	1.545	0.336	1.144	1.400	2.909	0.34	1.318	0.502	0.849
1.8000	0.174	0.607	2.136	1.200	1.574	0.321	1.143	1.400	2.803	0.33	1.313	0.502	0.873
1.8500	0.161	0.594	2.101	1.202	1.603	0.306	1.143	1.400	2.698	0.32	1.307	0.502	0.897
1.9000	0.149	0.581	2.069	1.204	1.630	0.293	1.144	1.400	2.593	0.31	1.301	0.503	0.922
1.9500	0.138	0.568	2.038	1.206	1.656	0.280	1.145	1.400	2.491	0.30	1.295	0.503	0.948
2.0000	0.128	0.556	2.009	1.208	1.681	0.268	1.148	1.400	2.390	0.29	1.288	0.504	0.975
2.0500	0.118	0.543	1.982	1.211	1.706	0.257	1.151	1.400	2.292	0.28	1.280	0.505	1.003

16

TABLE 5

CASE 4

CONSTANT GEOMETRY
CONSTANT AREA, SUPERSONIC
PRIMARY VAPOR AIR   SECONDARY GAS AIR
PR= 6.000 TR= 3.700 GP=1.400 GS=1.400 WR= 1.00 WP= 29.00 WS= 29.00
A/AP*= 14.552   AP/AP*= 2.078   AP/AS= 0.167
MP= 2.24 TIP/TOP=0.499 PIP/POS=0.088

| MS	PIS	TIS	VP/VS	VM/VS	MM	PM/	TM/	GM	MS/MP	EFPOS	POM/	EFAVL	SR
0.0500	VIOLATION OF 2ND LAW: REQUIRES NEGATIVE TEMPERATURES											
0.1000	VIOLATION OF 2ND LAW: REQUIRES NEGATIVE TEMPERATURES											
0.1500	VIOLATION OF 2ND LAW: REQUIRES NEGATIVE TEMPERATURES											
0.2000	VIOLATION OF 2ND LAW: REQUIRES NEGATIVE TEMPERATURES											
0.2500	VIOLATION OF 2ND LAW: REQUIRES NEGATIVE TEMPERATURES											
0.3000	VIOLATION OF 2ND LAW FOR ADIABATIC SYSTEMS: REQUIRES WORK INPUT AND COOLING											
0.3500	VIOLATION OF 2ND LAW FOR ADIABATIC SYSTEMS: REQUIRES WORK INPUT AND COOLING											
0.4000	VIOLATION OF 2ND LAW FOR ADIABATIC SYSTEMS: REQUIRES WORK INPUT AND COOLING											
0.4500	0.870	0.961	6.900	4.786	2.322	0.183	0.827	1.400	2.761	0.95	2.364	0.935	0.292
0.5000	0.843	0.952	6.238	3.983	2.024	0.235	0.922	1.400	2.985	0.76	1.905	0.721	0.467
0.5500	0.814	0.943	5.700	3.374	1.907	0.287	0.995	1.400	3.187	0.63	1.666	0.644	0.566
0.6000	0.784	0.933	5.253	2.905	1.642	0.338	1.052	1.400	3.366	0.55	1.530	0.593	0.621
0.6500	0.753	0.922	4.877	2.534	1.510	0.389	1.097	1.400	3.522	0.49	1.449	0.558	0.651
0.7000	0.721	0.911	4.557	2.237	1.404	0.438	1.133	1.400	3.654	0.46	1.401	0.535	0.665
0.7500	0.689	0.899	4.281	1.997	1.316	0.484	1.164	1.400	3.764	0.43	1.372	0.521	0.670
0.8000	0.656	0.887	4.041	1.800	1.243	0.528	1.189	1.400	3.852	0.42	1.355	0.512	0.670
0.8500	0.624	0.874	3.831	1.639	1.184	0.567	1.210	1.400	3.918	0.42	1.346	0.507	0.668
0.9000	0.591	0.861	3.644	1.509	1.137	0.600	1.227	1.400	3.964	0.42	1.342	0.505	0.665
0.9500	0.559	0.847	3.481	1.408	1.106	0.623	1.238	1.400	3.991	0.42	1.340	0.504	0.663
1.0000	0.528	0.833	3.335	1.337	1.095	0.631	1.242	1.400	(3.999)	0.42	1.339	0.504	0.662
1.0500	0.498	0.819	3.203	1.294	1.105	0.624	1.239	1.400	3.991	0.42	1.340	0.504	0.663
1.1000	0.469	0.805	3.084	1.268	1.129	0.606	1.230	1.400	3.968	0.42	1.340	0.504	0.665
1.1500	0.440	0.791	2.977	1.252	1.160	0.583	1.220	1.400	3.931	0.41	1.341	0.504	0.670
1.2000	0.412	0.776	2.879	1.241	1.194	0.558	1.209	1.400	3.881	0.41	1.341	0.504	0.676
1.2500	0.386	0.762	2.790	1.233	1.229	0.533	1.198	1.400	3.821	0.41	1.342	0.505	0.685
1.3000	0.361	0.747	2.709	1.227	1.265	0.508	1.188	1.400	3.750	0.40	1.342	0.505	0.694
1.3500	0.337	0.733	2.634	1.222	1.301	0.484	1.179	1.400	3.672	0.40	1.342	0.505	0.706
1.4000	0.314	0.718	2.565	1.219	1.337	0.461	1.170	1.400	3.587	0.40	1.342	0.505	0.718
1.4500	0.293	0.704	2.502	1.216	1.372	0.438	1.163	1.400	3.496	0.39	1.341	0.506	0.733
1.5000	0.272	0.690	2.444	1.214	1.407	0.417	1.156	1.400	3.400	0.38	1.340	0.506	0.748
1.5500	0.253	0.675	2.390	1.213	1.441	0.397	1.150	1.400	3.301	0.38	1.339	0.506	0.765
1.6000	0.235	0.661	2.339	1.212	1.474	0.378	1.145	1.400	3.199	0.37	1.337	0.506	0.784
1.6500	0.213	0.647	2.293	1.212	1.506	0.360	1.141	1.400	3.095	0.36	1.335	0.506	0.803
1.7000	0.203	0.634	2.249	1.213	1.538	0.343	1.138	1.400	2.990	0.35	1.332	0.507	0.824
1.7500	0.188	0.620	2.209	1.213	1.569	0.327	1.136	1.400	2.884	0.35	1.329	0.507	0.845
1.8000	0.174	0.607	2.171	1.214	1.598	0.312	1.135	1.400	2.779	0.34	1.325	0.508	0.868
1.8500	0.161	0.594	2.136	1.215	1.627	0.298	1.134	1.400	2.675	0.33	1.320	0.508	0.892
1.9000	0.149	0.581	2.102	1.217	1.655	0.285	1.135	1.400	2.571	0.32	1.315	0.509	0.916
1.9500	0.138	0.568	2.071	1.219	1.682	0.273	1.136	1.400	2.470	0.31	1.310	0.510	0.942
2.0000	0.128	0.556	2.042	1.222	1.707	0.261	1.138	1.400	2.370	0.30	1.303	0.511	0.967
2.0500	0.118	0.543	2.014	1.224	1.732	0.250	1.141	1.400	2.272	0.29	1.297	0.512	0.994
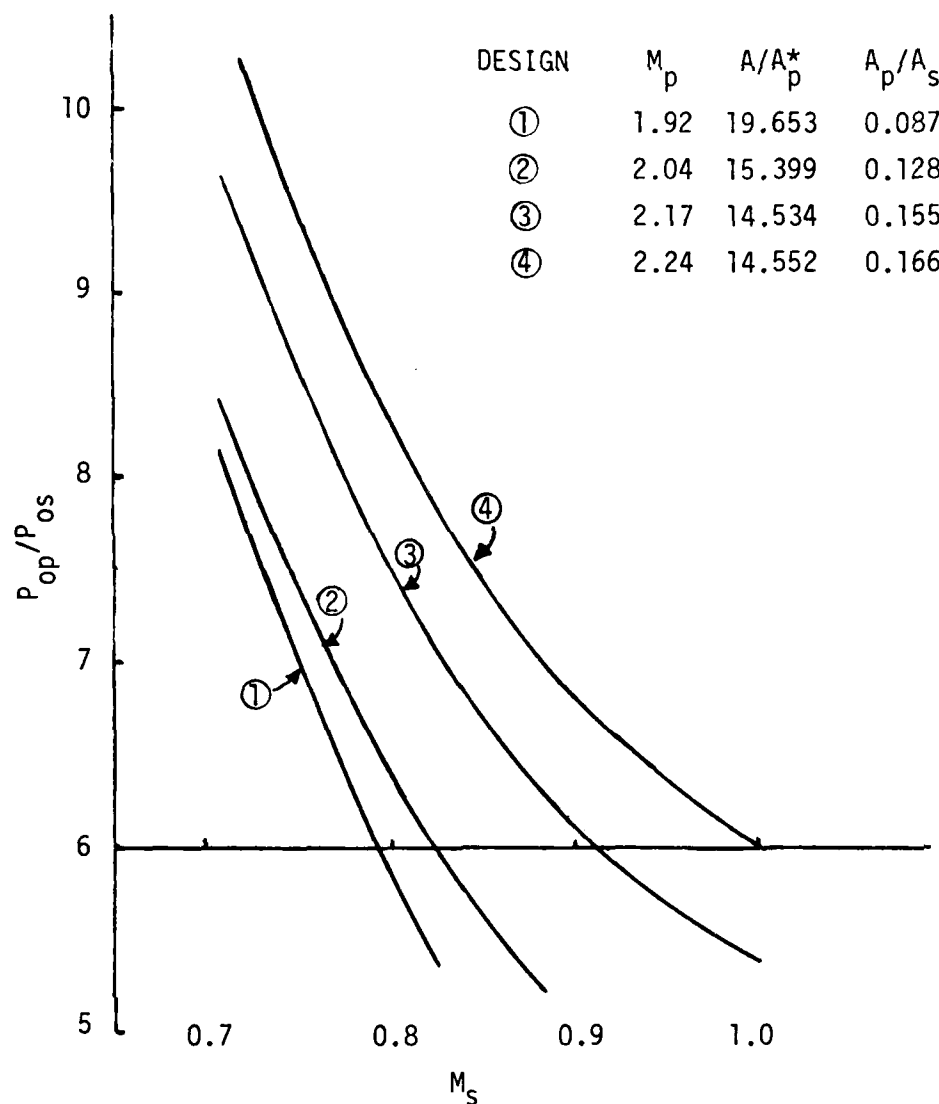
Figure 6. Total Pressure Ratio Required to Operate at the Indicated Value of M_s for Each of the Four Designs. The Intersection with the Pressure Ratio of Six Yields the Actual Operating Point at the Design Pressure Ratio.

18

We have plotted the results of our study on Figure 7 where we
show the supersonic branch solution for the bypass ratio of four
where $P_{1p} = P_{1s}$ (solid line, data from Table 1) and the four
operating characteristic curves (dashed lines with data from
Tables 2, 3, 4 and 5) with their actual operating points indicated
as determined from Figure 6. Thus, we see that an ejector cannot
operate on the supersonic solution branch when $M_s < 1$ and the mass
flow is given and $P_{1p} = P_{1s}$. Designs chosen from this branch
actually operate at efficiencies lower than the design value
and lower than the value of efficiency at $M_s = 1$.

In general, the design curves for which the bypass ratio
is given and the value of $P_{1p} = P_{1s}$ are valid in the supersonic
solution branch only for values of $M_s \geq 1$. The curves of the sub-
sonic solution branch are valid over the entire range of M_s.
As discussed in Appendix C an isolated point may exist on the
supersonic solution branch for which $P_{1p} = P_{1s}$ and $M_s < 1$. Indi-
cations are that this point occurs in the flat region (e.g.,
from $M_s = 0.8$ to 1 in Table 1) or dips below the efficiency at
$M_s = 1$. The value of efficiency at $M_s = 1$ has always been the
highest efficiency obtainable if $M_s \leq 1$ for a given mass flow.

In the rest of our studies we used the value of efficiency
at $M_s = 1$ as representative of the maximum efficiency achievable
for the given mass flow and $M_s \leq 1$.

If the value of $M_s = 1$ lies within the forbidden region,
we then used the value of M_s (less than one) found from simul-
taneous solution of Equations (1) and (2) in the studies presented
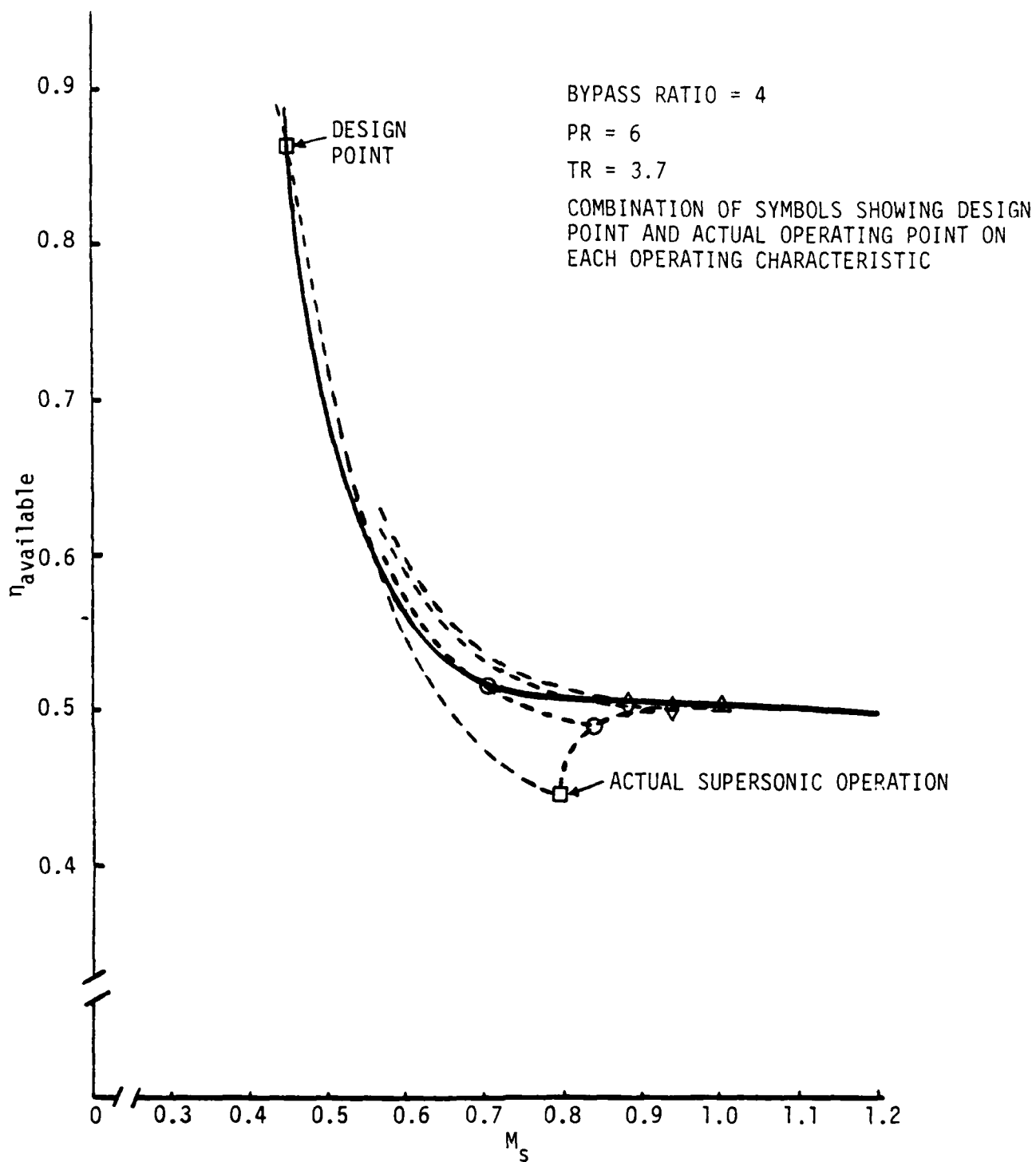in Section 5.

19

Figure 7. Results of the Study Showing the Actual Operation of the Designs at Values of $M_s \leq 1$. Note: Although the Bypass Ratio is Four at the Design Points It Would Not be Four on the Actual Operating Curve.

SECTION 4

IDEAL THRUST AUGMENTATION OF AN EJECTOR

In order to assess the potential of ejectors used for thrust augmentation we have made the following assumptions:

(1) For a given bypass ratio, the efficiency on the supersonic solution branch of an ejector at $M_s = 1$ and $P_{1p} = P_{1s}$ is representative of the maximum efficiency achievable at that bypass ratio;

(2) Inlets, nozzles, and diffusers are ideal and operate at 100 percent efficiency.

As explained in the last section, if we restrict operation of an ejector to subsonic inlet Mach numbers ($M_s \leq 1$) then the value of efficiency at $M_s = 1$ is a maximum (or very close to it) when the inlet restriction is considered (see Figures 4 and 7).

If supersonic secondary inlet Mach numbers are considered, then at low temperature ratios, higher efficiencies can be achieved at supersonic, secondary, inlet Mach numbers (e.g., see Figure 5).

These efficiencies, however, are not sufficiently higher to make a major change in the results.

The equations for thrust augmentation using ideal conditions were developed in reference 7 and are given in Appendix A. Figure 8 presents thrust augmentation for a pressure ratio of six, temperature ratio of 3.7, and four bypass ratios (0.5, 1, 2, and 4) as a function of flight Mach number M_∞. The thrust augmentation is good at high and low values of the flight Mach number, but in the range of 0.7 to 1.1 it is low or even less than one for all four bypass ratios.

Figure 9 presents similar curves for a pressure ratio of three and a temperature ratio of two. Again the thrust
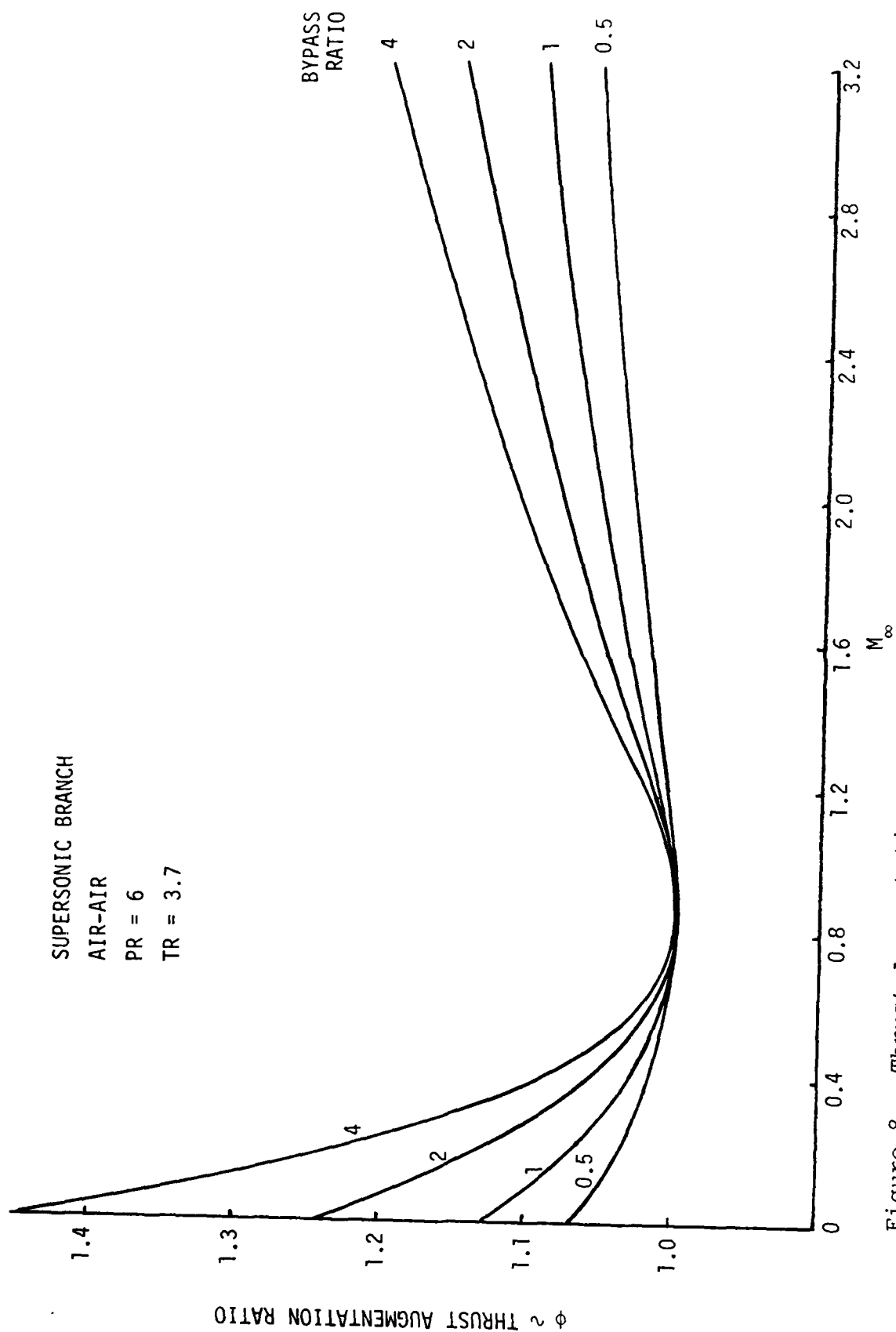
Figure 8. Thrust Augmentation as a Function of Flight Mach Number for an Ejector Operating on the Supersonic Branch at $M_s = 1$ at Various Bypass Ratios at the Indicated Conditions.
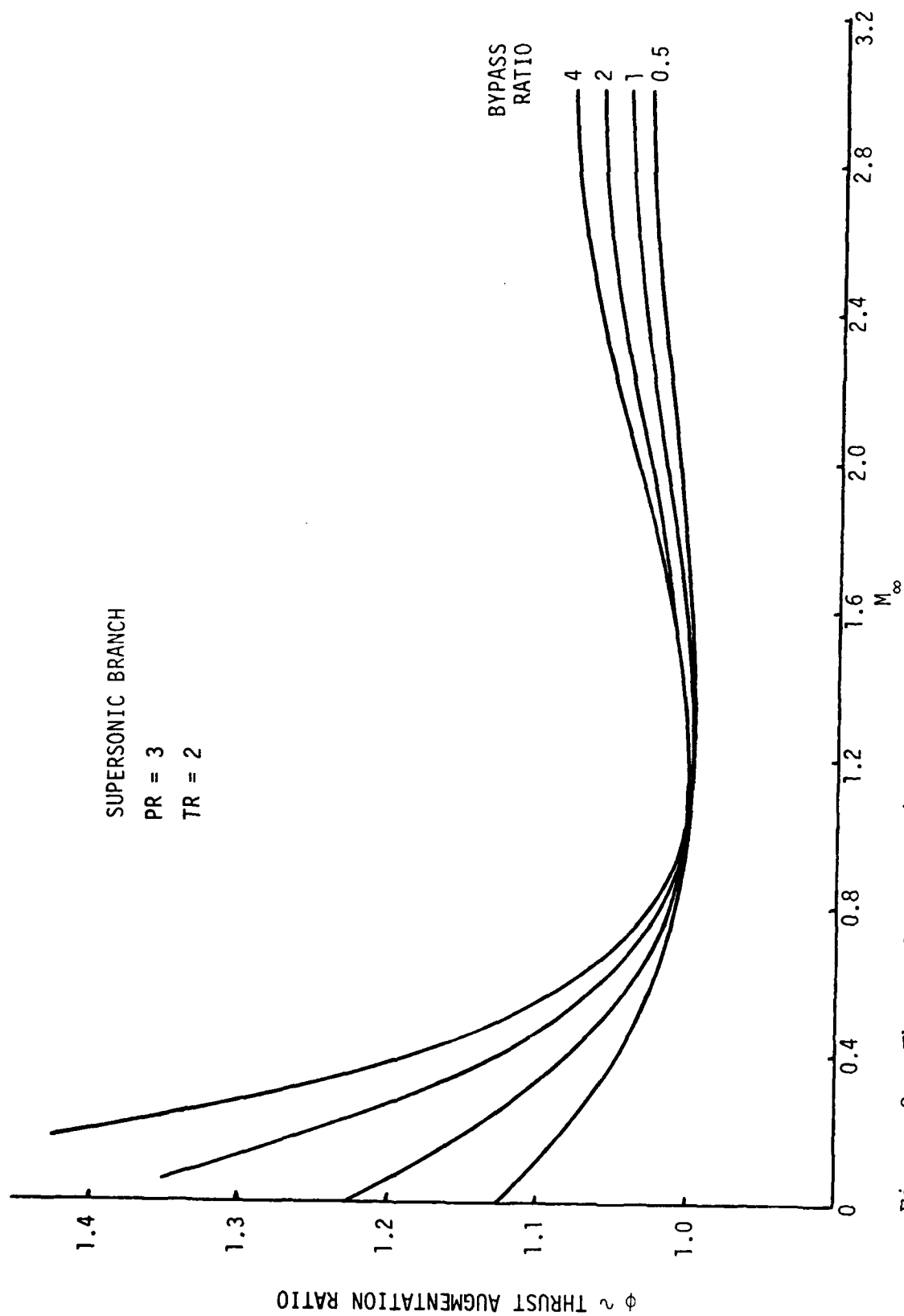
22

Figure 9. Thrust Augmentation as a Function of Flight Mach Number for an Ejector Operating on the Supersonic Branch at $M_s = 1$ at Various Bypass Ratios at the Indicated Conditions.

augmentation is good at low and high Mach numbers but poor in the range of Mach numbers from 0.9 to 1.5.

Figures 10 through 14 present the effects of temperature ratio on thrust augmentation, ϕ, for five pressure ratios: two, three, four, five, and six.

Figures 10 through 12 are for a bypass ratio of 0.5 and Figures 13 and 14 are for a bypass ratio of two. On each of the five figures the flight Mach number is the curve parameter.

Examination of the figures indicates only a weak dependence of ϕ on pressure ratio. The dependence of ϕ on temperature is reversed as we change from subsonic to supersonic flight Mach number. It also becomes obvious from these figures that the thrust augmentation in the neighborhood of Mach one is small or less than one for all pressure ratios, temperature ratios, and bypass ratios.

The low temperature end of the curves could be improved slightly by operating the ejector at supersonic values of M_s. It is doubtful, however, that this effect would raise the low-temperature-ratio end of the curves above one for supersonic flight Mach numbers, M_∞.

At supersonic flight Mach numbers the thrust augmentation is more like a ram jet effect than an ejector effect since it depends so strongly on the energy transfer due to the high temperature of the primary gas.

In the next section we will examine the thrust augmentation of an ejector when operating with a hypothetical engine.
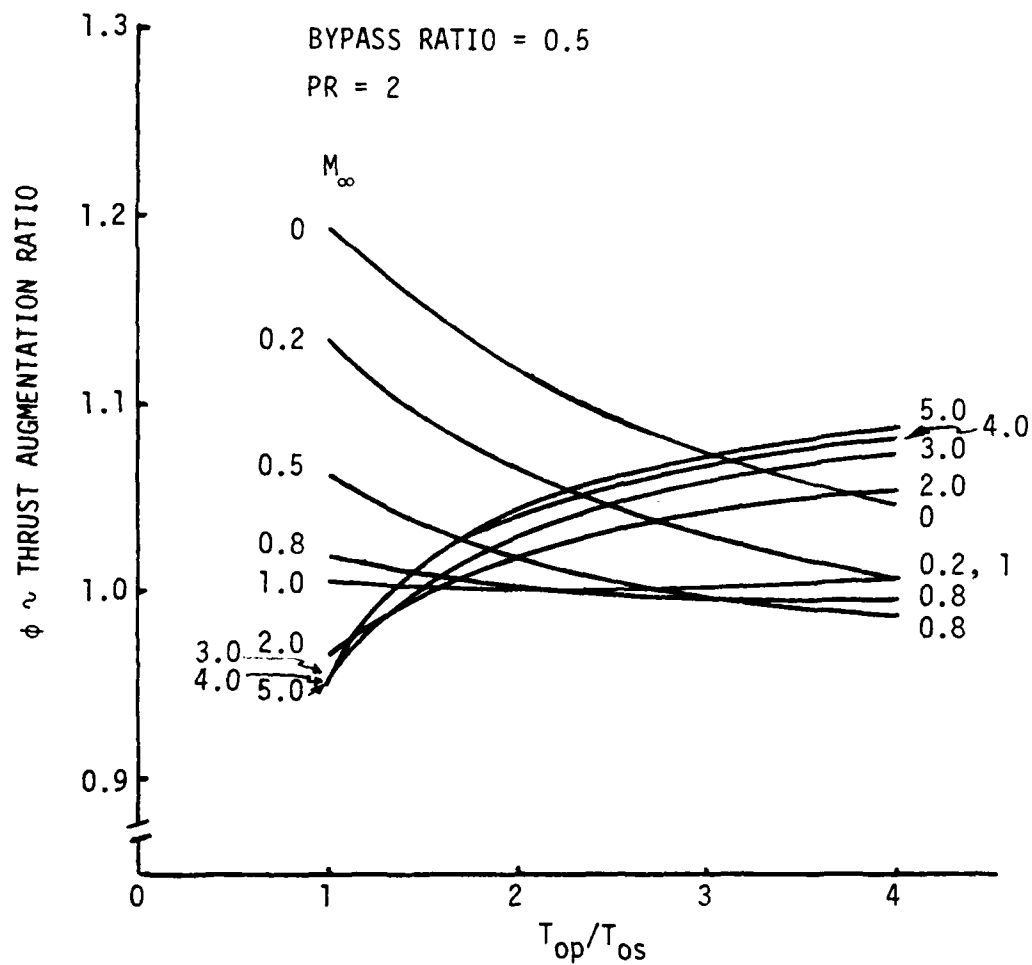
Figure 10. Effect of Temperature Ratio at a Pressure
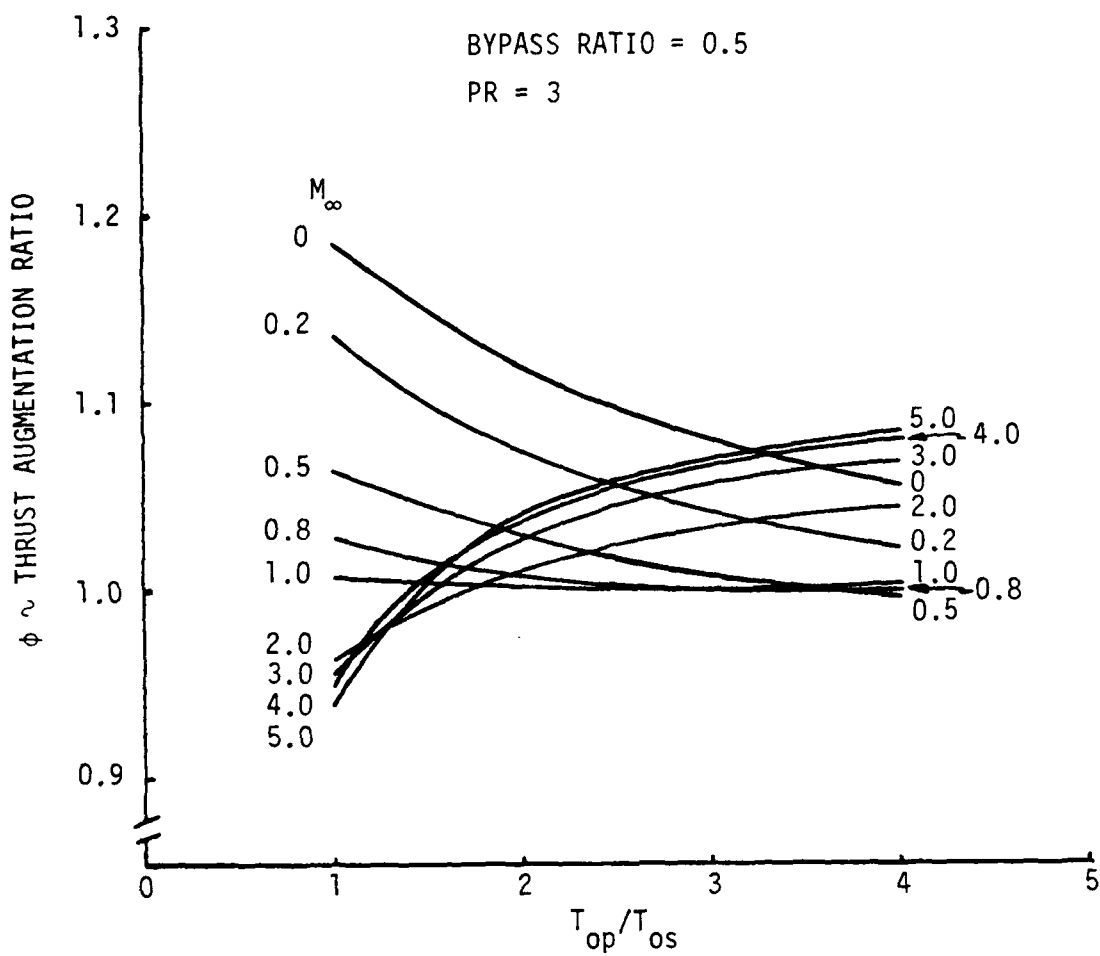Ratio of Two and a Bypass Ratio of 0.5.

25

Figure 11. Effect of Temperature Ratio at a Pressure
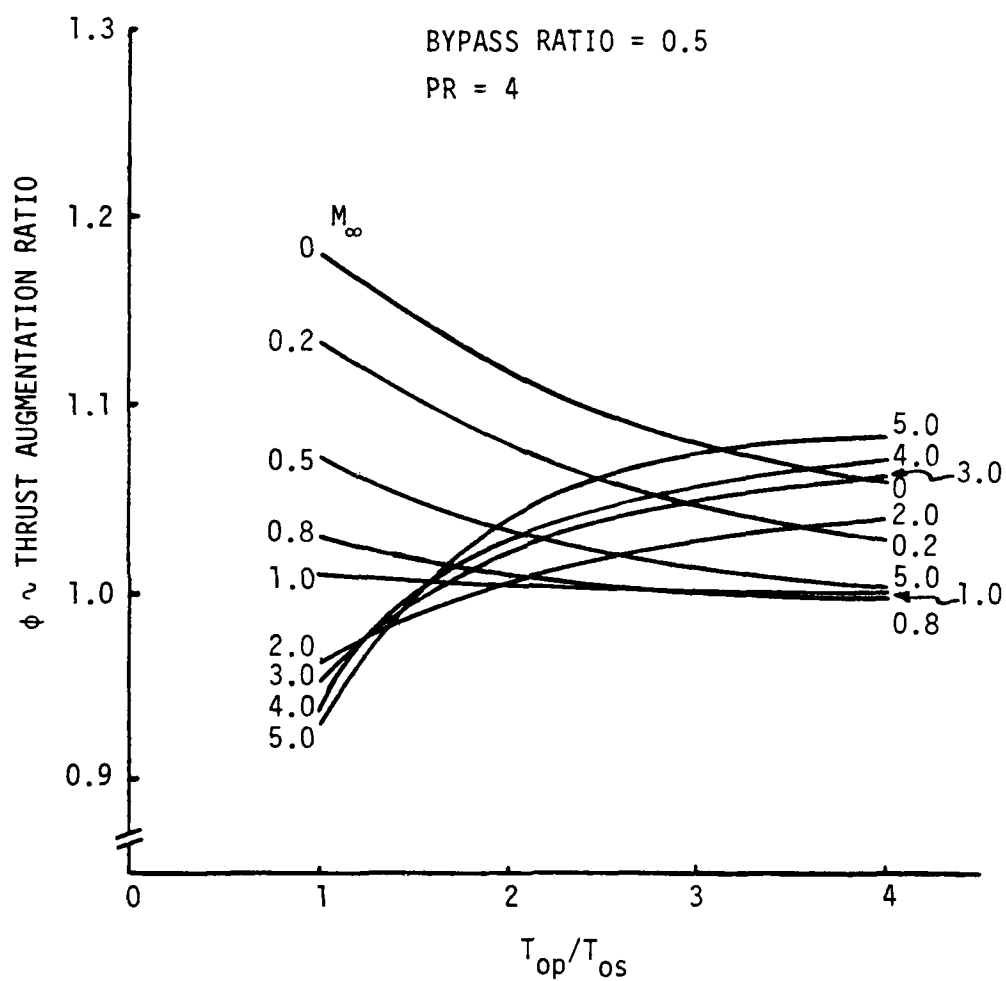Ratio of Three and a Bypass Ratio of 0.5.

Figure 12. Effect of Temperature Ratio at a Pressure
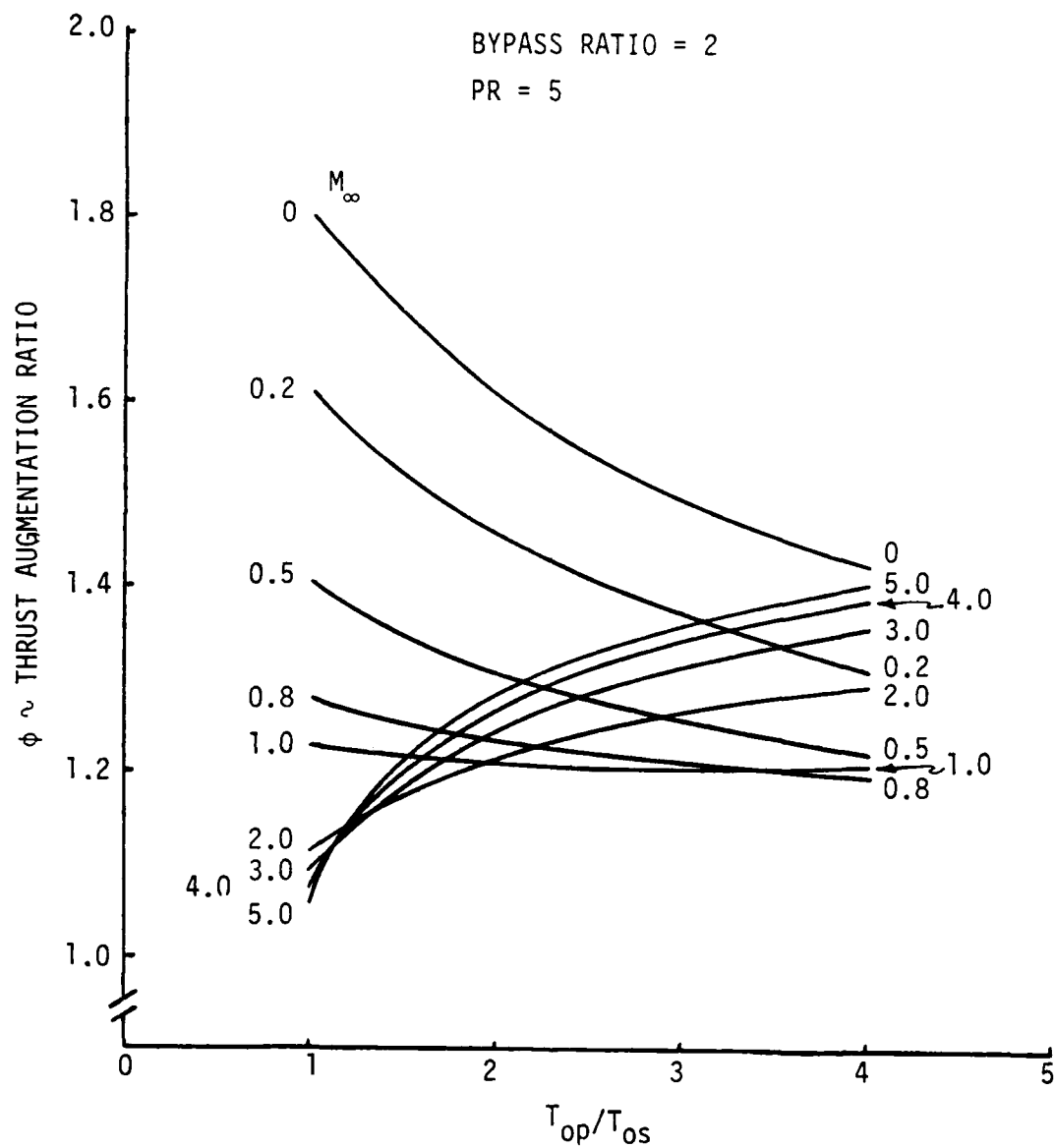Ratio of Four and a Bypass Ratio of 0.5.

Figure 13. Effect of Temperature Ratio at a Pressure Ratio of Five and Bypass Ratio of Two.
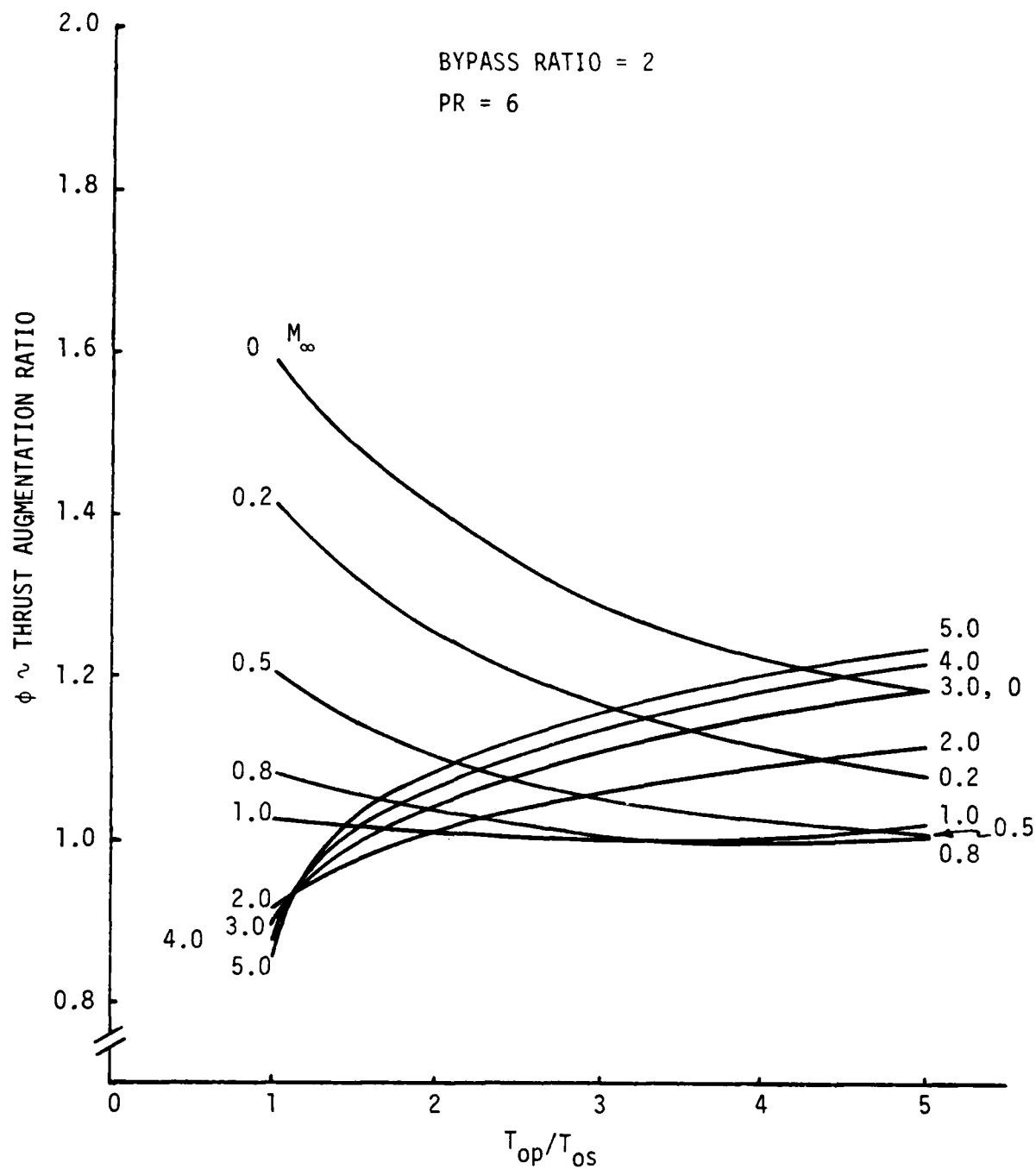
Figure 14. Effect of Temperature Ratio at a Pressure
Ratio of Six and a Bypass Ratio of Two.

SECTION 5

AN EJECTOR ENGINE COMBINATION

The performance of an ejector when coupled to a jet engine was studied for hypothetical engines over a range of flight Mach numbers and altitudes. Hypothetical engines with pressure ratios ranging from 5 to 40 were investigated for two turbine inlet temperatures: 2500°F and 3000°F. We investigated cycles with ideal processes as well as those with nonideal processes. Figure 15 shows a sketch of a T-s diagram for an engine with losses.

The process from 1 to 2 involves ram compression which is isentropic in the ideal case, or according to MIL-E-5007D as quoted in reference 9:

$$\frac{P_{02}}{P_{01}} = 1 \qquad M_\infty = 0 \text{ to } 1.0 \tag{3}$$

$$\frac{P_{02}}{P_{01}} = 1.0 - 0.076(M_\infty - 1)^{1.35} \quad M_\infty > 1.0 \text{ to } 5. \tag{4}$$

The compression process from 2 to 3 was assumed to be adiabatic with a polytropic efficiency of 1 in the ideal case, and 0.85 in the nonideal case. The rpm of the engine was assumed to vary with flight Mach number so that the pressure ratio remained constant (i.e., a constant specific speed was assumed).

In the combustor, process 3 to 4, the temperature was assumed to be raised to the maximum allowable turbine inlet temperature with no loss in total pressure in the ideal case or a 5 percent loss in total pressure in the nonideal case.

In the turbine the gas expands in process 4 and 5 and supplies the work required to drive the compressor. No account was taken for work supplied to accessories and C_p and γ were assumed constant and equal to those of air. The polytropic efficiency was set to 1 for the ideal case and to 0.85 for the nonideal case.
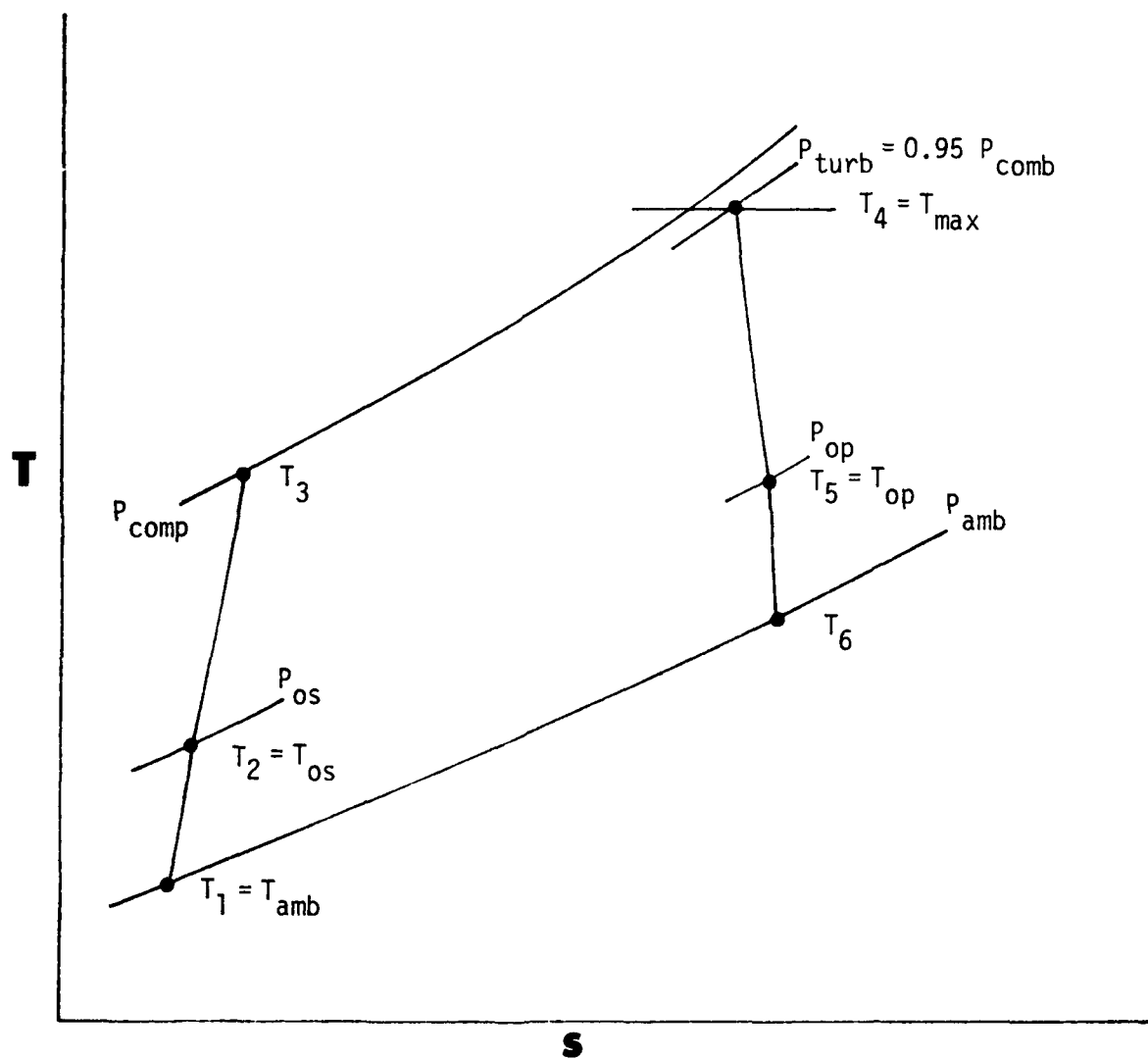
Figure 15. Sketch of T-s Diagram for a Hypothetical Engine.

31

The process from 5 to 6 represents the adiabatic expansion
to ambient pressure in the nozzle with a polytropic efficiency of
1.0 in the ideal case and 0.98 in the nonidealized case. The thrust
per unit of mass flow of the engine is calculated as a function
of the flight Mach number from the change in momentum.

Figures 16 and 17 show the primary engine thrust per unit
of mass flow at two altitudes as a function of the flight Mach
number for engines with a compressor pressure ratio, Pe, of 5 and
35, and turbine inlet temperatures, T_4, of 2500°R and 3500°R.

The low pressure ratio engine can, of course, achieve higher
Mach numbers than the high pressure ratio engine before its
thrust fall off to zero because of the high temperature limit.
At each flight Mach number the pressure ratio, PR, can be deter-
mined (PR=P_5/P_2); and the temperature ratio, TR, can be determined
(TR=T_5/T_2). The performance of an ejector for the values of PR
and TR can then be calculated at $M_s = 1$ and various bypass ratios.
If the ejector is choked, the ejector performance is calculated
on the boundary of the forbidden region for that bypass ratio.

Once the total pressure and temperature of the mixed flow
is known, the thrust per unit mass of the mixed flow can readily
be calculated assuming an adiabatic expansion to ambient pressure.
A polytropic efficiency of 1.0 was assumed in the ideal case,
and 0.98 in the nonideal case. The thrust per unit mass flow
can be determined from the momentum change and the thrust augmen-
tation, ϕ, calculated from the following equation:

$$\phi = (1 + \beta)(\tau_m/\dot{m}_m)/(\tau_p/\dot{m}_p). \tag{5}$$

The calculations were terminated when the pressure ratio, PR,
dropped below one.

In addition to thrust augmentation of an ejector, we also
calculated the performance of a mixing-fan jet engine. Using the
same polytropic efficiencies as for the engine alone, we determined
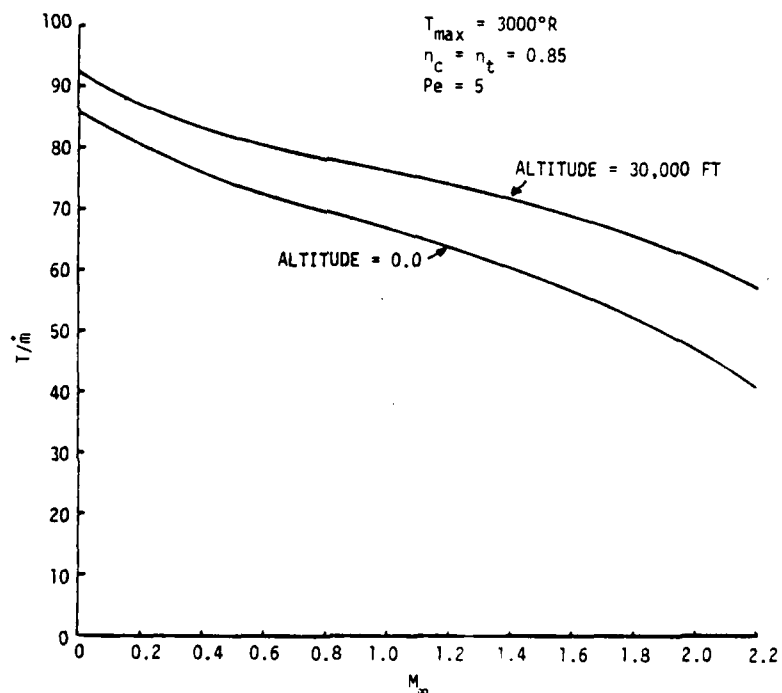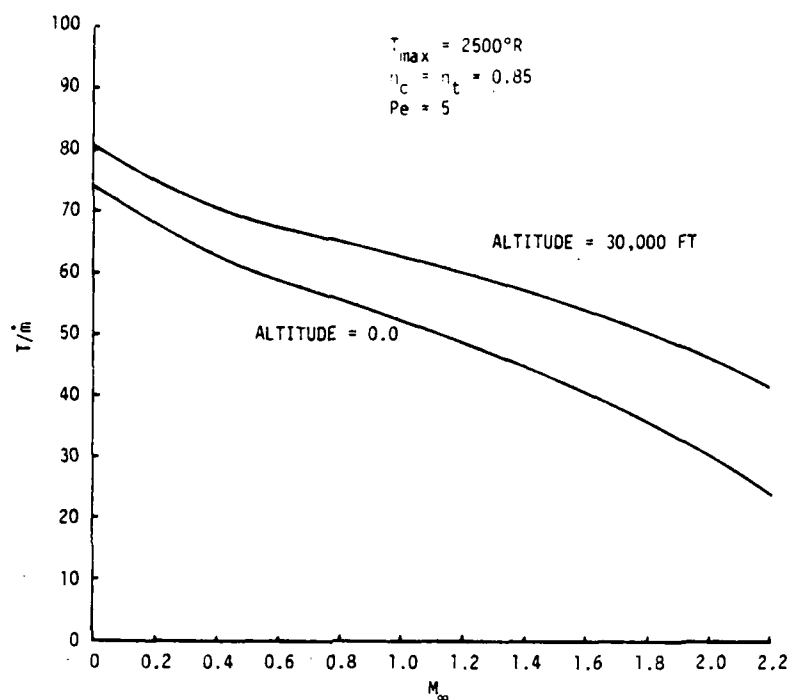a common pressure at the exits of the turbine and fan which matched

Figure 16.   Basic Engine Specific Thrust for a Compressor
Pressure Ratio of Five at a Turbine Inlet
Temperature of 2500°R (16a) and 3000°R (16b)
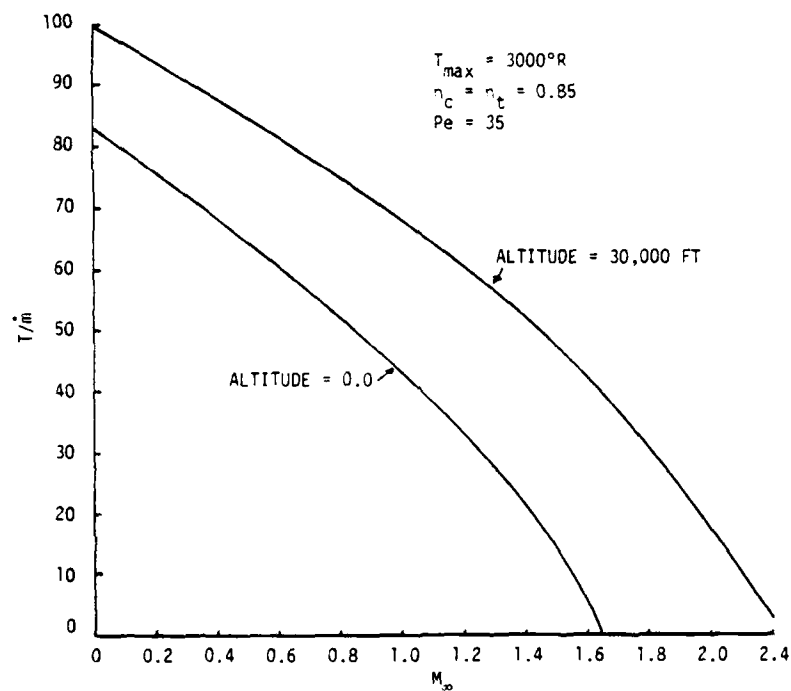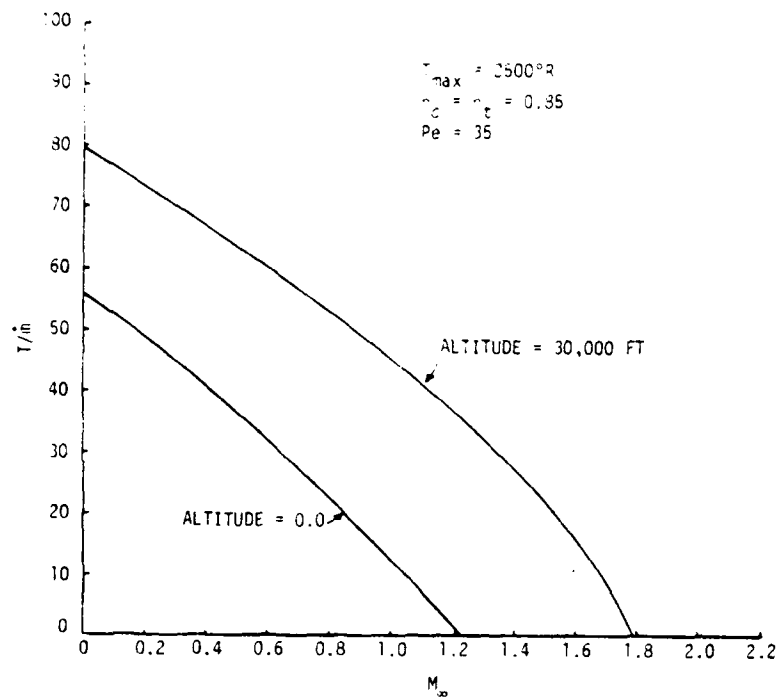at Sea Level and 30,000 feet.

Figure 17. Basic Engine Specific Thrust for a Compressor
Pressure Ratio of 35 at a Turbine Inlet
Temperature of 2500°R (17a) and 3000°R (17b)
at Sea Level and 30,000 feet.

34

the work required by the fan (at a particular bypass ratio) and the work produced by the turbine. The two flows are then mixed at this pressure at low velocity; the common pressure is then the stagnation pressure of the mixture. Since the exit temperatures from the fan and turbine are also known, the mixed total temperature can be evaluated and the final state of the mixed gas is known. Thus, the thrust per unit mass can be calculated and the thrust augmentation determined from Equation (5).

A substantial amount of data were obtained from this study and Table 6 details the various conditions used to present Figures 18 through 29. As indicated in Table 6, Figures 18 through 21 present results for the ideal case for compressor pressure ratio of 35. As with the previous study in the neighborhood of Mach one the thrust augmentation is near one or less than one for the ejector. However, for the high pressure ratio engine it remains low even in the supersonic region, although it does slightly exceed one in that region. On the other hand, the thrust augmentation for the ejector is substantial at low subsonic Mach numbers on all the figures, even after taking account for losses.

The mixing fan shows substantial thrust augmentation throughout the entire Mach number range even after reasonable component efficiencies are assumed on the later figures; Figures 22 through 29.

If we consider the low pressure ratio engine in the non-ideal case, Figures 26 through 29, we see that the ejector again shows a thrust augmentation at the supersonic Mach numbers. Again this is the result of an action more like a ram jet since it results from the energy transfer which results from the temperature difference between the primary and secondary.

Generally mass flow entrainment in ejectors would be very large (i.e., of the order of 10 or more). If one considers a mixing fan with similar flow rates being pumpted into the system, then the size of the engine will make integration with airframe a very difficult problem. On the other hand, distributing the engine air and entraining the outside air in large volumes will

not present insurmountable problems for integration. Ejectors
therefore are attractive devices from the point of view of
simplicity and integrability.

Curves such as the ones in Figures 18 to 29 must be viewed
in the light of the comments made above. Otherwise, it might
deter consideration of ejectors.

TABLE 6

THRUST AUGMENTATION DATA ARE PRESENTED FOR THE
FOLLOWING COMBINATIONS OF FIGURES 18 to 29

Figure Number	Compressor Pressure Ratio, Pe	Turbine Inlet Temperature °R	Altitude (kilofeet)	$\eta = \eta_t = \eta_c$
18	35	2500	0	1
19	35	3000	0	1
20	35	2500	30	1
21	35	3000	30	1
22	35	2500	0	0.85
23	35	3000	0	0.85
24	35	2500	30	0.85
25	35	3000	30	0.85
26	5	2500	0	0.85
27	5	3000	0	0.85
28	5	2500	30	0.85
29	5	3000	30	0.85

Figure 18. Thrust Augmentation for an Ejector Operating on the Supersonic Branch at $M_s = 1$ (or the Boundary of the Forbidden Region) and a Mixing-Fan at Various Bypass Ratios, Sea Level, Pe = 35, η = 1, 2500°R.

Figure 19. Thrust Augmentation for an Ejector Operating on the Supersonic Branch at $M_s = 1$ (or the Boundary of the Forbidden Region) and a Mixing-Fan at Various Bypass Ratios, Sea Level, Pe = 35, $\eta = 1$, 3000°R.

Figure 20. Thrust Augmentation for an Ejector Operating on the Supersonic Branch at $M_s = 1$ (or the Boundary of the Forbidden Region) and a Mixing-Fan at Various Bypass Ratios, 30,000 feet, $Pe = 35$, $\eta = 1$, 2500°R.

Figure 21. Thrust Augmentation for an Ejector Operating on the Supersonic Branch at $M_s = 1$ (or the Boundary of the Forbidden Region) and a Mixing-Fan at Various Bypass Ratios, 30,000 feet, $P_e = 35$, $\eta = 1$, 3000°R.
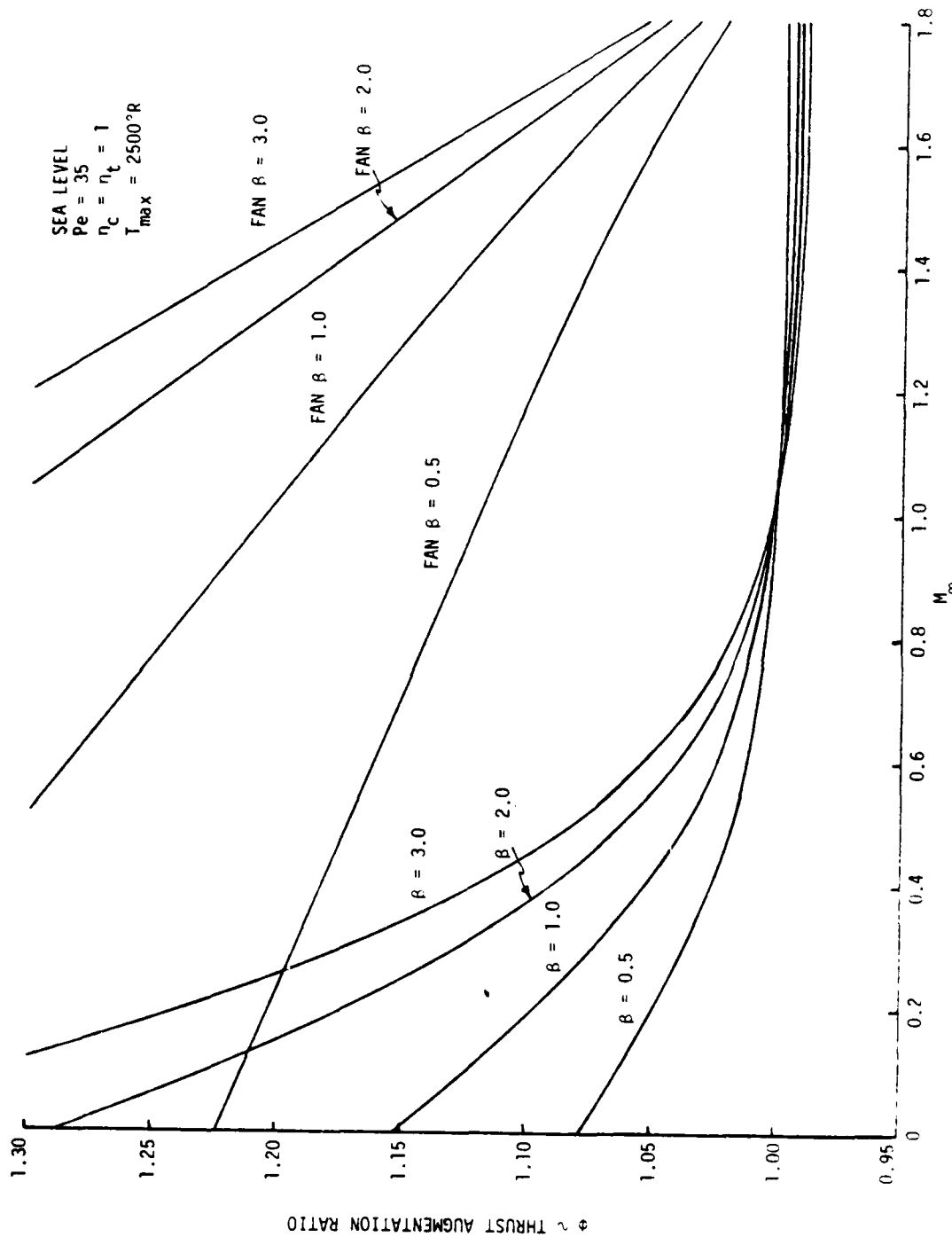
Figure 22.   Thrust Augmentation for an Ejector Operating on the Supersonic Branch at
$M_s = 1$ (or the Boundary of the Forbidden Region) and a Mixing-Fan at
Various Bypass Ratios, Sea Level, $P_e = 35$, $\eta = 0.85$, 2500°R.

Figure 23. Thrust Augmentation for an Ejector Operating on the Supersonic Branch at $M_\infty = 1$ (or the Boundary of the Forbidden Region) and a Mixing-Fan at Various Bypass Ratios, Sea Level, Pe = 35, $\eta = 0.85$, 3000°R.
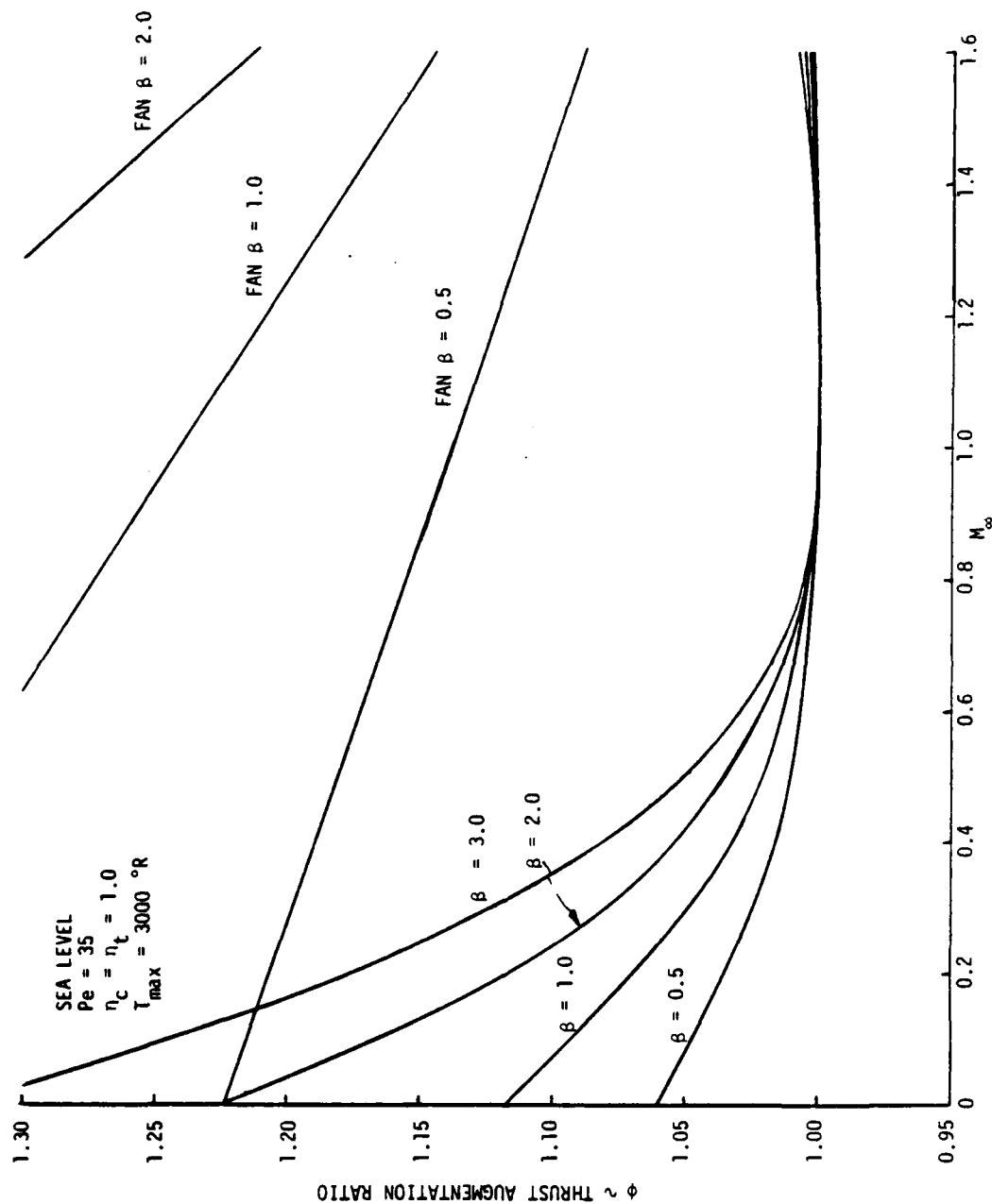
43

Figure 24. Thrust Augmentation for an Ejector Operating on the Supersonic Branch at $M_s = 1$ (or the Boundary of the Forbidden Region) and a Mixing-Fan at Various Bypass Ratios, 30,000 feet, Pe = 35, η = 0.85, 2500°R.

Figure 25. Thrust Augmentation for an Ejector Operating on the Supersonic Branch at $M_s = 1$ (or the Boundary of the Forbidden Region) and a Mixing-Fan at Various Bypass Ratios, 30,000 feet, Pe = 35, η = 0.85, 3000°R.

45
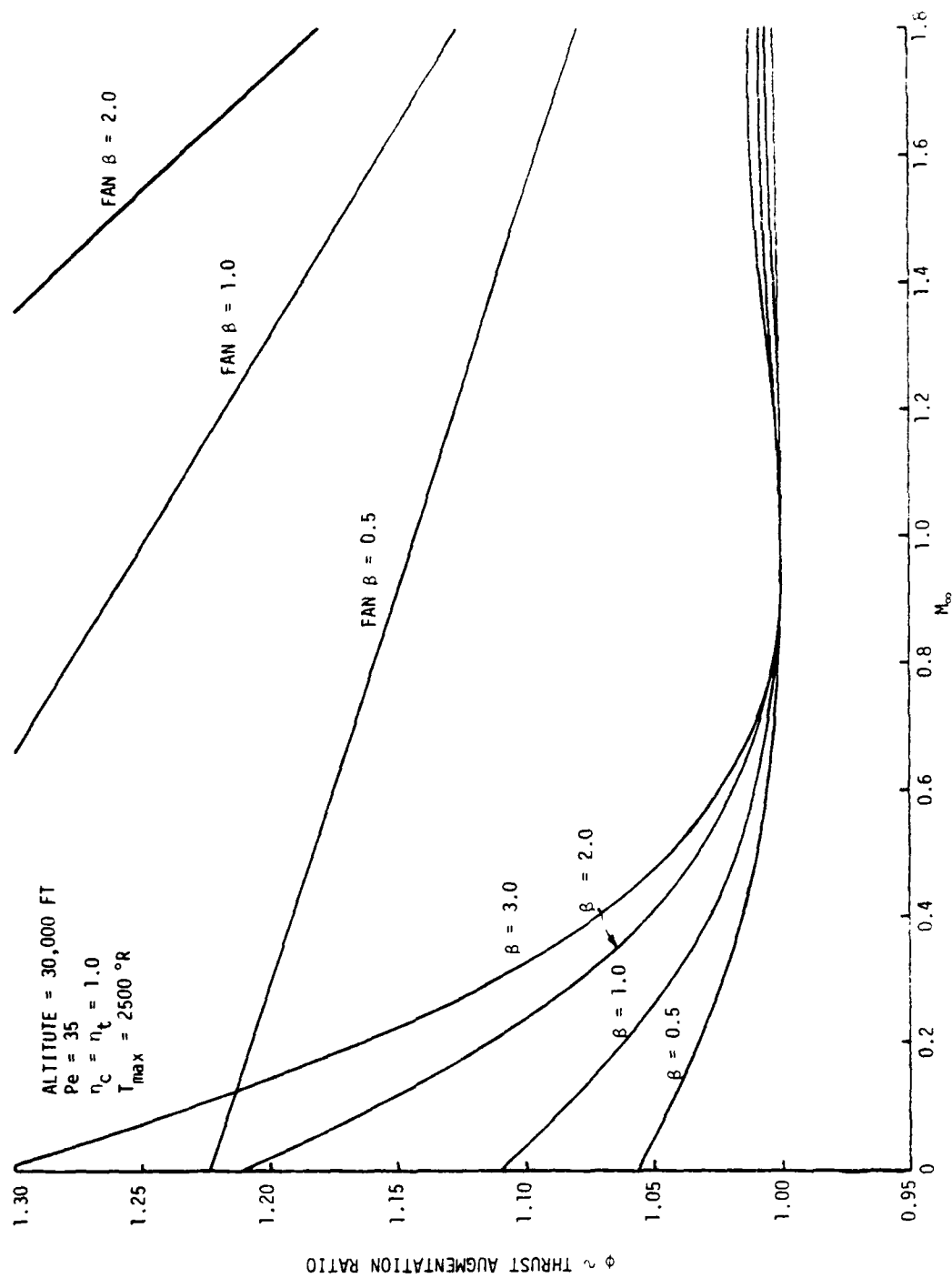
Figure 26. Thrust Augmentation for an Ejector Operating on the Supersonic Branch at $M_s = 1$ (or the Boundary of the Forbidden Region) and a Mixing-Fan at Various Bypass Ratios, Sea Level, $P_e = 5$, $\eta = 0.85$, $2500°R$.
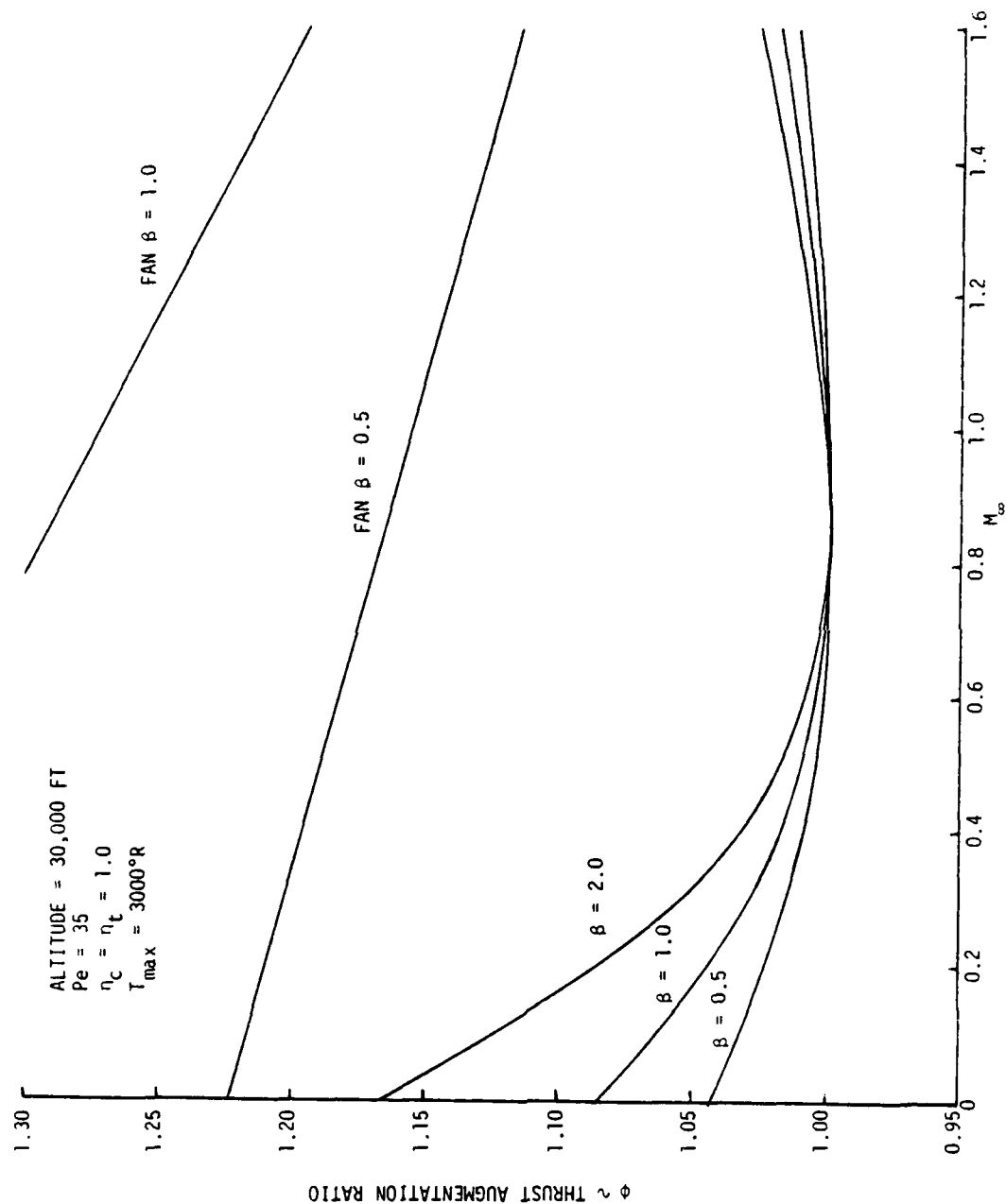
46
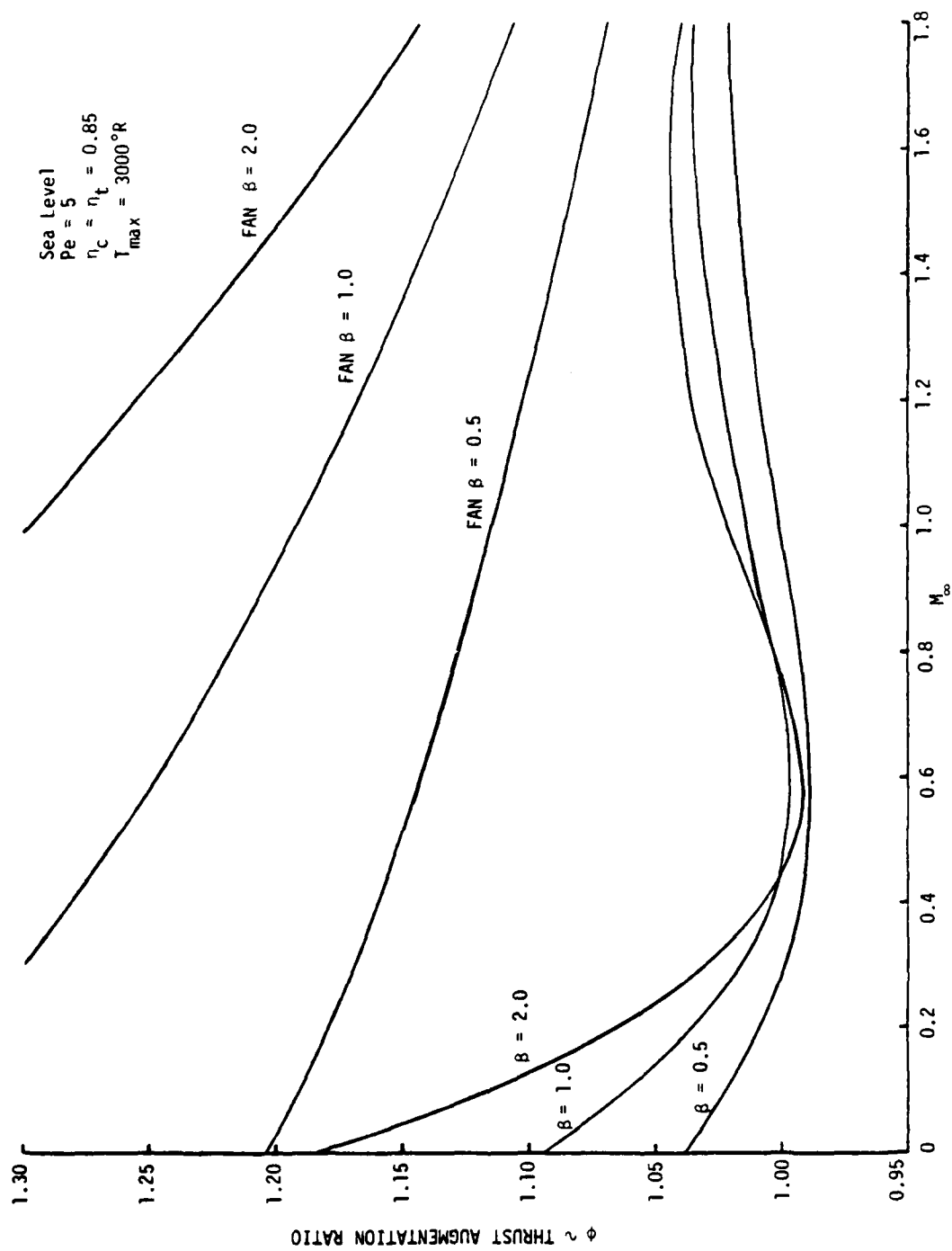
Figure 27. Thrust Augmentation for an Ejector Operating on the Supersonic Branch at $M_s = 1$ (or the Boundary of the Forbidden Region) and a Mixing-Fan at Various Bypass Ratios, Sea Level, Pe = 5, $\eta = 0.85$, 3000°R.

47
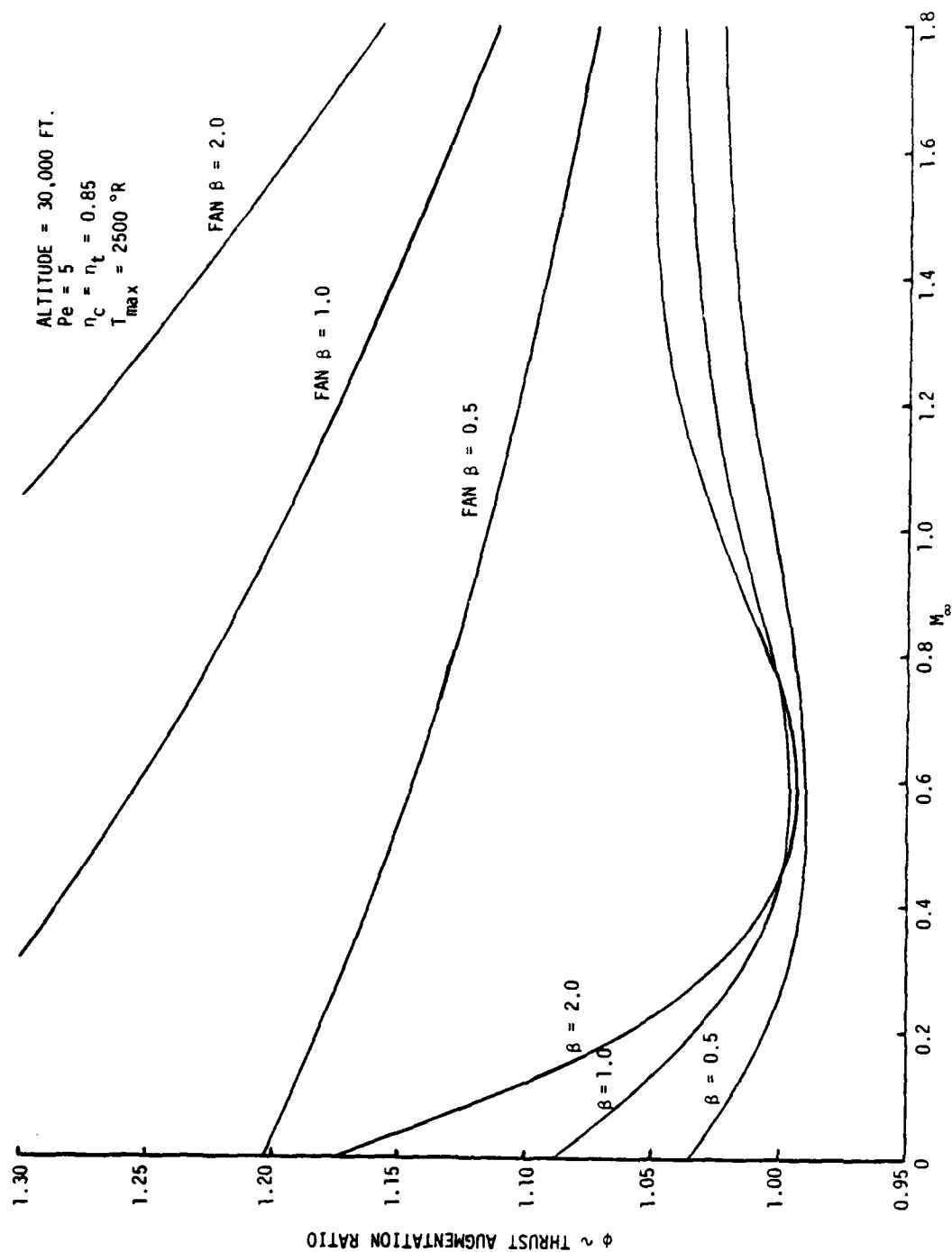
Figure 28. Thrust Augmentation for an Ejector Operating on the Supersonic Branch at $M_s = 1$ (or the Boundary of the Forbidden Region) and a Mixing-Fan at Various Bypass Ratios, 30,000 feet, Pe = 5, η = 0.85, 2500°R.

48
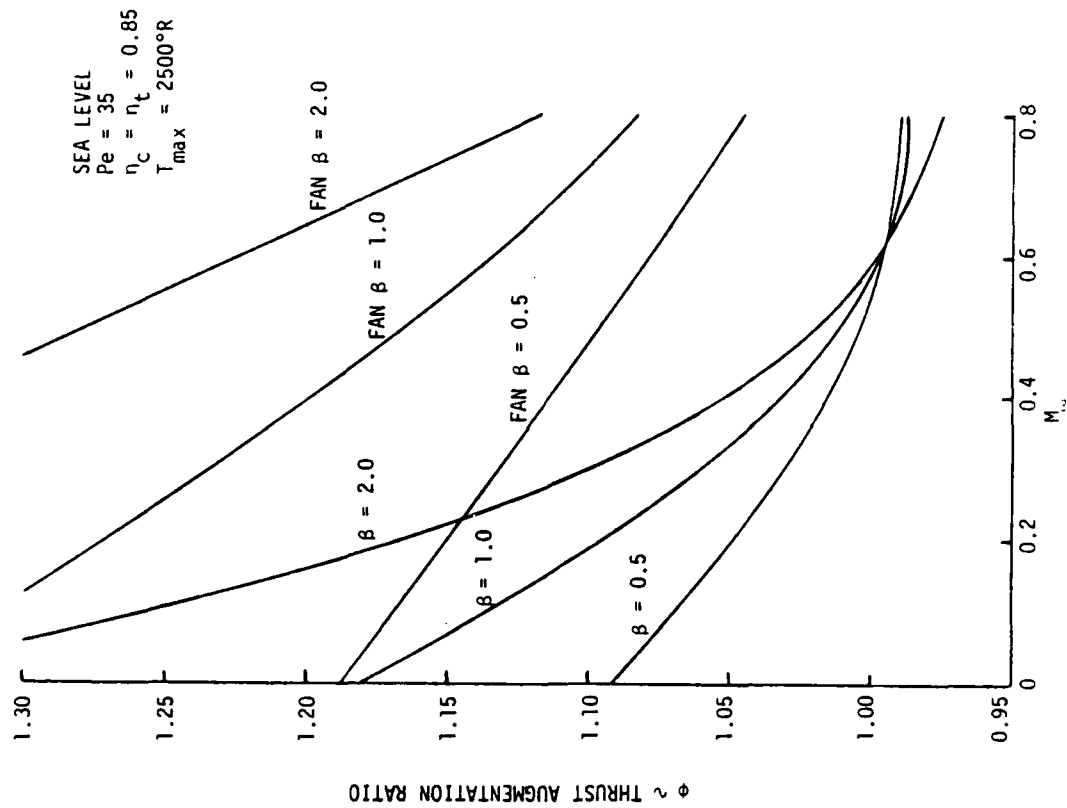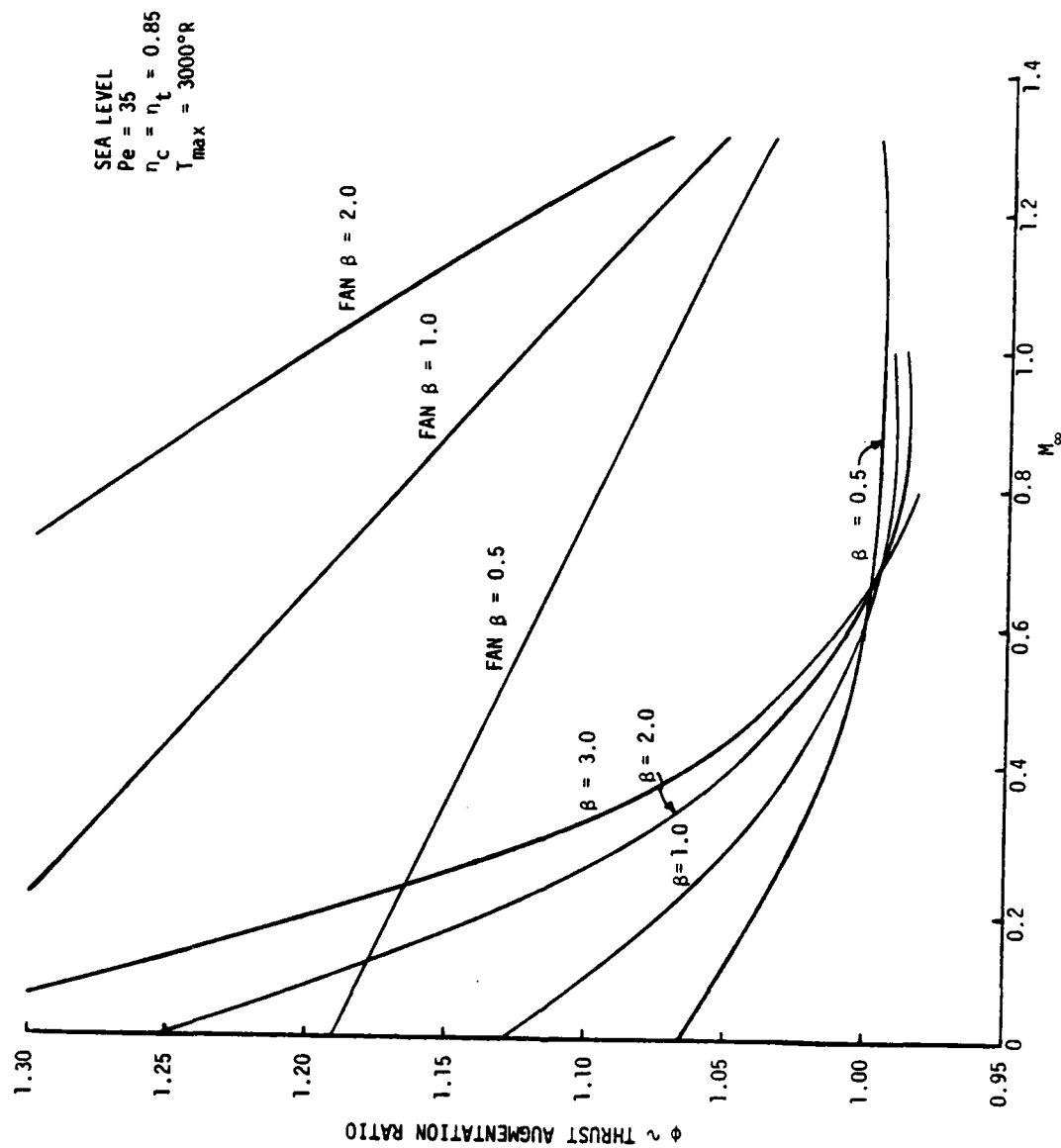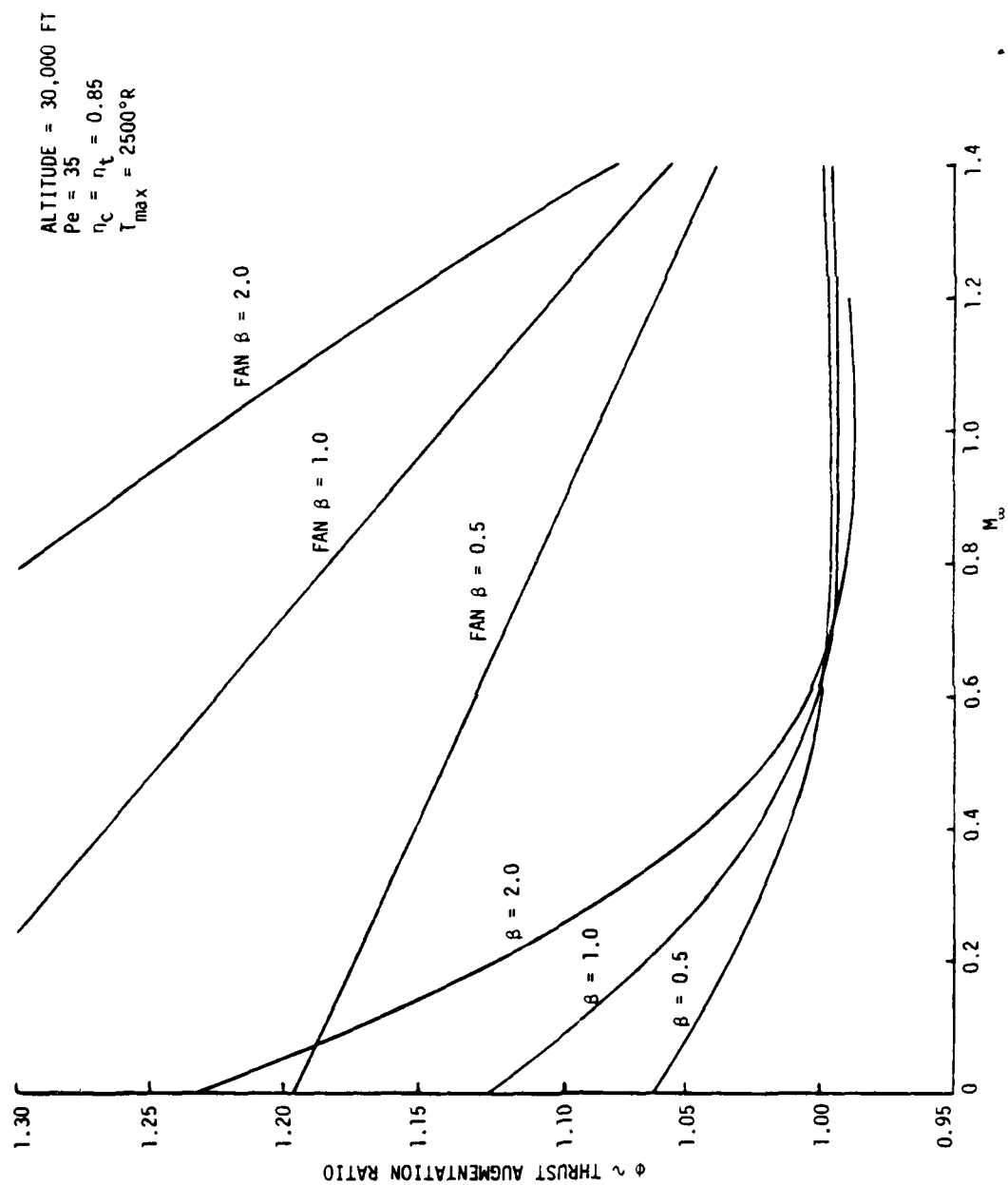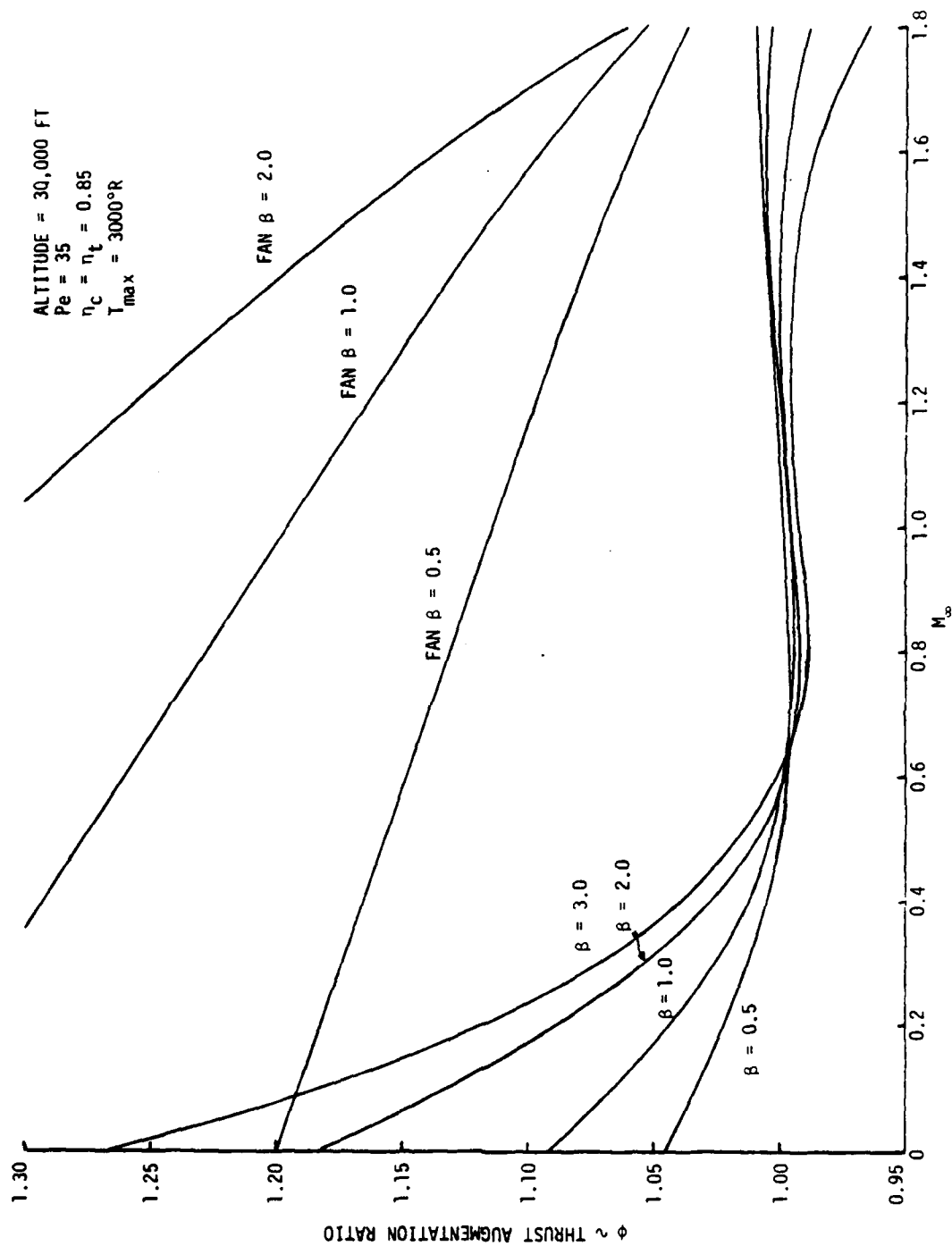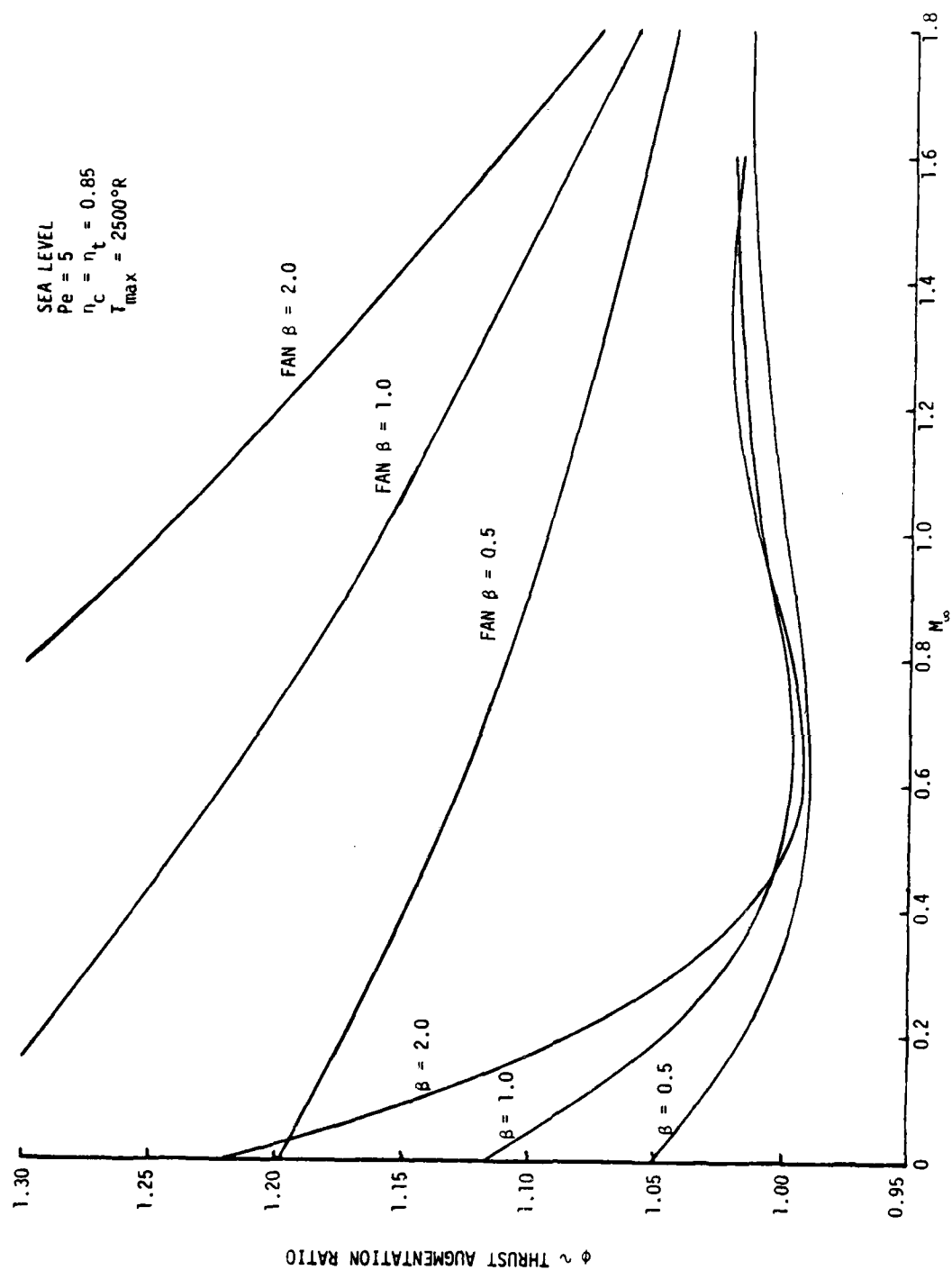
Figure 29. Thrust Augmentation for an Ejector Operating on the Supersonic Branch at $M_s = 1$ (or the Boundary of the Forbidden Region) and a Mixing-Fan at Various Bypass Ratios, 30,000 feet, $Pe = 5$, $\eta = 0.85$, 3000°R.

49

SECTION 6
CONCLUSIONS FROM THE EJECTOR STUDY

Based on the results of the studies presented in the previous sections for constant area ejectors, we have drawn the following conclusions:

(1) In general, on the supersonic branch of the design curves constructed for a given bypass ratio and T , the curves cannot be realized in an ejector of values : M (see Figure 7).

(2) In general, these curves, therefore,   for values of $M_s \geq 1$ on the supersonic solution branch   .

(3) Isolated points on the supersonic solution   be achieved at values of $M_s < 1$ but the efficiency   may not exceed the value of efficiency at $M_s = 1$ (see Appendix   for an example).

(4) The value of the efficiency at $M_s = 1$ on the supersonic branch is representative of the maximum efficiency if not the actual maximum efficiency (see Figures 4, 7, and 2).

(5) At lower temperature ratios the efficiency on the supersonic solution branch may be higher at values of $M_s > 1$ than at $M_s = 1$ (see Figure 5). However, conclusion (4) is still valid since these higher efficiencies are probably not high enough to make a significant difference in the overall conclusions.

(6) All of the thrust augmentation studies presented herein indicated little or no thrust augmentation at flight Mach numbers near one.

(7) The basic study of thrust augmentation shows a reversal of the effect of temperature at subsonic and supersonic flight Mach numbers: at subsonic flight Mach numbers, increases in temperature reduce thrust augmentation while at supersonic flight Mach numbers, increases in temperature result in increases in thrust augmentation ratio (see Figures 10 through 14).

(8) Pressure ratio has only a very small effect on thrust augmentation ratio (see Figures 10 through 12 and 13 to 14).

(9) Thrust augmentation ratios at low subsonic flight Mach numbers were substantial for all cases studied.

(10) Thrust augmentation levels at supersonic flight Mach numbers were adequate for the low pressure ratio engine cycle, but less than one for the high pressure ratio cycle.

(11) As expected, mixing-fan thrust augmentation was superior to the ejector for the same bypass ratio and flight Mach numbers (see Figures 18 through 29). This superior performance is achieved at the cost of complex rotating machinery and total weight.

(12) The thrust augmentation of the mixing-fan also fell off substantially with increasing flight Mach numbers.

Since no analytical technique was found that could determine the maximum efficiency of an ejector, it was necessary to base our results on a numerical study of an ejector. The Fabri and Siestrunck inlet condition enabled us to determine a reasonable representation of the maximum efficiency that would be obtained for a wide range of parameters. Even though we know of some cases where higher efficiencies could be achieved (low temperature ratios and $M_s > 1$) we do not believe that an actual ejector (with wall friction for example) could achieve efficiencies higher than those that we used. Thus, we believe that our results give reasonable estimates of the upper limits to performance that one can expect from an ejector over the range of parameters studied.

Conclusion (6) states that the thrust augmentation ratio of "constant area ejectors" is less than one at a flight Mach number around one. Therefore, this type of thrust augmenting ejector cannot be considered as a potential substitute for a turbo fan in a propulsion system for transonic aircraft. This raises two questions: (1) is thrust augmentation less than one near a Mach number of one an inherent characteristic of all types of thrust augmenting ejectors, and more broadly, of any type of momentum

51

exchange process not employing rotating machinery? And, (2) can ejector techniques in view of the limitation near Mach one be of any use for aircraft applications?

We feel that many useful applications of ejectors to aircraft are still possible at low flight speeds and that there are methods available to obtain thrust augmentation at Mach numbers near one. Some of the application areas are as follows:

(1) ejectors for STOL and VSTOL;

(2) boundary layer ejector systems;

(3) new approaches to momentum exchange

- co-flowing

- cross flow

- counter flow.

Thrust augmenting ejectors for VSTOL and STOL have the following advantages:

(1) high thrust augmentation capability of advanced compact ejectors at take-off and low flight speeds;

(2) feasibility of a large variety of shapes for the ejector shroud (from axisymmetrical to high aspect ratio slot configurations);

(3) resulting high performance capabilities and synergistic effects of ejector and wing

- prevention of flow separation by wing-boundary layer energization

- strong supercirculation; very high $C_{L,max}$; improved L/D

- favorable transition from "hover" to conventional flight (as flight speed increases, the vertical thrust component of the ejector decreases to a lesser degree than the aerodynamic lift increases).

In the boundary layer ejector systems the trailing edge region of the wing is configured as a very compact two-dimensional

ejector, which uses only wing boundary layer air as secondary ejector fluid medium. This results in performance characteristics and synergistic effects as follows:

(1) thrust augmentation does not drop to zero at flight Mach number around one and is extended into the supersonic flight regime;

(2) drag reduction due to restoration of the wake to free stream velocities;

(3) prevention of flow separation by boundary layer energization;

(4) improved wing characteristic (increased $C_{L,max}$ and L/D);

(5) possibility of boundary layer control by suction (if desired, the boundary layer ejector can be employed for a greatly simplified flow laminarization system).

In order to capitalize on the potential that these systems have, we recommend the following approach toward an ejector-aircraft design:

(1) Determination of major performance and design (geometry) parameters of two-dimensional ejectors under true environmental conditions, including simulated wing-boundary layer air for secondary fluid medium.

(2) Ejector-aircraft systems are major long-range projects requiring team efforts which combine expertise in ejector-engine-aircraft design.

However, before building an ejector-aircraft prototype, lessons learned from past failures of ejector-aircraft must be carefully avoided. This requires:

● a thorough comparison analysis of potential ejector wing fuselage configurations

● functional development of all critical system components and

● performance verification under true environmental conditions of these components.

In order to further our understanding of ejector processes we also recommend that studies of co-flowing ejectors be made using computational fluid dynamics (CFD). The code used by Scott and Hankey[10] to study the flow in combustors would be ideal for this purpose. Fundamental understanding of the processes could be greatly enhanced by such studies. In addition, studies of ejectors not having a constant area can also be studied with this code to determine the performance of such ejectors.

In addition to the more traditional approaches just discussed, we present some entirely new concepts in the next section. These new concepts have the potential of providing improved methods of transferring availability between fluid streams without using moving parts.

SECTION 7

NEW CONCEPTS AND RESEARCH APPROACHES IN THE FIELD OF DIRECT ENERGY TRANSFER PROCESS

Processes of transferring energy from one working medium of high energy content to one of lower energy content play a key role in aeropropulsion and other technology areas. Usually, in these processes, turbines and compressors are employed transferring the energy from one working substance to another, except in the so-called direct energy transfer processes. In these processes the energy transfer is accomplished by direct contact of the interacting media without the use of machinery.

Direct energy transfer processes have attracted a great deal of interest because of their inherent structural simplicity, low weight and cost, and high reliability; their problem, however, is to achieve high energy transfer efficiencies.

Distinction can be made between two major classes of direct energy transfer processes, namely:

- unsteady flow energy transfer processes
- steady flow energy transfer processes.

Examples for processes in which energy is transferred from one fluid medium to another one by means of unsteady flow are:

- shock tubes
- pulse jets
- dynamic pressure exchangers
- non-steady flow ejectors (non-steady flow in either primary or secondary flow or both).

Examples of steady flow direct energy transfer processes are:

- Continuous flow ejectors (for jet pumps, thrust augmentors, and other applications).

The following discussion deals with steady flow direct energy transfer processes, specifically with continuous flow

ejector-type devices for various applications in the field of thrust augmentation and pumps. Before discussing new approaches and concepts which depart from conventional ejectors, it will be most beneficial to briefly synopize the major characteristics of current ejector processes:

(a) Current ejector processes are based on momentum exchange between two mass-streams flowing in the same direction through a mixing duct (Figure 1). In the following, such processes will be referred to as "co-flowing momentum exchange processes." The momentum exchange in these processes is accomplished by mixing. The shape of the mixing duct is not limited to simple geometries, i.e., straight, constant duct cross-section. The mixing duct may be curved and its cross-section may vary with length.

(b) At the onset of mixing, the two interacting media have differences in one or more of the following fluid flow parameters:

- velocity
- total and/or static pressure
- total and/or static temperature
- physical or chemical characteristics (chemical reactions during mixing will not be considered).

The medium having at the onset of mixing the greater total pressure is called the "primary medium", the medium having the lower total pressure is called the "secondary medium."

(c) Within the mixing duct:

- the total mass flow is conserved
- in case of an adiabatic mixing process, the stagnation enthalpy is conserved

- if the internal flow does not exert a force
  component in the flow direction upon the inner
  surface of the mixing duct, then the impulse
  functions at mixing duct entrance and exit are
  equal.

(d) In "co-flow" type ejectors, mass and momentum trans-
port are coupled by the transport velocity $U(x,y)$ as
follows

- mass transport $\dot{m} = \int_{area} \rho(x,y) \cdot U(x,y) \, dA$

- momentum transport $\dot{M} = \int_{area} \rho(x,y) \, U^2(x,y) \, dA$

where $\rho(x,y)$ and $U(x,y)$ are, respectively, the
mass density and transport velocity at a given
duct cross-section as a function of position
(x,y).

(e) Two major categories of loss mechanisms can be iden-
tified in current ejectors:

- intrinsic losses associated with the mixing
  process
- parasitic drag losses.

The parasitic drag losses are due to skin friction
and possible flow separation at the inner surfaces
of the ejector shroud, which consists of inlet duct,
mixing duct and diffuser (a diffuser is employed if
necessary for matching mixing duct exit conditions
with environmental conditions).

The parasitic drag is not of a fundamental nature;
it can be strongly influenced by the design of the
ejector shroud and method of primary injection.
For example, the parasitic drag can be reduced by
reducing the mixing duct length required for adequate
mixing. This can be made possible, for example,

by employing a multiplicity of primary nozzles, by hypermixing nozzle shapes, or by accepting a certain degree of incomplete mixing.

The intrinsic losses associated with the mixing process are of a more fundamental nature and depend on the particular co-flow geometry chosen. For obtaining an upper bound of ejector performance and efficiency, the mixing losses can be determined analytically without taking parasitic drag losses into account. In flows where the total enthalpy is conserved, the ejector performance is completely determined by the total pressure after mixing, when mass flows and total pressures and temperatures of primary and secondary media are given.

The ratio of actual ejector performance to the performance resulting from an idealized mixing process having constant entropy for the system is most conveniently given by the ratio of availabilities, before and after mixing. We refer to this as the availability efficiency (η_{av}).

Another useful pseudo efficiency is the ratio of actual ejector exiting kinetic power to the kinetic power of the primary working medium expanding to a pressure equal to the stagnation pressure of the secondary working medium. This is called the kinetic energy efficiency (η_K).

(f) Perhaps the most important characteristic of all co-flowing ejectors is that the differences between the flow parameters of the interacting working media (as previously defined under "b") are greatest at the beginning of the mixing process and decrease through the process of mixing. At the end of the mixing process (in the ideal case), the mixed flow has a homogeneous gas composition, temperature,

58

pressure, and velocity. The consequences of
this type of equilibration process are, two-fold,
namely:

- An intrinsic increase in system entropy (or
  loss in availability) will occur during the
  mixing process. This increase in system entropy
  will be substantial, if at the onset of mixing
  the differences between the flow parameters such
  as temperature, pressure, velocity of the inter-
  acting fluid media, are large.

- Only a fraction of the initial momentum of the
  primary working medium can be transferred to the
  secondary working medium, because the primary
  and secondary working media are brought by
  mixing to equal speed pressure and temperature
  (v_m, P_{om}, T_{om}, respectively).

From the above synopsis it follows that major, intrinsic
performance shortcomings of current ejectors are a direct con-
sequence of the co-flowing momentum exchange process. In the
following, a discussion is given about momentum exchange processes
which depart from the co-flowing type.

7.1 FUNDAMENTAL RESEARCH AND NEW CONCEPTS IN THE FIELD OF MOMENTUM EXCHANGE PROCESSES

Practically all research and development efforts on mixing
phenomena and ejectors have been conducted in the area of co-
flowing momentum exchange processes under shrouded and unshrouded
(free jet mixing) conditions. Basic research as well as devel-
opment work is needed on novel momentum exchange processes of the
cross flow as well as the counter flow momentum exchange types.
(These terms are chosen because of their close analogy to heat
exchange processes, which are categorized according to co-flow,
cross flow, and counter flow types of heat exchange; the most
efficient heat transfer processes are of the counter flow type.)

First, the counter flow momentum exchange process will be described. In one-dimensional flow, only co-flow momentum exchange processes are possible. However, in axisymmetrical or two-dimensional flow configurations both a co-flow and a counter flow momentum exchange process can be realized, as illustrated in Figures 30 and 31, respectively. In Figure 31 the flow conditions are similar to those in fluid flow machinery: the mass flow per second is determined by the axial flow component, the density, and the annular area, while the angular momentum per second is determined by the tangential velocity component and the mass flow per second.

Since the axial velocity component can be small in comparison to the tangential velocity component, the primary and secondary gas flows can have either the same or opposite axial flow directions. It is important to realize the inherent functional differences resulting from these two possibilities; the latter allows for a counter flow momentum exchanger.

In the co-flowing process the greatest differences in total pressure exist at the onset of the mixing between the primary and secondary fluid media. As a consequence, this mixing process results in intrinsic losses or in an increase in total system entropy. In contrast, in the counter flow mixing process the secondary fluid medium comes first in contact with the primary medium after the energy of the primary medium is attenuated. As a consequence, the intrinsic mixing losses or system entropy increase are greatly reduced (under ideal conditions they can become zero).

In Figure 30 a cross flow concept is illustrated for a two-dimensional configuration. In the schematic shown, a rotor is used to establish vortices at a frequency corresponding to the natural Strouhal number of about 0.3 for the configuration (other configurations would not require a rotor). Eddies produced would exist for a longer duration before breaking into smaller scales. Because of the curvature of the channel, the eddies flow across

60
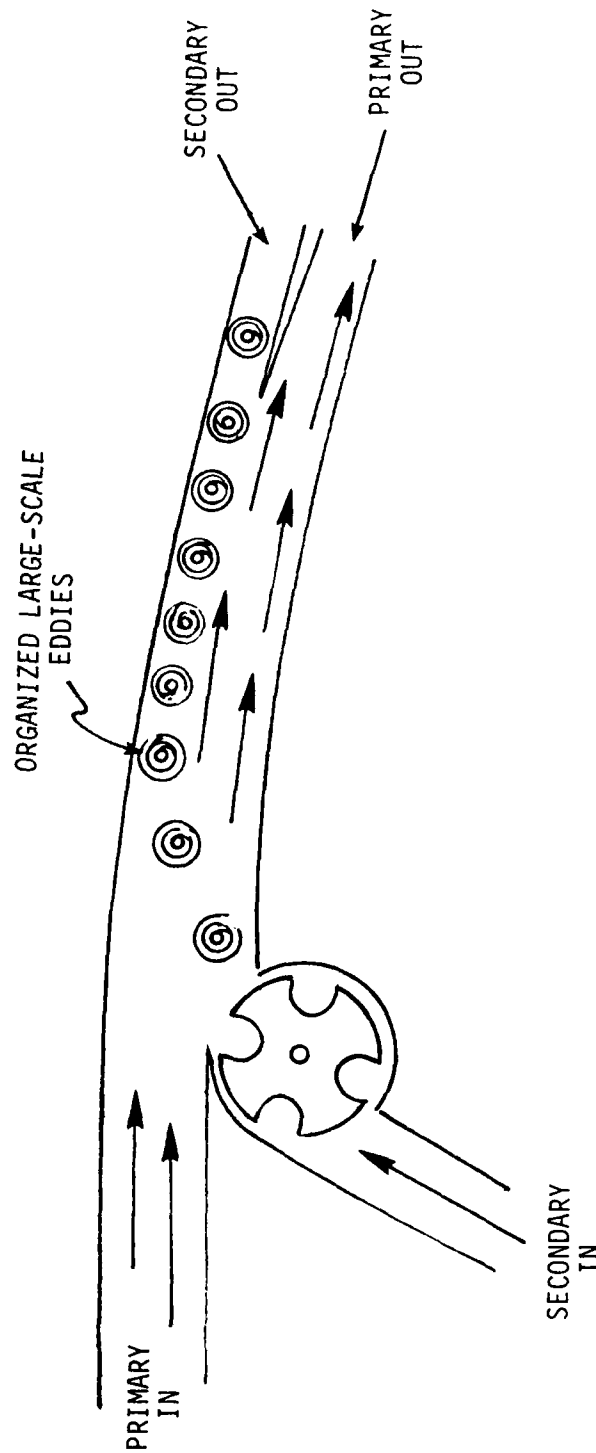
Figure 30. Schematic of a Cross Flow Momentum Exchanger Utilizing Organized Large-scale Eddies.
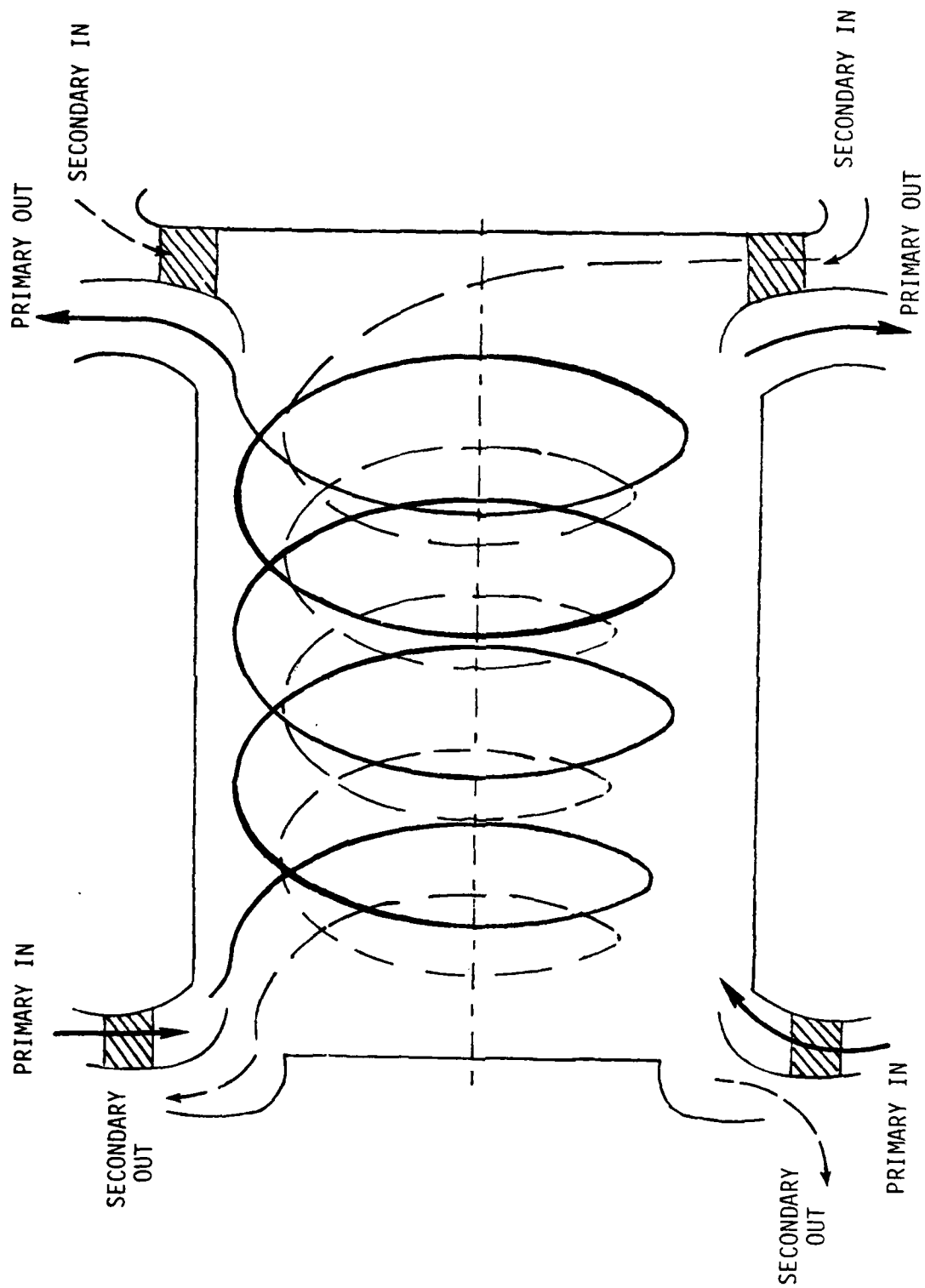
Figure 31. Schematic of a Counter Flow Momentum Exchanger.

62

the primary flow and can be accelerated to higher velocities with little exchange of thermal energy. (The primary and secondary are in general at different total temperatures.) The primary and secondary flows are separated at the exit.

Thus, we see that it is possible to describe momentum exchangers that operate on counter flow and cross flow configurations and permit, to some degree, the uncoupling of the thermal energy transport from the momentum transport. Such devices may have applications in many fields and could produce fundamental information concerning mixing phenomena. Thus, we believe that a research program should be established to investigate these concepts in view of many promising Air Force applications that can be envisioned.

REFERENCES

1. E. D. Kennedy, "The Ejector Flow Process," Master of Science Thesis, University of Minnesota, Minneaplis, Minnesota, 1955.

2. J. Fabri and R. Siestrunck, "Supersonic Ai₊ Ejectors," Advances in Applied Mechanics, Vol. 5, Academic Press, Inc. New York, New York, 1958.

3. H. J. Hoge, On the Theory of Mixing of Fluid Streams, Quartermaster Research and Engineering Center, Pioneering Research Division, Technical Report PR-2, February 1959.

4. B. Kiselev, Calculation on One-Dimensional Gas Flows, USAF Technical Report No. F-TS-1209-1A, January 1949, (translated from the Russian by Brown University).

5. M. Alperin and J. Wu, High Speed Ejectors, AFFDL-TR-79-3048, May 1979.

6. J. E. Minardi, et al., Ejector Turbine Studies and Experimental Data, DOE/ER/10509-1, November 1982.

7. Minardi, J. E., Characteristics of High Performance Ejectors, AFWAL-TR-81-3170, Air Force Wright Aeronautical Laboratories, Dayton, Ohio, January 1982.

8. Minardi, J. E., "Compressible Flow Ejector Analysis with Application to Energy Conversion and Thrust Augmentation," AIAA 82-0133, AIAA 20th Aerospace Sciences Meeting, 11-14 January 1982, Orlando, Florida.

9. Aeronautical Vest Pocket Handbook, United Technologies, Pratt and Whitney Aircraft, PWA Part No. 79500, Nineteenth Edition, Thirty-first Printing, August 1981

10. Scott, J. N. and Hankey, W. L., Jr., "Numerical Simulation of Cold Flow in an Axisymmetric Centerbody Combustor," AIAA-83-1741, AIAA 16th Fluid and Plasma Dynamics Conference, 12-14 July 1983, Danvers, Massachusetts.

RELEVANT EJECTOR EQUATIONS

MIXING FORMULA

$$C_{p_m} \dot{m}_m = C_{p_p} \dot{m}_p + C_{ps} \dot{m}_s$$

$$C_{v_m} \dot{m}_m = C_{v_p} \dot{m}_p + C_{v_s} \dot{m}_s$$

$$R_m \dot{m}_m = R_p \dot{m}_p + R_s \dot{m}_s$$

$$\bar{W} = \frac{W_p}{W_s}$$

$$\bar{m} = \frac{\dot{m}_p}{\dot{m}_s}$$

$$\beta = \frac{1}{\bar{m}}$$

$$\gamma_m = \gamma_p \frac{\dfrac{\bar{m}\Gamma}{\bar{W}} + 1}{\dfrac{\bar{m}\Gamma}{\bar{W}} + \dfrac{\gamma_p}{\gamma_s}}$$

$$\Gamma \equiv [\gamma_p/(\gamma_p-1)]/[\gamma_s/(\gamma_s-1)]$$

$$C_{pp}/C_{ps} = \Gamma/\bar{W}$$

$$C_{pm}/C_{ps} = (\Gamma\bar{m} + \bar{W})/[\bar{W}(\bar{m} + 1)]$$

$$R_m/R_s = (\bar{m} + \bar{W})/[\bar{W}(\bar{m} + 1)]$$

$$C_{pp}\dot{m}_p/C_{pm}\dot{m}_m = \Gamma\bar{m}/(\Gamma\bar{m} + \bar{W})$$

$$R_p\dot{m}_p/R_m\dot{m}_m = \bar{m}/(\bar{m} + \bar{W})$$

$$\frac{T_{om}}{T_{os}} = \left(1 + \frac{\Gamma\bar{m}}{\bar{W}} \cdot TR\right)\bigg/\left(1 + \frac{\Gamma\bar{m}}{\bar{W}}\right)$$

67

ISENTROPIC FLOW

$$\frac{T_O}{T} = 1 + \frac{\gamma-1}{2} M^2$$

$$\frac{P_O}{P} = \left(1 + \frac{\gamma-1}{2} M^2\right)^{\frac{\gamma}{\gamma-1}}$$

$$\frac{\rho_O}{\rho} = \left(1 + \frac{\gamma-1}{2} M^2\right)^{\frac{\gamma}{\gamma-1}}$$

$$\frac{A}{A^*} = \frac{1}{M} \left[\frac{2}{\gamma+1} \left(1 + \frac{\gamma-1}{2} M^2\right)\right]^{\frac{\gamma+1}{2(\gamma-1)}}$$

$$\frac{T_O}{T} \frac{V^2}{2h_O} = \frac{\gamma-1}{2} M^2$$

$$\frac{\dot{m}}{A} = \sqrt{\frac{\gamma W}{R}} \frac{P_O}{\sqrt{T_O}} \frac{M}{\left(1 + \frac{\gamma-1}{2} M^2\right)^{\frac{\gamma+1}{2(\gamma-1)}}}$$

EJECTOR EQUATIONS

$$C1 = \frac{\Gamma\bar{m}\,\bar{T}_O + \bar{W}}{\Gamma\bar{m} + \bar{W}} \left(1 + \frac{\gamma_s-1}{2} M_s^2\right)$$

$$C2 = \frac{\bar{W}(\bar{m} + 1)}{\Gamma\bar{m} + \bar{W}} \frac{\gamma_s - 1}{2} M_s^2$$

$$C3 = \left(\bar{P}_1\bar{A} + 1 - \frac{2\tau\ell}{P_{1s}r} (1 + \bar{A})\right) \frac{\bar{W}}{\bar{m} + \bar{W}}$$

$$C4 = \frac{\bar{m}\,\bar{W}\,\bar{V}}{\bar{m} + \bar{W}} \gamma_s M_s^2$$

$$C5 = \frac{\bar{W}}{\bar{m} + \bar{W}} \gamma_s M_s^2$$

$$C6 + \frac{\bar{W}(\bar{m} + 1)}{\bar{W} + \bar{m}} \gamma_s M_s^2$$

68

$$(C2 - C6)\,\overline{V}_m^2 + (C3 + C4 + C5)\,\overline{V}_m - C1 = 0$$

$$\overline{V}_m = V_m/V_{1s}$$

$$\frac{T_m}{T_{os}} = \frac{1 + \overline{m}}{1 + \dfrac{\Gamma\overline{m}}{\overline{W}}}\left[\frac{1 + \dfrac{\Gamma\overline{m}}{\overline{W}}\, TR}{(1 + \overline{m})} - \left(1 - \frac{T_{1s}}{T_{os}}\right)\overline{V}_m^2\right]$$

$$\frac{P_m}{P_{os}} = \frac{\overline{m} + \overline{W}}{\overline{W}(1 + AR)} \cdot \frac{T_m}{T_{1s}} \cdot \frac{P_{1s}}{P_{os}} \cdot \frac{1}{\overline{V}_m}$$

$$M_m = \overline{V}_m\, M_s \left/ \sqrt{\frac{\gamma_m}{\gamma_s}\,\frac{T_m}{T_{op}}\,\frac{\overline{W} + \overline{m}}{\dfrac{T_{1s}}{T_{os}}\,\overline{W}(1 + \overline{m})}} \right.$$

$$M_m = \frac{\overline{V}_m\, M_s}{\sqrt{\dfrac{\gamma_m}{\gamma_s}\,\dfrac{T_m}{T_{1s}}\,\dfrac{\overline{W} + \overline{m}}{\overline{W}(1 + \overline{m})}}}$$

The remaining Equations are for a single species (e.g, air-air)

$$\phi = \frac{\dot{m}_m}{\dot{m}_p}\,\frac{\sqrt{\dfrac{\dot{m}_p}{\dot{m}_m}\,\dfrac{T_{op}}{T_{os}} + \dfrac{\dot{m}_s}{\dot{m}_m}}\;\sqrt{\left(1 + \dfrac{\gamma-1}{2}\,M_\infty^2\right) - \left(\dfrac{P_{om}}{P_{os}}\right)^{-\frac{\gamma-1}{\gamma}}} - \sqrt{\dfrac{\gamma-1}{2}\,M_\infty^2}}{\sqrt{\dfrac{T_{op}}{T_{os}}}\;\sqrt{\left(1 + \dfrac{\gamma-1}{2}\,M_\infty^2\right) - \left(\dfrac{P_{op}}{P_{os}}\right)^{-\frac{\gamma-1}{\gamma}}} - \sqrt{\dfrac{\gamma-1}{2}\,M_\infty^2}}$$

$$\eta = \left(N + \ln \frac{P_{om}}{P_{os}} \right) \Big/ D$$

$$D = \frac{\gamma}{\gamma-1} \frac{\dot{m}_p}{\dot{m}_m} \left[\frac{T_{op}}{T_{os}} - 1 - \ln \left(\frac{T_{op}}{T_{os}} \right) \right] + \frac{\dot{m}_p}{\dot{m}_m} \ln \left(\frac{P_{op}}{P_{os}} \right)$$

$$N = \frac{\gamma}{\gamma-1} \left[\frac{\dot{m}_p}{\dot{m}_m} \left(\frac{T_{op}}{T_{os}} - 1 \right) - \ln \left(\frac{\dot{m}_p}{\dot{m}_m} \frac{T_{op}}{T_{os}} - \frac{\dot{m}_s}{\dot{m}_m} \right) \right]$$

INLET CONDITIONS

$$\frac{1}{M^*_{ep}} \left(\frac{\gamma+1}{2} - \frac{\gamma-1}{2} M^{*2}_{ep} \right)^{-\frac{1}{\gamma-1}} = \frac{A}{A^*_p} - \frac{A_s}{A^*_o} M^*_s \left(\frac{\gamma+1}{2} - \frac{\gamma-1}{2} M^{*2}_s \right)^{\frac{1}{\gamma-1}}$$

$$\frac{1 + M^*_{ep}}{M^*_{ep}} = \frac{1 + M^{*2}_p}{M^*_p} + \frac{A_s}{A^*_p} \frac{P_{os}}{P_{op}} \left(\frac{\gamma+1}{2} - \frac{\gamma-1}{2} M^{*2}_s \right)^{\frac{1}{\gamma-1}} \left(1 - M^*_s \right)^2$$

APPENDIX B

THE INLET FLOW CONDITIONS ALWAYS ADMIT THE SOLUTION OF $P_{1p} = P_{os}$ AND $M_s = 1.0$

In order to determine the value of P_{os}/P_{op} at a value of $M_s^* = 1$, we can solve the second inlet condition equation given in Appendix A for P_{os}/P_{op}:

$$\frac{P_{os}}{P_{op}} = \frac{A_p^*}{A_s} \; \frac{\left(\dfrac{1 + M_{ep}^*}{M_{ep}^*}\right) - \left(\dfrac{1 + M_p^{*2}}{M_p^*}\right)}{\left(1 - M_s^*\right)^2 \; \left(\dfrac{\gamma+1}{2} - \dfrac{\gamma-1}{2} \; M_s^{*2}\right)^{\frac{1}{\gamma-1}}} \; . \tag{B.1}$$

Now from the first Equation of the inlet conditions we see that if $M_s^* = 1$ then $M_{ep}^* = M_p^*$. Thus, Equation B.1 gives a 0/0 or indeterminate form when $M_s^* = 1$. However, L'Hospital's Rule can be used to determine the value of $M_s^* = 1$. A double application of L'Hospital's Rule is required. It results in:

$$\frac{P_{os}}{P_{op}} = \frac{1}{2} \; \frac{A_p^*}{A_s} \; \frac{M_p - 1}{M_p^{*2}} \; \left.\frac{d^2 M_{ep}^*}{d\,M_s^{*2}}\right|_{M_s^* = 1} \; . \tag{B.2}$$

In order to evaluate Equation B.2 we must use the first of the inlet equations given in Appendix B:

$$M_{ep}^{*-1}\left(\frac{\gamma+1}{2} - \frac{\gamma-1}{2} \; M_{ep}^{*2}\right)^{-\frac{1}{\gamma-1}} = \frac{A}{A_p^*} - \frac{A_s}{A_p^*} \; M_s^*\left(\frac{\gamma+1}{2} - \frac{\gamma-1}{2} \; M_s^{*2}\right)^{\frac{1}{\gamma-1}}$$

$$\tag{B.3}$$

71

After differentiating Equation B.3 twice we obtain:

$$\left. \frac{d^2 M^*_{ep}}{d\,M^{*2}_s} \right|_{M^*_s = 1} = 2\,\frac{A_s}{A^*_p}\cdot\frac{M^{*2}_p}{M^*_p - 1}\cdot\left(\frac{\gamma+1}{2} - \frac{\gamma-1}{2}\,M^{*2}_p\right)^{\frac{\gamma}{\gamma-1}}\,. \qquad \text{(B.4)}$$

Substitution of Equation B.4 into Equation B.2 results in

$$\left(\frac{P_{os}}{P_{op}}\right)_{M^*_s = 1} = \left(\frac{\gamma+1}{2} - \frac{\gamma-1}{2}\,M^{*2}_p\right)^{\frac{\gamma}{\gamma-1}}\,. \qquad \text{(B.5)}$$

Now

$$\left(\frac{P_{1s}}{P_{op}}\right)_{M^*_s = 1} = \frac{P_{1s}}{P_{os}}\cdot\frac{P_{op}}{P_{op}}\cdot\frac{P_{os}}{P_{op}} \qquad \text{(B.6)}$$

Using Equation B.5 along with the well known isentropic realtions yield

$$\left(\frac{P_{1s}}{P_{1p}}\right)_{M^*_s = 1} = 1\,. \qquad \text{(B.7)}$$

Therefore, the inlet conditions always admit the solution where $M^*_s = M_s = 1$; $P_{1s}/P_{op} = 1$ and the ratio P_{os}/P_{op} is determined from Equation B.5.

APPENDIX C

AN EXAMPLE OF AN ISOLATED POINT ON THE
SUPERSONIC BRANCH WHERE $M_s < 1$ AND $P_{1p} = P_{1s}$

As stated in the text an isolated point may exist on the supersonic branch where $M_s < 1$ and $P_{1p} = P_{1s}$. The investigation of the supersonic solution branch where $M_s < 1$ showed that most points could not be achieved in an ejector. However, one can show, by an inverse procedure, that an isolated point may exist where $M_s < 1$ and $P_{1p} = P_{1s}$.

Table C.1 presents the result of applying the Fabri and Siestrunck inlet conditions to an ejector design where $M_p^* = 1.7$ ($M_p = 2.1555$), $A_p/A_p^* = 1.928$ (Al in Table C.1), $A_s/A_p^* = 2.000$ (as in Table C.1) and TR = 1.15. Note that $A/A_p^* = 2 + 1.928 = 3.928$. Using the procedure described in reference 7, we found pressure ratios, PR, required to achieve various values of M_s^* (MS in the table). The ratio of P_{1p}/P_{1s} is also listed in Table 3.1 and we note that it achieves a value of 1 at $M_s^* = 1$ and about at $M_s^* = 0.7$ at which point the bypass ratio (MU in the table) is 0.25848 and PR = 7.40451.

Thus, if we run the design program with the values of β, PR, and TR indicated at $M_s^* = 0.7$ ($M_s = 0.6668$) we should recover this point and we know that it satisfies the Fabri and Siestrunck inlet conditions.

The computer output for this "inverse" run is shown in Table C.2. Indeed we see that at $M_s = 0.6668$, $M_p = 2.155$ is reasonable and $A/A_p^* = 3.928$ is also reasonable. Thus, this particular point on the curve can be achieved and the value of the efficiency is about 0.883. Note, however, that this value of efficiency is less than the value at $M_s = 1$, where it is 0.890. The value of the efficiency at $M_s = 1$ is slightly less than the values found at supersonic values of M_s.

TABLE C-1

MP*= 1.700 A1= 1.928 AS= 2.000 TR= 1.150

MS= 0.0000	MPE= 1.94594	AE/AP*= 3.92786	(A-AE)/AP*=-0.0000	PR= 18.45680	MU= 0.00000	P1P/P1S= 1.8505
MS= 0.0500	MPE= 1.93430	AE/AP*= 3.77028	(A-AE)/AP*= 0.1576	PR= 17.44470	MU= 0.00969	P1P/P1S= 1.7514
MS= 0.1000	MPE= 1.92287	AE/AP*= 3.61368	(A-AE)/AP*= 0.3142	PR= 16.45130	MU= 0.02048	P1P/P1S= 1.6591
MS= 0.1500	MPE= 1.91072	AE/AP*= 3.45905	(A-AE)/AP*= 0.4688	PR= 15.48250	MU= 0.03247	P1P/P1S= 1.5728
MS= 0.2000	MPE= 1.89786	AE/AP*= 3.30734	(A-AE)/AP*= 0.6205	PR= 14.54320	MU= 0.04576	P1P/P1S= 1.4927
MS= 0.2500	MPE= 1.88430	AE/AP*= 3.15952	(A-AE)/AP*= 0.7683	PR= 13.63760	MU= 0.06042	P1P/P1S= 1.4184
MS= 0.3000	MPE= 1.87008	AE/AP*= 3.01649	(A-AE)/AP*= 0.9114	PR= 12.76860	MU= 0.07654	P1P/P1S= 1.3497
MS= 0.3500	MPE= 1.85524	AE/AP*= 2.87915	(A-AE)/AP*= 1.0487	PR= 11.93930	MU= 0.09419	P1P/P1S= 1.2867
MS= 0.4000	MPE= 1.83992	AE/AP*= 2.74836	(A-AE)/AP*= 1.1795	PR= 11.15240	MU= 0.11342	P1P/P1S= 1.2291
MS= 0.4500	MPE= 1.82418	AE/AP*= 2.62493	(A-AE)/AP*= 1.3029	PR= 10.41010	MU= 0.13422	P1P/P1S= 1.1770
MS= 0.5000	MPE= 1.80920	AE/AP*= 2.50963	(A-AE)/AP*= 1.4182	PR= 9.71396	MU= 0.15657	P1P/P1S= 1.1304
MS= 0.5500	MPE= 1.79219	AE/AP*= 2.40318	(A-AE)/AP*= 1.5247	PR= 9.06450	MU= 0.18038	P1P/P1S= 1.0892
MS= 0.6000	MPE= 1.77639	AE/AP*= 2.30622	(A-AE)/AP*= 1.6216	PR= 8.46391	MU= 0.20546	P1P/P1S= 1.0538
MS= 0.6500	MPE= 1.76112	AE/AP*= 2.21935	(A-AE)/AP*= 1.7085	PR= 7.91073	MU= 0.23161	P1P/P1S= 1.0243
MS= 0.7000	MPE= 1.74673	AE/AP*= 2.14309	(A-AE)/AP*= 1.7848	PR= 7.40451	MU= 0.25846	P1P/P1S= 1.0003
MS= 0.7500	MPE= 1.73360	AE/AP*= 2.07789	(A-AE)/AP*= 1.8500	PR= 6.94541	MU= 0.28564	P1P/P1S= 0.9828
MS= 0.8000	MPE= 1.72214	AE/AP*= 2.02412	(A-AE)/AP*= 1.9037	PR= 6.53093	MU= 0.31259	P1P/P1S= 0.9718
MS= 0.8500	MPE= 1.71274	AE/AP*= 1.98207	(A-AE)/AP*= 1.9458	PR= 6.16001	MU= 0.33874	P1P/P1S= 0.9677
MS= 0.9000	MPE= 1.70574	AE/AP*= 1.95195	(A-AE)/AP*= 1.9759	PR= 5.83324	MU= 0.36325	P1P/P1S= 0.9716
MS= 0.9500	MPE= 1.70144	AE/AP*= 1.93387	(A-AE)/AP*= 1.9940	PR= 5.55356	MU= 0.38503	P1P/P1S= 0.9851
MS= 1.0000	MPE= 1.70000	AE/AP*= 1.92786	(A-AE)/AP*= 2.0000	PR= 5.26906	MU= 0.40705	P1P/P1S= 1.0000

74

TABLE C-2

CONSTANT MASS FLOW
CONSTANT AREA SUPERSONIC
PRIMARY VAPOR AIR SECONDARY GAS AIR
PR- 2 405 TR= 1 150 GP=1 400 GS=1 400 WR= 1 00 WP= 29 00 WS= 29 00
BY-PASS RATIO= 0.258

MS	PIS/	TIS/	VP/VS	VM/VS	MM	PM/	TM/	GM	MP	TIP/TOS	PIP/POP	AP/AS	A/AP*	EFPOS	POM/	EFAVL	SR
0 0500	VIOLATION OF 2ND LAW REQUIRES NEGATIVE TEMPERATURES																
0 1000	VIOLATION OF 2ND LAW REQUIRES NEGATIVE TEMPERATURES																
0 1500	VIOLATION OF 2ND LAW REQUIRES NEGATIVE TEMPERATURES																
0 2000	VIOLATION OF 2ND LAW FOR ADIABATIC SYSTEMS REQUIRES WORK INPUT AND COOLING																
0 2500	VIOLATION OF 2ND LAW FOR ADIABATIC SYSTEMS REQUIRES WORK INPUT AND COOLING																
0 3000	VIOLATION OF 2ND LAW FOR ADIABATIC SYSTEMS REQUIRES WORK INPUT AND COOLING																
0 3500	VIOLATION OF 2ND LAW FOR ADIABATIC SYSTEMS REQUIRES WORK INPUT AND COOLING																
0 4000	0 896	0 969	4 099	4 397	2 401	0 330	0 520	1 400	2 04	0 547	0 121	0 613	4 576	1 00	4 83	0 987	0 001
0 4500	0 870	0 961	3 677	3 914	2 363	0 380	0 553	1 400	2 05	0 542	0 118	0 693	4 353	0 98	4 48	0 940	0 096
0 5000	0 843	0 952	3 342	3 377	2 171	0 420	0 576	1 400	2 07	0 538	0 114	0 751	4 188	0 96	4 29	0 913	0 140
0 5500	0 814	0 943	3 071	3 039	2 109	0 451	0 592	1 400	2 10	0 532	0 110	0 818	4 071	0 94	4 18	0 898	0 166
0 6000	0 784	0 933	2 847	2 772	2 069	0 473	0 603	1 400	2 12	0 526	0 106	0 882	3 991	0 94	4 12	0 888	0 181
0 6500	0 753	0 922	2 661	2 557	2 044	0 487	0 610	1 400	2 15	0 520	0 102	0 944	3 940	0 93	4 09	0 884	0 188
0 7000	0 721	0 911	2 502	2 382	2 032	0 495	0 613	1 400	2 17	0 514	0 097	1 003	3 913	0 93	4 07	0 882	0 192
0 7500	0 689	0 899	2 367	2 236	2 030	0 497	0 614	1 400	2 20	0 507	0 093	1 061	3 908	0 93	4 07	0 982	0 192
0 8000	0 656	0 887	2 250	2 114	2 035	0 493	0 612	1 400	2 23	0 500	0 089	1 116	3 921	0 93	4 08	0 982	0 191
0 8500	0 624	0 874	2 149	2 010	2 047	0 485	0 609	1 400	2 27	0 493	0 084	1 169	3 950	0 93	4 09	0 883	0 189
0 9000	0 591	0 861	2 060	1 922	2 064	0 474	0 604	1 400	2 30	0 486	0 080	1 219	3 996	0 93	4 10	0 885	0 186
0 9500	0 559	0 847	1 981	1 845	2 085	0 460	0 599	1 400	2 34	0 478	0 076	1 267	4 055	0 93	4 11	0 887	0 182
1 0000	0 528	0 833	1 912	1 779	2 110	0 444	0 592	1 400	2 37	0 470	0 071	1 313	4 129	0 94	4 13	0 890	0 179
1 0500	0 498	0 819	1 850	1 720	2 139	0 426	0 585	1 400	2 41	0 462	0 067	1 357	4 216	0 94	4 14	0 892	0 175
1 1000	0 468	0 805	1 794	1 669	2 170	0 408	0 576	1 400	2 45	0 454	0 063	1 399	4 316	0 94	4 16	0 894	0 171
1 1500	0 440	0 791	1 745	1 623	2 203	0 388	0 568	1 400	2 49	0 446	0 059	1 439	4 429	0 94	4 17	0 896	0 168
1 2000	0 412	0 776	1 700	1 583	2 239	0 369	0 559	1 400	2 53	0 438	0 056	1 477	4 556	0 94	4 19	0 899	0 164
1 2500	0 386	0 762	1 659	1 547	2 276	0 349	0 550	1 400	2 57	0 430	0 052	1 513	4 695	0 95	4 20	0 901	0 161
1 3000	0 361	0 747	1 622	1 514	2 315	0 329	0 540	1 400	2 62	0 422	0 049	1 548	4 848	0 95	4 22	0 903	0 159
1 3500	0 337	0 733	1 589	1 484	2 355	0 310	0 531	1 400	2 66	0 414	0 046	1 580	5 015	0 95	4 23	0 905	0 155
1 4000	0 314	0 718	1 558	1 458	2 397	0 291	0 521	1 400	2 71	0 405	0 042	1 611	5 196	0 95	4 24	0 902	0 152
1 4500	0 293	0 704	1 530	1 434	2 440	0 273	0 511	1 400	2 75	0 397	0 040	1 641	5 392	0 95	4 25	0 908	0 149
1 5000	0 272	0 690	1 504	1 411	2 484	0 256	0 501	1 400	2 80	0 389	0 037	1 669	5 603	0 95	4 26	0 910	0 146
1 5500	0 253	0 675	1 481	1 391	2 529	0 239	0 491	1 400	2 85	0 381	0 034	1 696	5 829	0 96	4 27	0 911	0 144
1 6000	0 235	0 661	1 459	1 373	2 575	0 223	0 481	1 400	2 90	0 373	0 032	1 721	6 072	0 96	4 28	0 913	0 141
1 6500	0 218	0 647	1 439	1 356	2 622	0 208	0 471	1 400	2 95	0 365	0 029	1 745	6 331	0 96	4 29	0 914	0 139
1 7000	0 203	0 634	1 420	1 340	2 670	0 194	0 461	1 400	3 00	0 358	0 027	1 768	6 608	0 96	4 30	0 915	0 137
1 7500	0 188	0 620	1 403	1 326	2 718	0 180	0 452	1 400	3 05	0 350	0 025	1 790	6 904	0 96	4 31	0 917	0 135
1 8000	0 174	0 607	1 387	1 312	2 767	0 167	0 442	1 400	3 10	0 342	0 024	1 811	7 218	0 96	4 32	0 918	0 133
1 8500	0 161	0 594	1 372	1 300	2 816	0 156	0 433	1 400	3 15	0 335	0 022	1 830	7 553	0 96	4 33	0 919	0 131
1 9000	0 149	0 581	1 358	1 288	2 866	0 144	0 423	1 400	3 20	0 328	0 020	1 849	7 909	0 96	4 34	0 920	0 130
1 9500	0 138	0 568	1 345	1 277	2 917	0 134	0 414	1 400	3 26	0 321	0 019	1 867	8 296	0 96	4 34	0 921	0 128
2 0000	0 128	0 556	1 333	1 267	2 968	0 124	0 405	1 400	3 31	0 314	0 017	1 884	8 692	0 96	4 35	0 922	0 127
2 0500	0 118	0 543	1 321	1 258	3 019	0 115	0 396	1 400	3 36	0 307	0 016	1 900	9 110	0 96	4 35	0 922	0 126

75

END

FILMED

8